CHARACTERIZATION AND THERAPEUTIC TARGETING OF SURFACE MARKERS IN GLIOBLASTOMA PRE-CLINICAL MODELS

CHARACTERIZATION AND THERAPEUTIC TARGETING OF SURFACE MARKERS IN GLIOBLASTOMA PRE-CLINICAL MODELS

By NEIL SAVAGE, (H)B.Sc.

A Thesis Submitted to the School of Graduate Studies of McMaster University in Partial Fulfillment of the Requirements for the Degree of

DOCTOR OF PHILOSOPHY in BIOCHEMISTRY AND BIOMEDICAL SCIENCES

DOCTOR OF PHILOSOPHY (2023)

Biochemistry and Biomedical Sciences

Faculty of Health Science, McMaster University

Hamilton, ON Canada

TITLE: Characterization and Therapeutic Targeting of Surface Markers in Glioblastoma Pre-Clinical Models

AUTHOR: Neil Savage, (H)B.Sc.

SUPERVISOR: Dr. Sheila Kumari Singh

NUMBER OF PAGES: 206

Lay Abstract

Glioblastoma (GBM) remains an aggressive and incurable brain cancer despite decades of intense research. Treatment failure is due to the untargeted approaches currently undertaken in the clinic. The current work uses multiples methods to interrogate how GBM grows and develops over time. Using GBM samples from consenting patients, I investigated an important population of the tumor using a surface marker CD133 and CRISPR to study which genes influenced it. I then successfully validated SOX2 as a direct regulator of CD133 expression. Next, I combed multiple data sets for a target to kill GBM cells without harming healthy tissue in patients. I found Glycoprotein Non-Metastatic Melanoma Protein B (GPNMB) to be exploitable and used several experimental methods to investigate its role in GBM progression. Finally, we used a novel immunotherapy to eliminate cells which express GPNMB. Together, these findings could apply to the broader field of stem cell biology and be used for a more targeted method to eliminate the cancer entirely.

Abstract

Glioblastoma (GBM) remains the most aggressive primary brain tumor in adults. Since 2005, Standard of Care (SoC) consists of surgical resection followed by radiation and adjuvant chemotherapy with temozolomide. Treatment failure is attributed to intratumoral heterogeneity with populations capable of mechanisms to repair damaged DNA. Given the lack of progress to improve patient outcomes, the current work encompasses how multi-omic approaches can be utilized to uncover novel biology in GBM and develop precision medicines to exploit these cancer specific phenomena.

Using patient derived GBM samples I first used the surface marker CD133 to interrogate glioblastoma stem cells, a subpopulation of cells identified to withstand conventional therapies and lead to tumor relapse. I used a genome-wide CRISPR-Cas9 library to conduct an unbiased loss-of-function phenotypic screen to identify regulators of CD133. I then validated SOX2 as a direct transcription factor to *PROM1* encoding CD133. These findings further show the untapped potential of CRISPR to uncover novel biology to directly apply to broader fields of stem cells and cancer biology.

Next, I combed GBM data sets at transcriptomic and proteomic levels to identify understudied proteins as potential targets for immunotherapies. Glycoprotein nonmetastatic melanoma protein B (GPNMB) has previously been identified as a clinically relevant target in GBM and shown to be active in the tumor immune microenvironment. I found GPNMB to be upregulated in recurrent GBM and macrophage populations which can be exploited in a more comprehensive manner to treat GBM. Through a series of models, I elucidated how GPNMB influences GBM biology, its effectiveness as a target for Chimeric Antigen Receptor T-cells, and how it can be paired with CD133 therapies to

provide better coverage of tumor cells. Together, these studies highlight how advances in pre-clinical models and technologies can be leveraged to develop new therapies in a rational manner.

Acknowledgements

First and foremost, I would like to express my deepest gratitude to my supervisor, Dr. Sheila K. Singh, for her unwavering support, guidance, and encouragement throughout my doctoral studies. She has been a constant source of inspiration, challenge, and motivation and her insights and feedback have been invaluable in shaping the direction and quality of my research.

I would also like to thank my committee members, Dr. Jason Moffat and Dr. Karun Singh, for their invaluable feedback, constructive criticism, and insightful suggestions that have greatly enhanced the quality and impact of my research. Their diverse expertise, intellectual curiosity, and passion for scholarship have been a constant source of inspiration and challenge.

I owe a debt of gratitude to my colleagues and friends at McMaster University, particularly Dr. Chitra Venugopal, who have all supported and encouraged me in countless ways. Their kindness, generosity, and camaraderie have made this journey even more rewarding and memorable. We will end up around the world in the coming years, but our time together has shaped an unbreakable bond.

I would also like to thank my family for their unwavering love, support, and patience throughout my studies. Their belief in me, their sacrifices, and their unconditional love have sustained me through the highs and lows of this journey. I am forever grateful.

Most importantly, my deepest appreciation goes to my current fiancée who I cannot wait to make my wife later this year. To be on this journey from before I started my studies, no one sacrificed more. As I write this, I cannot help but feel overwhelmed with gratitude and love for you. For all I understand about immunotherapy in brain tumors now, I'll never

learn your kindness, your generosity, your selflessness – all the qualities that I aspire to emulate. Thank you for making me a better person and for helping me see the world in a brighter light. I dedicate this thesis to you, my beloved, with all my heart. I look forward to the journey ahead, with you by my side, and I promise to love and cherish you always.

Thank you all.

Neil Savage

Table of Contents

Chapter 5: Discussion

Figures

List of Abbreviations and Symbols

ACT – Adoptive Cell Transfer

ADC – Antibody Drug Conjugate

BBB – Blood-Brain Barrier

bFGF – Basic Fibroblast Growth Factor

BiTEs – Bispecific T Cell Engagers

BT – Brain Tumor

BTICs – Brain Tumor Initiating Cells

CAR – Chimeric Antigen Receptor

CAR-T – Chimeric Antigen Receptor T-Cell

CD – cluster of differentiation

CRS – Cytokine Release Syndrome

EDTA – ethylenediaminetetraacetic acid

CNS – Central Nervous System

CRS – Cytokine release syndrome

DCs – Dendritic Cells

DNA – deoxyribonucleic acid

ECM – extra cellular matrix

EGFR – Epidermal Growth Factor Receptor

ELISA – Enzyme Linked Immunosorbent Assay

FDR – False Discovery Rate

FFPE – formalin-fixed paraffin-embedded

GAPDH – glyceraldehyde 3-phosphate dehydrogenase

GBM – Glioblastoma

GSCs – Glioblastoma Stem Cells

GSEA – Gene Set Enrichment Analysis

GV – Glembatumumab Vedotin

H&E – Hematoxylin and Eosin

HHS – Hamilton Health Sciences

HRP – Horseradish Peroxidase

ICIs – Immune Checkpoint inhibitors

IDH – Isocitrate Dehydrogenase

IFN – Interferon

IHC – Immunohistochemistry

IL – Interleukin

KO – Knock Out

MDSCs – Myeloid-Derived Suppressor Cells

MGMT – O6-methylguanine methyltransferase

MHC – Major Histocompatibility Complex

MMR – DNA Mismatch Repair

MRI – Magnetic Resonance Imaging

NCC – NeuroCult Complete Media

NES – Normalized Enrichment Scores

NK – Natural Killer

NPC – Neural-Progenitor Cell

NSCs – Neural Stem Cells

OS – Overall Survival

PBMCs – Peripheral Blood Mononuclear Cells

PBS – Phosphate Buffer Saline

PDGFR – Platelet Derived Growth Factor Receptor

PD-1 – Programmed Cell Death Protein-1

PDX – Patient Derived Xenograft

pGBM – Primary GBM

PI3K – phosphatidylinositol 3-kinase

PTEN – Phosphatase and Tensin Homolog

RB1 – Retinoblastoma

RFS – Relapse-Free Survival

rGBM – Recurrent GBM

RNA – Ribonucleic acid

RT – Radiotherapy

RTK – Receptor tyrosine kinase

scFvs – Single-Chain Variable Fragments

sci-RNA-seq3 – Single-cell Combinatorial Indexing RNA Sequencing

SoC – Standard of Care

SVZ – Subventricular Zone

TAA – Tumor Associated Antigen

TAM – Tumor Associated Macrophages

TCGA – The Cancer Genome Atlas

TCR – T Cell Receptor

TILs – Tumor-Infiltrating Lymphocytes

TIME – Tumor Immune Microenvironment

TKOv3 – Toronto Knockout Library Version 3

TMA – Tissue Microarray

TMZ – Temozolomide

TNF – Tumor Necrosis Factor

WHO – World Health Organization

WT – Wildtype

Declaration of Academic Achievement

This thesis represents my original work that I conceptualized throughout my PhD and now contribute to the scientific community. I designed and performed experiments, conducted data analysis and interpretation, and wrote the manuscripts along with all sections of this thesis. This thesis does not include contributions I have made to other projects, whether they are published or in the process of being published by other academic groups. The entirety of my PhD work was under the supervision of Dr. Sheila K. Singh. Contributions of co-authors to each publication have been noted in the premable of Chapters 2-4. This thesis is presented in the format of a sandwich thesis as outlined in McMaster University's Guide for Preparation of Master's and Doctoral Theses (v2021).

Chapter 1 provides my modern perspective of the current research fields regarding glioblastoma and immunotherapy with a summary of all relevant topics to this thesis. I acknowledge the breadth of these fields and respect all the differences of philosophies the vastness inevitably generates.

Chapter 2 is an original article focused on a biological question regarding glioblastoma. Its purpose is borne from a phenotypic screen of glioblastoma stem cells to determine the genetic regulators of CD133, a widely used cancer stem cell marker but its function and regulation remains undetermined. Using multiple cutting edge high throughput techniques, I validate SOX2 as a transcription factor to directly regulate *PROM1*. This manuscript is currently being submitted to journals for publication.

Chapter 3 is an original article focused on uncovering the biology of an exploitable tumor associated antigen for glioblastoma therapies. Using the newest technologies in the field such as CRISPR and single-cell RNA-sequencing in patient derived glioblastoma

I explored how glycoprotein non-metastatic melanoma protein B (GPNMB) contributes to cancer aggression. This manuscript is in the process of being submitted to high impact journals in the field.

Chapter 4 is an original article focused on a novel therapeutic strategy, targeting GPNMB in glioblastoma using CAR-Ts. Building on Chapter 3, I use some of the newest methods in the field to not only measure how effective CAR-Ts are at reducing tumor burdens, but also how they modulate the tumor immune microenvironment. By combining the GPNMB CAR-T in combination with a CD133 CAR-T, I show a proof-of-concept example for how data driven combinations of therapies offer synergistic efficacy for future clinical development. This manuscript is also in the process of being submitted to high impact journals in the field.

Chapter 5 reflects on the work conducted in this thesis and discusses the implications it proposes to compliment currently available data. Future possibilities to improve our understanding of recurrent GBM biology, identify novel targets and develop better therapies for the treatment of recurrent GBM.

Chapter 1: Introduction

Section 1

Clinical Characteristics - Standard of Care and Disease Prognosis

Glioblastoma (GBM) is a highly aggressive tumor which originates within the brain (Louis *et al.* 2021). Its incidence is low compared to other cancers, affecting less than 5 per 100,000 citizens in North America, but its rapid progression typically results in death within 16 months of diagnosis and a patient 5-year survival rate of only 5% (Lin *et al.* 2021, Tran *et al.* 2010). Until recently, tumor grading of central nervous system (CNS) cancers relied strictly on histological features. GBM is identified by marked hypercellularity, nuclear atypia, microvascular proliferation, and necrosis (Alessio D'Alessio *et al.* 2019). The advent of personalized genetic tests has added a powerful dimension to diagnosis. In 2021, the Consortium to Inform Molecular and Practical Approaches to CNS Tumor Taxonomy (cIMPACT-NOW) updated the CNS tumor classifications to remove all isocitrate dehydrogenase (IDH)-mutants from GBM to classify them as IDH-mutant astrocytomas (Louis *et al.* 2021b). Other genetic identifiers of GBM include: *TERT* promoter mutation, *EGFR* amplification, and chromosomes 7 and 10 copy number changes (Louis *et al.* 2021b).

Once diagnosed, GBM patients typically undergo the Stupp protocol which has become the current Standard of Care (SoC) consisting of surgical resection, fractionated radiation therapy and adjuvant temozolomide (TMZ) (Stupp *et al.* 2005). GBM can arise anywhere in the brain but typically occurs in the supratentorial region (Larjavaara *et al.* 2007). If operable, surgical resection is the most effective intervention to prolong patient survival times (Incekara *et al.* 2020). However, due to the highly infiltrative nature of GBM,

tumor cells escape beyond the margins of resection requiring the subsequent TMZ and radiation. Radiation is commonly administered over six weeks (2 Gy per day, Monday to Friday) for a total dose of 60 Gy (Stupp *et al.* 2005). TMZ is a prodrug derivative of dacarbazine, an alkylating chemotherapy given to melanoma and Hodgkin's lymphoma. TMZ is orally administered and readily penetrates the blood–brain barrier (BBB) and into tumor cells due to its lipophilic nature (Wesolowski *et al.* 2010). Its primary mechanism of action is to methylate the O6 site of guanine bases leading to mismatching nucleobases during DNA replication causing cells to initiate DNA mismatch repair pathways or undergo cell death (Zhang *et al.* 2012). MGMT (O(6)-methylguanine-DNA methyltransferase) is a DNA repair enzyme that plays a critical role in the repair of alkylated DNA damage. The methylation status of the *MGMT* promoter has emerged as a significant predictor of patient prognosis, where patients with methylated promoters have a better prognosis compared to those with unmethylated MGMT promoter because the methylated promoter leads to lower MGMT expression, and therefore, decreased ability to repair DNA damage. The clinical status of *MGMT* methylation status is determined using a variety of techniques, including methylation-specific PCR, restriction fragment length polymorphism, and next-generation sequencing (NGS). Variable methylation status of *MGMT* in patients and conflicting reports of how well patients respond to TMZ, radiation or both according to the MGMT status confounds the ability of it being a routine clinical decision maker. Therefore, all patients are given the Stupp protocol when appropriate despite limited clinical advantage**.** Despite this, GBM inevitably recurs with majority of tumors recurring within 2cm of the original mass visible by MRI (J Sherriff *et al.* 2013).

Molecular Classification of GBM

There is no single cause for therapy failure in GBM. The complexity and resistance to treatment is partially attributed to cellular and genetic heterogeneity within the tumour and among patients (Davis *et al.* 2019, Qazi *et al.* 2022). The Cancer Genome Atlas (TCGA) attempted to classify GBM into distinct subtypes to better characterize the molecular profiles and predict beneficial treatments for patients (McLendon *et al.* 2008, Verhaak *et al.* 2010). In 2008 using over 200 GBM specimens interrogated by DNA copy number, gene expression, and DNA methylation profiling, TCGA was able to identify the three most common dysregulated signaling networks: Receptor tyrosine kinase (RTK) signaling, p53 signaling, and RB signaling. Of the tumors examined, 74% of GBMs displayed dysregulation in all three pathways suggesting critical roles in tumorigenesis. Together, these pathways show the tight regulation required for healthy cell division and multiple junctures at which breakdowns can occur leading to uninhibited GBM progression.

Receptor tyrosine kinases (RTKs) encompass 20 classes of cell surface receptors with high affinities for several growth factors, cytokines and hormones (Du *et al.* 2018). They play critical roles in regulating cellular processes during normal development but actively contribute to progression of many cancers when mutations lead to activation of signaling cascades causing upregulation and/or downregulation of downstream protein functions (Du *et al.* 2018). Of the GBMs specimens examined for DNA sequencing, 88% displayed somatic alterations in RTK pathways lead by *EGFR* mutations and amplifications, followed by Phosphatidyl Inositol 3 Kinase (PI3K) mutations, and *PDGFRA*

amplifications. Tumor suppressors which inhibit RTK signaling were also identified to be commonly mutated/inactivated, lead by *PTEN* and *NF1* alterations.

Tumor protein P53, also known as “p53”, are critical proteins for conserving genomic stability and preventing tumor formation by regulating gene expression (Mantovani *et al.* 2019). In GBM, 87% of samples exhibited dysfunctional p53 signaling. Amplifications in *MDM2* and *MDM4* (a combined 21% of samples) which inhibit p53 lead to altered p53 activity, while mutations or deletions in *CDKN2A* and *TP53* more commonly lead to inactivation and therefore genomic instability. Altogether, these genomic alterations contribute to GBM progression and survival by avoiding p53 induced cell death (Gomez-Manzano *et al.* 1997).

Retinoblastoma protein (Rb) is another tumor suppressor commonly mutated in several cancers and was identified in 78% of GBMs. Its role is to prevent excessive cell growth by inhibiting cell cycle progression until the cell is ready to divide at which point Rb is phosphorylated to be inactivated. Rb activation occurrs alongside CDK4 amplification in 18% of GBM tumors, while mutations or deletions in *P16/INK4A* and *CDKN2B* were the most common events leading to Rb inactivation (52% and 47% of GBM tumors respectively). The altered function of Rb has several avenues to promote cell cycle progression and drug resistance in GBM (Biasoli *et al.* 2013).

Building on the genomic interrogation of GBMs, transcriptomes were examined and integrated to categorize patients into four manageable subgroups based on gene expression profiles. From this, Classical, Mesenchymal, Proneural and Neural subtypes were established (Verhaak *et al.* 2010).

The Classical subtype was strongly associated with chromosome 7 and 10 alterations, particularly *EGFR* amplifications which corresponded with an increase in EGFR at the RNA level. EGFRvIII mutations were also found in the Classical subtype, where this mutation results in a truncated extracellular domain of the EGFR receptor causing constitutive downstream signaling despite an absence of EGF (Batra *et al.* 1997). Interestingly, despite *TP53* being the most frequently mutated gene in GBM, *TP53* mutations were absent in this population of samples. However, deletion of *CDKN2A* (encoding for both p16INK4A and p14ARF) was commonly associated with the Classical subtype and occurred alongside *EGFR* amplifications. Interestingly, *CDKN2A* deletions were almost mutually exclusive with other alterations of the RB pathway suggesting patients could be stratified into distinct cohorts.

The Mesenchymal subtype was most strongly identified by hemizygous deletion of the chromosome region 17q11.2 which contains the gene *NF1* and subsequently lead to lower transcript levels. Co-mutations of *NF1* and *PTEN* were identified in this GBM subtype, and with both being instrumental in the AKT signaling pathway can potentially be used to stratify patients into cohorts for treatment options. The Mesenchymal subtype also exhibited higher RNA levels of mesenchymal markers such as *CHI3L1/YKL40* and *MET*, previously proposed by Phillips *et al.* 2006 (Phillips *et al.* 2006). Mesenchymal markers (CD44) and tumor necrosis factor super family members and NF-κB pathway members such as *TRADD*, *RELB*, *TNFRSF1A* were highly expressed in this subtype which was attributed to higher overall necrosis and inflammatory infiltrates.

The Proneural subtype was originally suggested to be the subtype with more favorable patient outcomes (Phillips *et al.* 2006). However, this group was

overrepresented by younger patients who can withstand more extensive surgical resections (Carson *et al.* 2007) and point mutations in *IDH1* (now classified as classified as astrocytomas which have longer survival times than GBMs (Louis *et al.* 2021). Beyond this, amplifications in *PDGFR* and mutations in *TP53* more frequently occurred in this subtype. Copy number changes of chromosomes 7 and 10 were less common in Proneural GBMs, although they still occurred in 54% of samples. Other markers included *PIK3CA/PIK3R1* mutations, increased *PDGFRA* and *OLIG2* transcripts, as well as development genes such as *SOX* family members and *TCF4*.

The Neural subtype displayed neuron markers such as *NEFL*, *GABRA1*, *SYT1* and *SLC12A5*. Gene Ontology associated this subtype with neuron projection, and transmission of axons and synaptic junctures. This subtype remains controversial as its presence was later proposed to be the presence of normal neuronal tissue along tumor margins (Wang *et al.* 2017). However, researchers used pathology slides of GBMs and found few normal cells present. Also confounding the data was the two normal brain tissue sample included in the dataset were categorized within the Neural subtype.

This classification system was quickly upended when it was discovered through single cell RNA-sequencing that all subtypes are represented within a single GBM tumor (Patel *et al.* 2014). This finding strengthened the position held by Sottoriva *et al.* in 2013 that geographically distinct regions of the tumour can be classified into different subtypes (Sottoriva *et al.* 2013). Thus, GBMs are dynamic structures, with subtypes varying spatially and temporally within a tumor (Sottoriva *et al.* 2013). A landmark paper by Neftel *et al.* 2019 reinforced the notion that GBM cells exist in four main cellular states but are influenced by the tumor microenvironment to exhibit plasticity (Neftel *et al.* 2019). The

proportion of cells in each state vary between patients and is influenced by copy number amplifications of the *CDK4*, *EGFR* and *PDGFRA* loci, and by mutations in the *NF1* locus.

Another heavily investigated area by researchers is how heterogeneity present within GBMs allow tumors to adapt to stresses, with the therapies acting as selective pressures (Heppner *et al.* 1983). When GBM inevitably relapses, the recurrent tumour can vary greatly from the primary tumour (Kim *et al.* 2015). Recurrence is a term used to describe the state of cancer after it has been treated and the patient was in remission. In the case of GBM, recurrence is almost inevitable with most patients experiencing a return of the cancer between 12 to 15 months after their initial diagnosis (Stupp *et al.* 2009). As mentioned before there are several reasons why GBM has a high rate of recurrence. Not only can the primary and recurrent tumours have distinct genomic profiles, but the therapies themselves can act as bottlenecks to drive the emergence of treatment-resistant sub-clones, no longer having mutations in the recurrent tumour that originally drove the primary tumour (Johnson *et al.* 2014). Due to the wide spectrum of patient phenotypes and a continually evolving genetic landscape, the requirement for precision medicine becomes more urgent as the intricacies of GBM become more evident.

Section 2

Stem Cells

Stem cells are specialized cells unique to multicellular organisms and since their discovery have become critical to our understanding of developmental biology, aging, and normal functioning of cells and tissues in the body (Poliwoda *et al.* 2022). Stem cells are considered to be "undifferentiated" or "pluripotent", meaning that they have the ability to

develop into many different cells types, including bone cells, nerve cells and skeletal muscle cells (Poliwoda *et al.* 2022). Stemness refers to the defining characteristic of stem cells that enable them to differentiate into various types of cells or to self-renew (Aponte *et al.* 2017). Stemness can be measured in several ways, including the expression of certain genes that are the fundamental molecular drivers regulating the balance between two cell fates (Cai *et al.* 2004). Stemness can also be measured by the capacity of cells to form colonies or spheres *in vitro*, the ability to differentiate into multiple cell types when induced, or a distinctive set of epigenetic modifications such as specific patterns of DNA methylation and histone modification (Cai *et al.* 2004, Wu *et al.* 2006).

There are two main types of stem cells: embryonic stem cells and adult stem cells. Embryonic stem cells are derived from the inner cell mass of the blastocyst, a structure that forms in the early stages of embryonic development (Zakrzewski *et al.* 2019). These cells are pluripotent, meaning they can differentiate into any cell type of the body. Adult stem cells on the other hand are “multipotent”, meaning they are more limited in their ability to differentiate into specific cell types based on the tissue they are found (Zakrzewski *et al.* 2019). Stem cells can be found in all regions of the body such as embryonic and fetal tissues, umbilical cord blood, and bone marrow (Zakrzewski *et al.* 2019). In the brain, neural stem cells (NSCs) can be found in the subgranular zone of the hippocampus, and the ventricular-subventricular zone around lateral ventricles (Bond *et al.* 2020).

Embryogenesis refers to the process by which a single cell called the zygote, a human’s original totipotent stem cell, transforms into a complex multicellular entity capable of generating all the different cell types and tissues of an individual (Zhai *et al.*

2022). During embryogenesis, the process initiates with fertilization, in which the sperm and egg fuse to form a single cell (the zygote) (Zhai *et al.* 2022). This cell undergoes a series of rapid cell divisions which results in the formation of a sphere of cells called the blastomere (Zhai *et al.* 2022). The blastomere then undergoes a process known as gastrulation, in which the cells begin to differentiate into the three primary germ layers: the ectoderm, mesoderm, and endoderm (Zhai *et al.* 2022). The ectoderm gives rise to the skin, hair, nails, and nervous system, while the mesoderm gives rise to the skeleton, muscles, and circulatory system (Cao *et al.* 2013). The endoderm gives rise to the lining of the digestive and respiratory tracts, as well as the liver and pancreas (Yiangou *et al.* 2018). The formation of these three germ layers is a critical step in embryonic development, as it lays the foundation for the subsequent formation of tissues and organs.

iPSCs and Yamanaka Factors

Induced pluripotent stem cells (iPSCs) are a type of stem cell that are generated by engineering a differentiated cell, such as a skin cell, to display stemness with a high degree of potency. This was first conducted by Dr. Shinya Yamanaka and his team in 2006 whereby mouse fibroblasts were induced to express four transcription factors (OCT4, SOX2, KLF4 and c-MYC) since called “Yamanaka factors” (Takahashi *et al.* 2006). Yamanaka factors regulate a delicate balance of gene expressions that are responsible for determining cell fates. Inducing their function reprograms a mature cell into an iPSC (Takahashi *et al.* 2006). When cells expressing all four factors were subcutaneously transplanted into nude mice, resulting tumours contained tissues from all

three germ layers observed in embryonic development (Takahashi *et al.* 2006). Findings were later replicated in human cells (Takahashi *et al.* 2007, Yu *et al.* 2007).

Formation of the Brain and Rise of SOX2

The formation of the brain during embryogenesis is a complex and highly regulated process that involves the coordinated expression of thousands of genes and the establishment of specific patterns of gene expression. From the ectoderm, the neuroectoderm arises, followed by differentiation into the neural plate and the neural crest, which goes on to form the peripheral nervous system (Elshazzly *et al.* 2022). Another critical event in embryogenesis is the formation of the notochord, a structure that provides a scaffold for the formation of the neural tube (Elshazzly *et al.* 2022). This neural tube eventually differentiates into the brain and spinal cord and is critical for the normal development of the CNS (Elshazzly *et al.* 2022). Most notably among these processes, SOX2 is the Yamanaka Factor to take most direct control of neural stem cells and is crucial for the maintenance of their pluripotency, and formation of neural progenitor cells that will go on to generate neurons and glia of the CNS (Kopp *et al.* 2008). The spatial organization of these different structures is the result of gradients of a variety of growth factors leading to highly coordinated signaling pathways, including the Wnt, Hedgehog, and TGF-beta pathways (Gurdon *et al.* 2001).

SOX2 (SRY-box 2) belongs to the SOX family of transcription factors, which are characterized by the presence of a high-mobility-group (HMG) DNA-binding domain (Schepers *et al.* 2002). Functional SOX2 is critical for inner cell mass development of embryos particularly by regulating ectodermal commitment and neuroectodermal

differentiation (Avilion *et al.* 2003, Kopp *et al.* 2008). Its regulation of gene expression is important for the proper specification and differentiation of various cell types, including neural stem cells (Kopp *et al.* 2008). Its ability to be a master regulator of gene transcription is found in its ability to be a pioneer transcription factor, meaning it can bind to nucleosome DNA in a closed chromatin structure to initiate chromatin opening (Dodonova *et al.* 2020). Recruitment of chromatin remodeling complexes such as coactivators can greatly increase the rate of transcription of a gene or set of genes in a highly specific manner (Wegner *et al.* 2010). Coactivators may have histone acetyltransferase (HAT) activity to weaken the association of histones to DNA by acetylating the N-terminal histone tail (Bannister *et al.* 2011). This provides more space for the transcription machinery to bind to the promoter which increases DNA accessibility and subsequent transcription.

SOX2 plays a key role in the biology of NSCs beyond embryogenesis into the developed adult brain. SOX2 regulates self-renewal and differentiation of NSCs by interacting with other transcription factors to modulate transcription rates of genes involved in processes such as responses to environmental stressors (Wegner *et al.* 2010). For example, SOX2 has been shown to regulate the cell cycle, specifically inhibiting cyclin-dependent kinase inhibitors to prevent NSCs undergoing cell division (Marqués-Torrejón *et al.* 2013). SOX2 has been shown to respond to injury and disease such as strokes, where it promotes the regeneration of neurons and glia (Lin *et al.* 2015). Further research in this area may provide important insights into the regulation of NSC biology and may lead to the development of new therapies for a variety of diseases and injuries of the CNS.

Glioblastoma Stem Cells

Stemness can also be used to measure and define a restricted population of cells in GBM called Glioblastoma Stem Cells (GSCs). Cancer stem cells were first proposed in 1997 in acute myeloid leukemia (Bonnet *et al.* 1997). Cancer stem cells share several characteristics with healthy stem cells, particularly the ability to self-renew a phenocopy of itself and give rise to a diverse range of differentiated cell types, which go on to produce the bulk of the tumor (Reya *et al.* 2001). Therefore, since these cells are credited with driving tumor growth and generating the heterogeneity of GBMs, understanding their biology and targeted elimination has been an intense area of focus in research.

SOX2 is expressed at high levels in several types of cancer, including GBM and used as a marker of GSCs (Gangemi *et al.* 2009). It is involved in the response to various environmental signals such as oxidative stress initiating autophagic response to withstand metabolic stresses, chemotherapy and radiotherapy (Wang *et al.* 2013). SOX2 has been shown to regulate the expression of genes involved in the regulation of cell cycle, cell migration and invasion, and resistance to apoptosis of GBM (Bulstrode *et al.* 2017, Alonso *et al.* 2011, Ferletta *et al.* 2011). Because SOX2 has been shown to be critical in maintaining tumorgenicity in GBM, developing therapies to selectively inhibit its activity has been an enticing option for researchers (Gangemi *et al.* 2009, Schmitz *et al.* 2007, Garros-Regulez *et al.* 2013). While more research is needed to fully understand the complex role of SOX2 in GBM, targeting this transcription factor has strong potential.

CD133, also known as Prominin-1, is a transmembrane protein first identified in 1997 as a marker for hematopoietic stem cells (Yin *et al.* 1997, Miraglia *et al.* 1997). Since then it has been used to as a marker of various types of stem cells including NSCs and

GSCs (Peh *et al.* 2009, Singh *et al.* 2004). The overlap of CD133 biology in normal stem cells and cancer has been shown in various types of cancer, including GBM as well as hepatocellular carcinoma and colon cancer (Glumac *et al.* 2018). In GSCs, CD133 expressing cells (CD133+) have been associated with greater proliferation, invasion, and resistance to therapies compared to their non-expressing (or CD133-) counterparts (Singh *et al.* 2004, Wang *et al.* 2018, Bao *et al.* 2006, Liu *et al.* 2006). CD133+ GSCs are suspected of causing tumor relapse once the therapeutic pressure has been removed (Tamura *et al.* 2013). This has made CD133 a valuable target for the development of new cancer therapies in a variety of modalities. Researchers have developed small molecules that specifically inhibit CD133+ cells growth (Venugopal *et al.* 2015). Clinical trials are underway to determine the efficacy of CD133 targeted therapies in the treatment of tumors (Wang *et al.* 2018) but more research is needed to fully understand its role in the biology of this aggressive cancer.

While the co-expression of SOX2 and CD133 has previously been shown, the association has been correlative without establishing a direct biological interaction (Song *et al.* 2016, Lv *et al.* 2018, Guerra-Rebollo *et al.* 2019). Establishing a physical interaction could help deconvolute their molecular functions and may be invaluable to both cancer and stem cell biology.

Section 3

CRISPR and Genetic Screens

CRISPR (Clustered Regularly Interspaced Short Palindromic Repeats) is a powerful tool developed in the early 2010s for editing the genome of prokaryotes and

eukaryotes alike (Jinek *et al.* 2012, Ran *et al.* 2013). It has revolutionized the field of genetics, enabling researchers to make precise incisions to the genome with unprecedented speed, accuracy and cost effectiveness compared to earlier technologies (Wiedenheft *et al.* 2012). CRISPR works by exploiting the natural defense mechanisms of certain bacteria to protect themselves from viral infections (Jinek *et al.* 2012). When a bacterium is infected by a virus, it retains a piece of the virus's DNA and incorporates it into its own genome as a CRISPR sequence for future reference, reminiscent of a human's adaptive immune system utilizing antibodies (Wiedenheft *et al.* 2012). The CRISPR system consists of two main components: a guide RNA (gRNA) and a Cas nuclease (Pickar-Oliver *et al.* 2019). The gRNA is a small RNA molecule that is complementary to the target DNA sequence and guides the Cas enzyme to the precise location in the genome where the cut is made. There have been several Cas enzymes identified, each with its own unique functions and properties which can be exploited by scientists (Pickar-Oliver *et al.* 2019).

CRISPR screens are a powerful tool for identifying the genetic interactions that contribute to a disease of interest or biological process such as drug resistance (Shalem *et al.* 2014). There are several different types of CRISPR screens, including knockout screens which involve the complete inactivation of a gene, or activation screens to increase activity of genes (Boettcher *et al.* 2015). These have replaced siRNA screens because of the more dramatic biological effects of complete elimination of gene function with CRISPR rather than decreased RNA levels of siRNA, and the more targeted elimination of individual genes compared to homologous RNA transcripts (Boettcher *et*

al. 2015). CRISPR screens can be performed in a variety of cell and animal models, including cultured cells, zebrafish, mice and others (Bock *et al.* 2022).

A CRISPR screen is conducted by first synthesizing a library of gRNAs complementary to the target DNA sequences (Bock *et al.* 2022). When the gRNA library is introduced into the cell or animal model, the Cas enzyme is guided to the precise location in the genome to eliminate gene activity (Bock *et al.* 2022). Following this, the cells or animals are subjected to a particular experimental condition where the effect of the gene in relation to the phenotype is measured, and the genes that are essential for the phenotype are identified (Bock *et al.* 2022). CRISPR screens have been used to identify the genetic factors that underlie a wide variety of biological processes and diseases, including development, immune function, cancer and drug resistance (Bock *et al.* 2022).

Section 4

Tumor Microenvironment and Immune Components

GBM is an “immune cold tumor”, meaning it is not very immunogenic. This is due to the tumor immune microenvironment (TIME) in GBM which consists of complex interplay between tumour cells, immune populations within the tumour, and other abiotic factors (Dapash *et al.* 2021). The TIME can influence the development and progression of GBM in several ways. For example, certain immune cells such as T cells can recognize and attack cancer cells, while myeloid immune cells such as macrophages promote cancer cell survival and growth in certain instances (Ravi *et al.* 2022). The influence of each immune population is determined by their abundance and presence of their

signaling molecules such as cytokines and chemokines to regulate the intercommunication of cells which plays a critical role in the development and progression of GBM in patients (Ravi *et al.* 2022).

The hypoxic niche in GBM refers to areas within the tumour that have low levels of oxygen (Park *et al.* 2022). Hypoxia is a common feature of solid tumors and can have several important effects on cancer cells and the TIME (Park *et al.* 2022). In GBM, hypoxia has been linked to both the development of cancer stem cells and resistance to therapy (Kolenda *et al.* 2011). Hypoxia has also been shown to promote the production of angiogenesis factors to stimulate the formation of new blood vessels and support the growth of the tumor (Nicolas *et al.* 2019). The lack of oxygen in GBM is also a source of immune evasion, as hypoxia can inhibit the function of immune cells such as T cells and promote the recruitment of immune suppressive cells, such as myeloid derived suppressor cells (MDSCs) and tumor associated macrophages (TAMs) (Park *et al.* 2021, Guo *et al.* 2016). Targeting the hypoxic niche in GBM is a promising approach for the treatment of this cancer (Tatari *et al.* 2022).

Tumor-infiltrating lymphocytes (TILs) are immune cells, specifically T cells and natural killer (NK) cells that have penetrated the TIME (Maddison *et al.* 2021, Liu *et al.* 2016, Sonmez *et al.* 2022). TILs are often present at low levels and have been shown to have a limited ability to recognize and attack GBM cells (Liu *et al.* 2016, Sonmez *et al.* 2022). The proportion of TILs in GBM has been correlated with patient prognosis and response to treatment with conflicting results although the mechanisms underlying these associations require further exploration (Han *et al.* 2014, González *et al.* 2020, Lohr *et al.* 2014). Enhancing the infiltration and function of TILs in the TIME is a promising approach

for the treatment of GBM and other types of cancer (Zhenjiang *et al.* 2014, Nguyen *et al.* 2014). Overall, TILs play a critical role in the immune response to cancer and are an important avenue for the development of new cancer therapies.

MDSCs are a heterogeneous population of cells that include immature myeloid cells, such as monocytes and neutrophils, as well as more mature myeloid cells such as macrophages and dendritic cells (Chai *et al.* 2019, Dubinski *et al.* 2016). They are present at elevated levels in the blood and tumors of GBM patients and are characterized by their ability to inhibit the activation and function of T cells, which are important for the immune surveillance and defense against GBM (Chai *et al.* 2019). MDSCs can be activated by a variety of stimuli, including inflammation and exposure to cancer-derived factors (Dubinski *et al.* 2016). The role of MDSCs in GBM is complex and not yet fully understood. They have been shown to exhibit varying biology in a context-dependent manner in GBM (Bayik *et al.* 2020). For example, MDSCs have been shown to promote GBM growth and angiogenesis but have also been shown to have anti-tumor effects by promoting the differentiation of T cells into anti-tumor effector cells (Lakshmanachetty *et al.* 2021). Inhibiting the activation and expansion of MDSCs or reprogramming them to adopt an anti-tumor phenotype is a viable strategy in cancers but indications are only in preliminary stages (Peng *et al.* 2022, Chen *et al.* 2021).

TAMs and microglia are immune cells also present within the TIME (Yin *et al.* 2017). TAMs are a type of macrophage that have infiltrated the tumor and can either have pro-tumor or anti-tumor functions depending on their activation state and the signals they receive (Yin *et al.* 2017). In contrast, microglia are a type of immune cell that reside within the CNS and are important for the immune surveillance and defense of the CNS (Yin *et*

al. 2017). Because TAMs and microglia constitute a large percentage of GBM populations, targeting them with drugs or other therapies is a promising approach to reduce the size of GBMs and alleviate the immunosuppressive microenvironment (Fu *et al.* 2020, Wang *et al.* 2022). Blocking the activation of TAMs or reprogramming them to adopt an anti-tumor phenotype has been shown to be effective in preclinical models of GBM with multiple clinical trials underway (Wang *et al.* 2022).

Advances in Immunotherapy and Chimeric Antigen Receptor (CAR) T Cells

Immunotherapy is a type of cancer treatment that seeks to harness the power of the immune system to fight cancer. Immune checkpoint blockade has made great strides in treating an assortment of solid tumors, even winning the 2018 Nobel Prize in Physiology and Medicine (Fennell *et al.* 2021, Topalian *et al.* 2014, Huang *et al.* 2019). Several studies have shown neoadjuvant blockade of Programmed cell death protein 1 (PD1) can modulate the GBM microenvironment to enhance anti-tumor responses, elevate expression of chemokines, increase immune cell infiltrates including more diverse T cell receptor clonality (Peng *et al.* 2012, Lee *et al.* 2021). Clinical trials have provided tantalizing results for clinicians and patients alike in small settings but the benefit in larger settings remains to be seen indicating single agent therapies (monotherapies) are unlikely to provide relief in the near future (Cloughesy *et al.* 2019, Reardon *et al.* 2020, Ahmad *et al.* 2019). Recent and ongoing clinical trials are attempting to develop new regimens to combine immunotherapies with existing SoC, but unfortunately are not achieving significantly improved progression free survival or overall survival (BMS *et al.* 2019a,

2019b). One confounding factor is the use of corticosteroids such as dexamethasone to reduce cerebral edema leading to a weakened immune response (Yang *et al.* 2021).

While antibodies and bi-specific T-cell engager (BiTE) modalities are advantageous over other methods of intervention due to their lower cost and "off the shelf" availability, their effectiveness and persistence lack compared to cell therapies (Subklewe *et al.* 2021). Adoptive cell transfer (ACT) therapy using T cells, where T cells are expanded *ex vivo* and then infused back into a patient have shown promising results in clinical trials for cancers (Zacharakis *et al.* 2018). Chimeric antigen receptor (CAR) T cells (CAR-Ts) are a form of ACT therapy, which involves genetically modifying T cells to express a CAR, which is a protein designed to recognize and bind a specific antigen on the surface of cancer cells (Subklewe *et al.* 2021). CAR-Ts can be administered in as little as a single dose (Subklewe *et al.* 2021). Target specificity is critically important for CAR modalities because once infused into the patient the cells are capable of freely traversing the entire body of the patient (Benmebarek *et al.* 2019). When the antigen of interest is engaged, CAR-Ts will produce perforin and granzyme B to lyse the cancer cells along with an upregulation of inflammatory markers such as IFN-gamma and TNF-alpha to recruit additional immune cells (Benmebarek *et al.* 2019). Provided the target is cancer specific, CAR-Ts will pass over healthy tissue without engaging or causing tissue damage (Benmebarek *et al.* 2019). This modality has been particularly successful in hematological cancers as the approved medications Carvykti against BCMA in multiple myeloma and Kymriah against CD19 in acute lymphoblastic leukemia show (Berdeja *et al.* 2021, Schuster *et al.* 2019). However, tumor regression and patient safety of CAR-Ts or other cell therapies against GBM tumors has yet to be proven to the same degree (Brown *et al.*

2015, Brown *et al.* 2016, O'Rourke *et al.* 2017, Liu *et al.* 2023). CAR-T cells can also have significant side effects including cytokine release syndrome (CRS) which is a systemic inflammatory response that causes severe symptoms and neurotoxicity (Cai *et al.* 2020). This can affect the function of the central nervous system and ultimately lead to death if not controlled (Cai *et al.* 2020).

The first generation of CAR-T cells (or first-generation CARs) were introduced in the early 1990s (Eshhar *et al.* 1993). These CAR-Ts contained a single-chain antibody that was fused to the T cell receptor designed to recognize a tumor associated antigen and when engaged, activated the T cell to lyse cancer cells in a non-major-histocompatibility-complex-restricted manner (Eshhar *et al.* 1993). This approach was effective in killing cancer cells *in vitro* but was limited by low persistence (Tomasik *et al.* 2022). Subsequent generations of CARs have incrementally improved aspects of anti-tumor activity, persistence in the body, and safety by including the use of multiple signaling domains, co-stimulatory domains, and the incorporation of additional effector functions (Tomasik *et al.* 2022). Fourth-generation CAR-Ts, the latest to be tested in human trials, are designed to target multiple antigens on cancer cells to provide a more comprehensive approach to tumor killing and incorporate advanced safety mechanisms to ensure the CAR-T cells can be rapidly eliminated in the event of severe side effects such as neurotoxicity (Tomasik *et al.* 2022). Fourth-generation CAR-Ts are still in development, but early results clinical trials are encouraging (Duan *et al.* 2021).

Section 5

Glycoprotein Non-Metastatic Melanoma Protein B

Glycoprotein non-metastatic melanoma protein B (GPNMB) is a transmembrane protein overexpressed in several types of cancer, including GBM (Kuan *et al.* 2006). In GBM, high levels of GPNMB have been linked to a more aggressive and treatment-resistant phenotype and to a worse prognosis for patients (Rich *et al.* 2003, Feng *et al.* 2020). GPNMB has been shown to play a role in the migration and invasion of cancer cells, as well as in the suppression of the immune response to cancer (Rich *et al.* 2003, Kobayashi *et al.* 2019). High levels of GPNMB have been linked to inhibition of the differentiation of T cells into anti-tumor effector cells and contribute to an immunosuppressive environment (Xiong *et al.* 2022, Kobayashi *et al.* 2019). GPNMB has also been shown to be upregulated along with the expression of immune checkpoint molecules, such as PD-L1 which can inhibit the immune response to cancer or inhibit T cells directly through binding with Syndecan-4 (Chung *et al.* 2019, Chung *et al.* 2007).

Reasons are yet to be elucidated for why GPNMB localizes to the extracellular membrane of GBM cells. In triple negative breast cancer heat shock protein 90 (HSP90) dysregulation causes lysosome membrane fusion with the plasma membrane, causing an accumulation of GPNMB to be targetable to antibody therapies (Biondini *et al.* 2022). Strategies to target GPNMB have centered around monoclonal antibodies to block GPNMB function, or antibody-drug conjugates (ADCs) to kills cancer cells (Kuan *et al.* 2010, Chung *et al.* 2019, Keir *et al.* 2012).

Attempts to target GPNMB with ADCs rely on the dileucine motif in the cytoplasmic tail which is commonly associated with functions such as rapid receptor internalization

(Bonaficino *et al.* 2003). In the quail ortholog of GPNMB, if either leucine residue is mutated, GPNMB is retained at the plasma membrane (Le Borgne *et al.* 2001). Glembatumumab Vedotin ("GV" or known as CDX-011 or CR011-vcMMAE) as an ADC has been in clinical trials for recurrent osteosarcoma, melanoma and breast cancer (Kopp *et al.* 2019, Ott *et al.* 2019, Yardley *et al.* 2015). GV is a fully human monoclonal antibody against the extracellular domain of GPNMB combined with a highly potent anti-mitotic agent called monomethyl auristatin E (MMAE) (Pan *et al.* 2015). When internalized, the valine-citrulline linker within cellular endosomes, freeing the MMAE toxin to inhibit β-tubulin and microtubule structure, causing death (Tse *et al.* 2006). Although GV has not been tested in CNS tumors, the clinical relevance for developing immunotherapies against GPNMB in a variety of cancers is a viable option with human clinical trials already setting precedent.

In GBM, targeting GPNMB could prove fruitful because expression is displayed by cancer cells and certain MDSCs of the immunosuppressive microenvironment. Macrophages exposed to GBM conditioned media increased expression of GPNMB along with a distinct profile of TAMs (Solinas *et al.* 2010, Szulzewsky *et al.* 2015) indication a conditional expression pattern. Simply put, macrophages can be polarized into different functional subsets depending on the microenvironment with the two main subsets being M1 and M2 macrophages degerming their responses to inflammation (Orecchioni *et al.* 2019). M1 macrophages are pro-inflammatory and are involved in host defense against pathogens, while M2 macrophages are anti-inflammatory and involved in tissue repair where GPNMB has previously been implicated (Silva *et al.* 2018). Therefore, understanding the role of GPNMB in macrophage function may provide insights into how

GBM progresses and potential intercommunication between tumor cells and immune cells. From this, novel therapeutic strategies can be developed to exploit unique biological processes of cancer.

Chapter 2: A Novel SOX2-STAGA(like) Transcription Factor Complex Regulates CD133 and Stemness in Glioblastoma Stem Cells

Preamble

In this chapter, I present an original manuscript describing functional genetic regulators of CD133 and stemness in glioblastoma using genome-scale CRISPR-Cas9 screening and a series of validation experiments:

Savage, N., Chokshi C., Custer S., Danis E., Venugopal, C., Brown, K. R., Moffat, J., & Singh, S. K. A Novel SOX2-STAGA(like) Transcription Factor Complex Regulates CD133 and Stemness in Glioblastoma Stem Cells.(manuscript in preparation)

Author contributions are as follows for the aforementioned manuscript: Conceptualization: N.S, S.K.S, J.M, and C.C; Resources: S.K.S, and J.M; Methodology, Investigation and Validation: N.S, and S.C; Software and formal analysis: C.C, E.D, K.R.B; Visualization: N.S, C.C, E.D, C.V; Writing – original draft preparation: N.S; Writing – review and editing: N.S, C.C, S.C, E.D, C.V, K.R.B, J.M, S.K.S; Project administration and supervision: S.K.S and J.M; Funding acquisition: S.K.S and J.M. All authors read and approved the manuscript.

I present data summarizing our findings from the genome-wide CRISPR-Cas9 screens. Together, we explore the functional drivers of CD133 and stemness in patient-derived GBM models and uncover novel interactions. These analyses map the

overlapping biology between healthy neural stem cells and cancerous glioblastoma stem cells. Mechanistically, eliminating SOX2 and histone acetyltransferase components reduces CD133 levels due to general transcription machinery no longer being recruited to the promoter region of *PROM1* for efficient gene transcription.

Abstract

Functional genomics was empowered by CRISPR to scale genome-wide screens to determine how phenotypes of interest arise. CD133, a pentaspan transmembrane glycoprotein encoded by *PROM1*, is the most used surface marker to identify cancer stem cells. However, its function is still unknown, and regulation remains undetermined. Using patient derived glioblastoma stem cells we conducted a large-scale loss-of-function phenotypic screen using CRISPR-Cas9 to identify regulators of CD133. We validated SOX2 as a direct transcription factor binding to *PROM1*. These findings further show the untapped potential of CRISPR screens to uncover new biological insights into phenotypes of interest. These findings may have broader implications for the fields of stem cells and cancer biology.

Introduction

Glioblastoma (GBM) is a highly aggressive form of brain cancer that is often resistant to current therapies, making it difficult to effectively treat and manage (Louis *et al.* 2021). Its dismal prognosis is attributed to Glioblastoma Stem Cells (GSCs) that possess the ability to self-renew and differentiate into multiple cell types which can contribute to tumor growth and recurrence. GSCs can be identified by the surface marker CD133, a pentaspan-transmembrane glycoprotein, and have been shown to be the chemo- and radio-therapy resistant population (Singh *et al.* 2004, Bao *et al.* 2006, Liu *et al.* 2006). Therefore, CD133 has been considered a promising target for the development of novel therapies for GBM (Venugopal *et al.* 2015, Vora *et al.* 2020). Herein, we define CD133+ populations as cells with the detectable AC133 epitope (Campos *et al.* 2011). One potential approach to improving patient outcomes is to identify specific regulators of GSCs, as targeting their regulators may provide a means of selectively targeting and eliminating the cancer cells.

Clustered Regularly Interspaced Short Palindromic Repeats (CRISPR) is a powerful genome editing tool that can be used to manipulate targeted genes and identify specific involvement in the development of a wide range of biological processes (Ran *et al.* 2013). Genome-wide CRISPR screens are a high throughput tool capable of analyzing the role of thousands of genes in complex biological systems, where genes can interact with one another to regulate a particular phenotype including the maintenance of GSCs (Shalem *et al.* 2014). The results of these screens can provide valuable insights into underlying molecular mechanisms and help to identify new therapeutic targets for cancer.

SRY (sex determining region Y)-box 2, commonly known as SOX2 is a transcription factor that has been extensively studied in stem cell populations (Novak *et al.* 2020). SOX2 is a member of the SOX family of transcription factors, which play key roles in embryonic development and stem cell maintenance(Novak *et al.* 2020). In GSCs, SOX2 has been shown to be involved in self-renewal, differentiation, and cell survival (Gangemi *et al.* 2009). Studies have demonstrated that SOX2 is often overexpressed in GBM and that increased expression of SOX2 correlates with a more aggressive tumor phenotype and a worse prognosis for patients (Berezovsky *et al.* 2014). SOX2 regulates the biology of GSCs through associations with other signaling pathways and transcription factors such as Wnt and Notch pathways, to regulate stem cell self-renewal and differentiation (Berezovsky *et al.* 2014). Additionally, SOX2 has been shown to interact with other transcription factors, such as Oct4 and Nanog, to regulate the expression of key stem cell genes (Lopez-Bertoni *et al.* 2015, Bradshaw *et al.* 2016. Understanding the role of SOX2 in GSCs is an important dimension to the development of new therapies for GBM.

Activity of transcription factors is regulated by complex networks of interactions with other proteins such as the availability of cofactors that are necessary for efficient gene transcription (Stallcup *et al.* 2020). Histone acetyltransferases (HATs) are a group of enzymes that catalyze the transfer of an acetyl group from acetyl-CoA to specific lysine residues on histones, which are proteins that help package and compact DNA into the nucleus of a cell (Marmostein *et al.* 2014). This process, known as histone acetylation, leads to the relaxation of the chromatin structure and the promotion of gene transcription, the first step in the synthesis of a functional RNA molecule (Marmostein *et al.* 2014).

Therefore, coactivators could provide promising therapeutic targets in the treatment of cancer.

Here we use fluorescence-activated cell sorting, the gold standard for isolating antibody-labelled cells of interest, to compare CD133+ and CD133- populations of GSCs to identify the most critical regulators of stemness.

Results

Identifying Regulators of CD133 Surface Expression

Patient derived GSC lines established in our lab were characterized by flow cytometry for CD133 surface expression with three of the highest expressing lines being expanded for functional assays (Figure 1A). Cells were sorted into CD133+ and CD133- populations to assess their ability to self-renew, or form secondary spheres (Figure 1B, left) and proliferate (Figure 1B, right). In all patient samples, the CD133+ population exhibited greater self-renewal capacity ($p<0.001$) and proliferation ($p<0.0001$). As BT935 displayed the highest surface expression of CD133 (the phenotype of interest), it was expanded to sufficient numbers to conduct a genome-wide CRISPR/Cas9 dropout screen using the Toronto Knockout Library version 3 (TKOv3)(Figure 1C). A low multiplicity of infection (MOI=0.3) was used to ensure single viral integrations per cell while non-transduced cells were eliminated using puromycin. 30 million transduced GSCs were plated in triplicate, translating to a 400+ representation per sgRNA in each replicate to ensure accuracy, efficiency, and scalability of our findings. GSCs were propagated for a total of twelve doublings when an unsorted bulk population of cells was sampled for sequencing while the remaining cells were sorted using flow cytometry into the top and bottom 5th

percentiles of CD133 surface expression. Approximately 4-5 million cells were collected in each group. The screen was deemed successful once sequencing reads were aligned and quality was assured by confirming essential genes dropped out with a high precision-recall (Figure 1D,E).

DrugZ analysis was used to rank genes according to phenotype-genotype interactions and distribution of sgRNAs between groups showed positive correlations between groups, with the greatest discrepancy being between the AC133-high vs. AC133-low cohorts (Figure 2A). As the phenotype the genome-wide CRISPR screen was based on was AC133 surface expression, it was important to have the *PROM1* gene as a highly ranked negative interaction hit, which successfully occurred as it was the top gene ranked of negative regulators (Figure 2B). Comparing the AC133-high population to AC133-low population, twelve genes met a stringent FDR <5% cutoff for negative interactions with relation to the CD133 surface expression, while one gene was detected for positive interactions (Figure 2C).

To validate our dataset further, we performed gene set enrichment analysis (GSEA) with our top hits and found several morphogenic processes including netrin activated signaling, glial differentiation, kidney epithelial differentiation and developmental cell division (Figure 2D). Strikingly, the strong statistical significance of STAGA/SAGA acetyltransferase components *TADA1* and *TADA2B* (#3 and #4 respectively in our DrugZ ranking) was of interest, due to their relatively unexplored association with embryonic stem cell regulation. Because our strict parameters analyzing the CRISPR screen resulted in a short list of gene candidates, we employed the STRING network to identify protein-protein interactions of our top 50 ranked genes (Figure 2E). Several components

of transferase complexes were highlighted, including TADA1 and TADA2B. Their indirect yet overlapping association with SOX2 and FBXW7 in embryonic stem cells lead us to the conclusion of a previously undefined transcription factor complex in glioblastoma stem cells. SOX2 is a well-defined transcription factor in GBM, but the direct involvement of SOX2 and CD133 in GSCs remains correlative rather than interactive.

Validating SOX2 as a Regulator of Stemness and CD133 Levels

Two sgRNA sequences per gene and one AAVS1 control (17 total) were individually ligated into plasmid backbones to validate their roles in regulating CD133 and stemness. For practical reasons, the gene candidates were limited to include CUX1 (the only positive interaction) and top seven negative interaction genes, using SOX2 as a cutoff because of its high RNA levels in GBM (Supplementary 1A) and well-known involvement in stemness of GSCs. The high expression of *SOX2* in brain tumors was also of interest for its localized expression levels Supplementary 1B). The total proportion of CD133+ cells in GSC populations was measured in biological triplicate (Figure 3A, Supplementary 1C) and the Mean Fluorescence Intensity (MFI) was also analyzed (Figure 3B, Supplementary 1D). *PROM1* knockouts predictably displayed the greatest reduction in both phenotypes. Surprisingly, SOX2 knockouts displayed a greater reduction on CD133 surface expression compared to other genes ranked higher in the DrugZ ranking, an observation consistent among all examined GSC lines. Of note, while the CD133% or MFI of BT935 could not reasonably be expected to rise higher than AAVS1 controls, levels were raised for certain genes in BT954, the naturally lowest expressing cell line tested.

Next, the influence of each gene knockout over whole cell CD133 protein levels was investigated by western blot (Figure 3C, Supplementary 2E) and normalized to AAVS1 levels. Again, eliminating *PROM1* functionally lead to the greatest decrease in total CD133 protein with SOX2 also displaying dramatic decreases. While CD133 surface expression (percent and MFI) did not decrease as dramatically as western blot levels, we attribute this to the CRISPR screen being conducted over the course of one month while validations only lasted 7 to 12 days between sgRNA transduction and experimental readouts. We suspect CD133 present at the cell surface at the time of transduction would have remained after the genes of interest were knocked out. Additionally, validations were conducted using pooled knockouts instead of deriving clones which could yield more dramatic changes.

Finally, standard *in vitro* assays were conducted in all cell lines to examine the role of each gene relating to stemness independent of CD133 expression. This was done by measuring the ability of GSCs to self-renew (Figure 3E, Supplementary 1G) and proliferate (Figure 3F, Supplementary 1H). The role of each gene regarding experimental readouts varied among cell lines. *KEAP1* knockouts exhibited reduced self-renewal and proliferation in BT935 while similar effects were not consistent in BT954 or MBT103. *SIAH1* and *FBXW7* knockouts showed significant ablation of self-renewal in BT935 and BT954 but not MBT103 despite marked reductions in proliferative capacities. In addition to SOX2, the most consistent impact on stemness was exhibited by TADA1 and TADA2B. Knockouts significantly decreased self-renewal and proliferation across all cell lines indicating an influential role in regulating stemness of GSCs. Confirmation of knockouts in all gene targets were validated using western blots (Supplementary 2A).

Mapping SOX2 Transcriptional Regulation Within Glioblastoma Stem Cells

Studies have shown SOX2 contributes to tumor relapse and therapy resistance in GBM while not being upregulated in recurrent GBM, suggesting that underlying mechanisms are not fully understood. SOX2 is upregulated in GBM relative to normal brain tissue (Figure 4A). Our screen was conducted in the context of stem cell enriching media without therapeutic pressures applied. In this context, we next validated the correlative trend of reduced CD133 protein with SOX2 knockouts across multiple cell lines (Figure 4B) with a commercial antibody compatible for CUT&RUN. An improvement of CUT&RUN over ChIP-seq is that the global chromatin profiling occurs *in situ* and provides high resolution in a time-efficient manner. Because the antibody is allowed to bind to the protein in its native state inside the cells without lysing the cells or sheering the chromatin, targeted DNA sequences are released into the supernatant to be collected and sequenced (Figure 4C). After successful alignment of reads with genome-wide mapping in our H3K4me3 samples (positive control) and few peaks called in our non-binding antibody samples (negative control) we determined SOX2 binds in the first intron of PROM1 (Figure 4F).

Discussion

At present, cancer research is focused on several key areas including understanding the genetic and molecular drivers of cancer and exploring innovative treatment options. Despite their differences, there is a growing body of evidence showing similarities of GSCs and NSCs. In this study, we examined the molecular regulators of the stem cell marker CD133 in GSCs. We first examined its variable expression among patients and their primary cell lines. Consistently, the CD133+ population exhibited higher rates of self-renewal and proliferation compared to their CD133- counterparts. Using our highest CD133-expressing GSC line we conducted a genome-wide CRISPR knockout screen to examine regulators of CD133 and stemness therein, in stem cell-enriching conditions.

As CD133 is a marker of stemness, CUX1 as the sole hit to be identified as a positive regulator stood out because of its well-known association with morphogenesis and cell differentiation by binding to DNA to effectively repress transcription in certain contexts. Another hit indicating the success of our screen was the #2 ranked gene, *KEAP1*. KEAP1 (Kelch-like ECH-associated protein 1) is a subunit of Cullin 3-based E3 ubiquitin ligase which regulates the activity of Nrf2 sensing oxidative and electrophilic stress in cells. Nrf2 (encoded by *NFE2L2* ranked #732) is well established regulator of stem cell self-renewal, proliferation, and differentiation. SOX2 as another top hit is a transcription factor that plays a critical role in the regulation of stemness in both NSCs and GSCs with studies showing that SOX2 is upregulated in GBM.

Of our top candidate genes, the transcription factor SOX2 produced the most dramatic results showing direct influence on CD133 protein and surface expression

levels. In combination with chromatin modifying subunits TADA1 and TADA2B, SOX2 proved to be essential in the regulation of stemness.

SOX2 is a heavily investigated transcription factor that can be present throughout the genome. The increased presence of SOX2 in GBM compared to normal tissue suggested the possibility of heightened activity. To examine the direct position of SOX2 throughout the genome we employed CUT&RUN, a successor to ChIP-seq because of reduced background noise and absence of crosslinking agents which reduces damage to DNA, ultimately affecting the results of protein-DNA interactions. Presence of SOX2 was not detected in the promoter regions of *PROM1,* but in the first intron. Transcription factors are known to bind within introns for a variety of reasons, including regulation of gene expression, alternative splicing, and regulation of non-coding RNA genes. These interactions are important for proper gene regulation and cellular function. Introns can contain enhancer elements that help to regulate gene expression by binding transcription factors. Because transcription coactivators are critically important in assisting transcription factors upregulate gene transcription in rapid and specific manner, we propose the existence of novel complexes that interact to regulate stemness in a cancer specific context.

Materials and Methods

Generation of Primary Cell Lines

Human GBM samples were acquired from consenting patients, as approved by Hamilton Health Sciences and the McMaster Health Sciences Research Ethics Board. Tumor specimens were processed using previously published protocols (Chokshi *et al.* 2020). GBMs were then cultured in Neurocult Complete (NCC) media, a defined and commercially available serum-free neural stem cell medium (STEMCELL Technologies, Cat#05751), supplemented with human recombinant epidermal growth factor (20ng/mL: STEMCELL Technologies, Cat#78006), basic fibroblast growth factor (20ng/mL; STEMCELL Technologies Cat#78006), heparin (2 µg/mL 0.2% Heparin Sodium Salt in PBS; STEMCELL technologies, Cat#07980), antibiotic-antimycotic (1X; Wisent, Cat# 450-115-EL). Tumorspheres derived from these cultures were expanded on polyornithine-laminin coated plates for adherent growth until sufficient populations were acquired for experimental purposes. Passaging consisted of dissociating a 10cm dish with 1 mL of TrypLE (ThermoFisher Cat. 25200056) for 5 min at 37°C followed by collection with PBS and centrifugation at 300g. Neural stem cells were derived and propagated in a similar fashion, as previously published (Suk 2022, STAR Protocols).

Flow Cytometry Analysis and Cell Sorting

Single cell GBM suspensions were generated from adherent cell cultures by dissociating with 3 mL of TrypLE on 15 cm dishes for 5 min at 37°C followed by collection with PBS and centrifugation at 300g. Cells were incubated with CD133/2 anti-human, PE-conjugated antibody (Miltenyi Cat. 130-113-186) at manufacturer's recommended

concentration for 15 minutes, followed by PBS washing, centrifugation (repeat as before) and resuspension. The viability dye 7AAD (1:10; Beckman Coulter, A07704) was used to exclude dead cells. Cells were sorted using Beckman Coulter MoFlo XDP Cell Sorter with all flow plots were generated using FlowJo software.

Sphere Formation Assay

Single cells were plated in a 96-well plate at a density of 1,000 cells/200 µL per well and incubated at 37°C and 5% CO^2 for five days. Spheres were counted manually with spheres formed being defined as clusters of three or more cells with no clearly defined border.

Cell Proliferation Assay

Single cells were plated in a 96-well plate at a density of 1,000 cells/200 µL per well and incubated at 37°C and 5% CO^2 for five days. 20 µL of Presto Blue (ThermoFisher, Cat.A13262), a fluorescent cell metabolism indicator, was added to each well four hours prior to reading out the assy. Fluorescence was measured using a FLUOstar Omega Fluorescence 556 Microplate reader (BMG LABTECH) with excitation and emission wavelengths of 544nm and 590nm respectively. Readings were then analyzed using Omega analysis software. Proliferation was calculated for each well by subtracting the average RFI of blank wells from the RFI of individual wells. Mean RFI was plotted for each well being tested as a side-by-side comparison of proliferation.

CRISPR sgRNA Lentivirus Library Generation

The TKOv3 lentivirus was produced as previously described (Hart *et al.* 2017). Briefly, HEK293T cells were seeded at 9×10^6 cells per 15 cm plate and incubated overnight. Transfection was conducted with a mixture of psPAX2 (4.8 µg; Addgene #12260), pMDG.2 (3.2 µg; Addgene #12259), TKOv3 plasmid library (8 µg) and X-tremeGENE 9 (48 µl; Roche Cat. 6365787001) in Opti-MEM (Gibco Cat.31985070). 24 hours after transfection the media was changed to DMEM with 1% BSA and 1% penicillin–streptomycin. Virus-containing medium was collected 48 hours after transfection, centrifuged at 1,500 rpm for 5 minutes and stored at −80 °C. Viral titres were determined by titration on HAP1 cells where 24 hours after infection the media was replaced with puromycin-containing medium (1 µg ml^{-1}) and incubated for 48 hours. The multiplicity of infection (MOI) was determined 72 hours after infection by comparing survival of infected cells with infected unselected and uninfected selected control cells.

Pooled Genome-Wide CRISPR Screen in Glioblastoma Stem Cells

The CRISPR screen was established, where 100×10^6 cells were transduced with the TKOv3 lentivirus library at an MOI of 0.3, representing more than 400-fold coverage per sgRNA after selection with puromycin. Media was changed 24 hours after infection to puromycin-containing medium (1.2µg/mL). 72 hours after transduction, 30×10^6 puromycin-selected cells were collected for genomic DNA extraction at starting timepoint, and 90×10^6 cells were evenly divided into triplicates (30×10^6 cells each, 2.5×10^6 cells per 15cm dish). Passaging subsequently occurred every 7 days (approximately 3 cell doublings), where 30×10^6 cells in each replicate were reseeded until the 12^{th} doubling

(T12) when sorting was performed. A representative portion of the final population of cells (bulk/unsorted) was collected for sequencing prior to staining for flow cytometry followed by the top and bottom 5th-percentiles of CD133 surface expression being collected in cooled flow tubes. Collected cells were centrifuged and stored at -80 °C until genomic extraction as described below.

Genomic DNA Extraction and Illumina Sequencing

Genomic DNA was extracted from experimental cell pellets using Wizard Genomic DNA Purification Kit (Promega Cat. A1120). Sequencing libraries were prepared by amplifying sgRNA inserts using a two-step PCR reaction using primers that include Illumina TruSeq adapters with i5 and i7 indices. Resulting libraries were then sequenced on an Illumina HiSeq2500 (RRID: SCR_016383) as previously published (Hart *et al.* 2017). Each read was completed with standard primers for dual indexing with Rapid Run V1 reagents. The first 20 cycles of sequencing were dark cycles or base additions without imaging. The actual 26 bp read begins after the dark cycles and contains two index reads, reading the i7 first, followed by i5 sequences.

Screen Data Processing and Quality Control

Reads were trimmed by extracting the flanking 20 bp after each 8bp anchor was found in barcoding primers. A 2 bp mismatch was allowed for the anchor search. After trimming, a quality-control alignment was performed using Bowtie v.0.12.8 (allowing for a maximum of 2 bp mismatches) and sgRNAs were quantified. Read counts for all samples in the screen were combined into a matrix (the percentage of recovered sgRNAs in each

sample is provided below; recovered is defined as ≥1 raw read) and normalized by dividing each read count by the sum of all of the read counts in the sample and then multiplying by the expected read number (10 million). Fold change was calculated to a reference sample (T12 unsorted). Calculated fold changes were then used to generate normalized Z scores using drugZ (v.1.1.0.2).

Generation of Validation Knockout Vectors

Individual lentiviral sgRNA constructs for knockout validations were generated as follows: Single-stranded sgRNA oligos (sequences provided below) were annealed using T4 polynucleotide kinase in T4 ligation buffer (NEB, Cat.B0202S) and ligated into BsmBI digested (NEB, Cat.R0580), phosphatase-treated (NEB, Cat.M0289S) and gel-purified modified pLCKO backbones using T4 DNA ligase (NEB, Cat.M0202T). All plasmids were verified by Sanger sequencing and virus was prepared as described above. GSCs were transduced with targeted or control lentiviruses by exposure for 24 hours in suspension, followed by plating cells onto laminin coated dished for an additional 24 hours. 48 hours after transduction, used media was replaced with fresh NCC media containing puromycin to eliminate all uninfected cells for 72 hours, at which point validation experiments were initiated.

Gene	sgRNA	Sequence	Gene	sgRNA	Sequence
AAVS1	(Control)	GGGGCCACTAGGGACAGGAT	FBXW7	KO-A	*AAGAGCGGACCTCAGAACCA*
PROM1	KO-A	*TGAATAGCAACCCTGAACTG*	FBXW7	KO-B	*TGAACATGGTACAAGCCCAG*
PROM1	KO-B	*GGCCCAGTACAACACTACCA*	SIAH1	KO-A	*AAGTTGCGAATGGATCCCAA*
KEAP1	KO-A	*GGGCCGCCTGATCTACACCG*	SIAH1	KO-B	*CGAAGTGTCCACCATCCCAG*
KEAP1	KO-B	*GAGGACACACTTCTCGCCCA*	SOX2	KO-A	*GATAAGTACACGCTGCCCGG*
TADA1	KO-A	*ACTGGGCTAACCTAAAGCTG*	SOX2	KO-B	*GGAGCCAAGAGCCATGCCAG*

TADA1	KO-B	*TGGGCTGGACAATGTCACCG*	CUX1	KO-A	*GTTCAAGAAGAACACTCCAG*
TADA2B	KO-A	*GCTGAAGCGCAAGATCACCA*	CUX1	KO-B	*GCTGGCCTCACAGATCCAGA*
TADA2B	KO-B	*AGCTGAAAGAGAGACAGCGG*			

Western Blots

Cells pellets were lysed in RIPA buffer (50mM Tris HCl pH 8.0, 150mM NaCl, 1% NP-40, 0.5% sodium deoxycholate, and 0.1% SDS) containing HALT™ Protease and Phosphatase Inhibitor Cocktail (ThermoFisher Cat.78440) and placed on an active nutator in 4°C for 1 hour. Once complete, centrifugation took place at 14,000rcf at 4°C for 10 minutes. Supernatant was collected and protein concentration was determined using the Bradford method (BioRad). 30µg total protein was loaded in all lanes, and proteins were resolved on 4%–12% Novex Bis-Tris gradient gels (Invitrogen) at 100V for 60 minutes and transferred to Immobilon-P PVDF membranes (Millipore) at 200mA for 120 minutes. Membranes were blocked in TBS-T containing 5% BSA for 30 minutes at room temperature followed by the addition of primary antibodies to be incubated at 4^{o}C on a rocker at slow speeds. The following morning, membranes were washed repeatedly with TBS-T followed by incubation with secondary antibodies in TBS-T containing 5% BSA for 60 minutes. After repeated washes in TBS-T membranes were imaged.

Antibodies were purchased and used at the following concentrations: CD133 (Abcam, 19898, 1:5000), KEAP1 (ThermoFisher, 10503-2-AP, 1:2000), TADA1 (Santa Cruz, Anti-STAF42 sc-398787, 1:2000), TADA2B (Santa Cruz, MB-56 sc-130479, 1:2000), SIAH1 (Novus Biologics, NBP2-20356, 1:1000), SOX2 (Cell Signaling Technology, D9B8N 23064, 1:5000), Beta-tubulin (ThermoFisher, MA5-16308, 1:5000), GAPDH (Abcam, ab8245, 1:5000), anti-Mouse IgG Secondary (LICOR, 926-68070,

1:10,000), anti-Rabbit IgG Secondary (LICOR, 926-32211, 1:10,000), Santa Cruz (m-IgG Fc BP-HRP sc-525409, 1:10,000).

Online Databses

To incorporate publicly available data sets, the GEPIA2 interface was utilized to compare correlations of individual genes, or genome-wide gene expression profiles between GBM specimens of The Cancer Genome Atlas (TCGA) and normal brain tissue of the Genotype-Tissue Expression (GTEx) portal as previously described (Tang *et al.* 2017).

CUT&RUN

Patient derived lines were acquired and propagated as previously described. CUT&RUN was performed using a magnetic bead-based protocol using CUTANA Kit (EpiCypher Cat.14-1048) according to manufacturer's instructions. The magnet was placed on ice for all steps. Cells were harvested by centrifugation (300g for 3 minutes at room temperature in a swinging bucket rotor) and washed in ice cold Wash Buffer. One million cells were added to low binding PCR tubes containing activated beads (in triplicate) for 10 minutes at room temperature. Cell Permeabilization Buffer consisted of Wash Buffer containing 0.01% Digitonin. Antibody Buffer consisted of Cell Permeabilization Buffer containing 0.5M EDTA). 0.5ug of each antibody (SOX2-test, H3K4me4-positive control, and IgG-negative control) was added to respective tubes and placed on a nutator overnight at 4ºC for incubation. Extracted DNA fragments were quantified using QubitTM fluorometer and stored at -20ºC until library preparation was

initiated.

Library Preparation, Sequencing and Analysis

Library preps were conducted using NEBNext® Ultra™ II DNA Library Prep Kit for Illumina according to manufacturer's instructions. Sequencing libraries were prepared by amplifying DNA fragments using a 2-step PCR using primers as follows: R1: 5'-[insert]-AGATCGGAAGAGCACACGTCTGAACTCCAGTCAC...-3' and R2: 5'-[insert]-AGATCGGAAGAGCGTCGTGTAGGGAAAGAGTGT...-3'. Resulting libraries were subsequently sequenced on an Illumina HiSeq2500 (RRID: SCR_016383). Analysis was conducted using previously published pipelines by Kong *et al.* 2021.

References

Arede L, Pina C. Buffering noise: KAT2A modular contributions to stabilization of transcription and cell identity in cancer and development. Exp Hematol. 2021 Jan;93:25-37. doi: 10.1016/j.exphem.2020.10.003. Epub 2020 Oct 22. PMID: 33223444.

Bao S, Wu Q, McLendon RE, Hao Y, Shi Q, Hjelmeland AB, Dewhirst MW, Bigner DD, Rich JN. Glioma stem cells promote radioresistance by preferential activation of the DNA damage response. Nature. 2006 Dec 7;444(7120):756-60. doi: 10.1038/nature05236. Epub 2006 Oct 18. PMID: 17051156.

Berezovsky AD, Poisson LM, Cherba D, Webb CP, Transou AD, Lemke NW, Hong X, Hasselbach LA, Irtenkauf SM, Mikkelsen T, deCarvalho AC. Sox2 promotes malignancy in glioblastoma by regulating plasticity and astrocytic differentiation. Neoplasia. 2014 Mar;16(3):193-206, 206.e19-25. doi: 10.1016/j.neo.2014.03.006. Epub 2014 Apr 13. PMID: 24726753; PMCID: PMC4094829.

Bowles J, Schepers G, Koopman P. Phylogeny of the SOX family of developmental transcription factors based on sequence and structural indicators. Dev Biol. 2000 Nov 15;227(2):239-55. doi: 10.1006/dbio.2000.9883. PMID: 11071752.

Bradshaw A, Wickremesekera A, Brasch HD, Chibnall AM, Davis PF, Tan ST, Itinteang T. Cancer Stem Cells in Glioblastoma Multiforme. Front Surg. 2016 Aug 26;3:48. doi: 10.3389/fsurg.2016.00048. PMID: 27617262; PMCID: PMC5001191.

Campos B, Zeng L, Daotrong PH, Eckstein V, Unterberg A, Mairbäurl H, Herold-Mende C. Expression and regulation of AC133 and CD133 in glioblastoma. Glia. 2011 Dec;59(12):1974-86. doi: 10.1002/glia.21239. Epub 2011 Sep 7. PMID: 21901757.

Chen YC, Dent SYR. Conservation and diversity of the eukaryotic SAGA coactivator complex across kingdoms. Epigenetics Chromatin. 2021 Jun 10;14(1):26. doi: 10.1186/s13072-021-00402-x. PMID: 34112237; PMCID: PMC8194025.

Chokshi CR, Savage N, Venugopal C, Singh SK. A Patient-Derived Xenograft Model of Glioblastoma. STAR Protoc. 2020 Nov 21;1(3):100179. doi: 10.1016/j.xpro.2020.100179. PMID: 33377073; PMCID: PMC7757408.

Colic M, Wang G, Zimmermann M, Mascall K, McLaughlin M, Bertolet L, Lenoir WF, Moffat J, Angers S, Durocher D, Hart T. Identifying chemogenetic interactions from CRISPR screens with drugZ. Genome Med. 2019 Aug 22;11(1):52. doi: 10.1186/s13073-019-0665-3. PMID: 31439014; PMCID: PMC6706933.

Cox JL, Mallanna SK, Luo X, Rizzino A. Sox2 uses multiple domains to associate with proteins present in Sox2-protein complexes. PLoS One. 2010 Nov 12;5(11):e15486. doi: 10.1371/journal.pone.0015486. PMID: 21103394; PMCID: PMC2980493.

Ellis P, Fagan BM, Magness ST, Hutton S, Taranova O, Hayashi S, McMahon A, Rao M, Pevny L. SOX2, a persistent marker for multipotential neural stem cells derived from embryonic stem cells, the embryo or the adult. Dev Neurosci. 2004 Mar-Aug;26(2-4):148-65. doi: 10.1159/000082134. PMID: 15711057.

Fong H, Hohenstein KA, Donovan PJ. Regulation of self-renewal and pluripotency by Sox2 in human embryonic stem cells. Stem Cells. 2008 Aug;26(8):1931-8. doi: 10.1634/stemcells.2007-1002. Epub 2008 Apr 3. PMID: 18388306.

Gangemi RM, Griffero F, Marubbi D, Perera M, Capra MC, Malatesta P, Ravetti GL, Zona GL, Daga A, Corte G. SOX2 silencing in glioblastoma tumor-initiating cells causes stop of proliferation and loss of tumorigenicity. Stem Cells. 2009 Jan;27(1):40-8. doi: 10.1634/stemcells.2008-0493. PMID: 18948646.

Hart T, Tong AHY, Chan K, Van Leeuwen J, Seetharaman A, Aregger M, Chandrashekhar M, Hustedt N, Seth S, Noonan A, Habsid A, Sizova O, Nedyalkova L, Climie R, Tworzyanski L, Lawson K, Sartori MA, Alibeh S, Tieu D, Masud S, Mero P, Weiss A, Brown KR, Usaj M, Billmann M, Rahman M, Constanzo M, Myers CL, Andrews BJ, Boone C, Durocher D, Moffat J. Evaluation and Design of Genome-Wide CRISPR/SpCas9 Knockout Screens. G3 (Bethesda). 2017 Aug 7;7(8):2719-2727. doi: 10.1534/g3.117.041277. PMID: 28655737; PMCID: PMC5555476.

Kong NR, Chai L, Tenen DG, Bassal MA. A modified CUT&RUN protocol and analysis pipeline to identify transcription factor binding sites in human cell lines. STAR Protoc. 2021 Aug 17;2(3):100750. doi: 10.1016/j.xpro.2021.100750. PMID: 34458869; PMCID: PMC8379522.

Liu G, Yuan X, Zeng Z, Tunici P, Ng H, Abdulkadir IR, Lu L, Irvin D, Black KL, Yu JS. Analysis of gene expression and chemoresistance of CD133+ cancer stem cells in glioblastoma. Mol Cancer. 2006 Dec 2;5:67. doi: 10.1186/1476-4598-5-67. PMID: 17140455; PMCID: PMC1697823.

Lopez-Bertoni H, Lal B, Li A, Caplan M, Guerrero-Cázares H, Eberhart CG, Quiñones-Hinojosa A, Glas M, Scheffler B, Laterra J, Li Y. DNMT-dependent suppression of microRNA regulates the induction of GBM tumor-propagating phenotype by Oct4 and Sox2. Oncogene. 2015 Jul 23;34(30):3994-4004. doi: 10.1038/onc.2014.334. Epub 2014 Oct 20. PMID: 25328136; PMCID: PMC4404208.

Louis DN, Perry A, Wesseling P, Brat DJ, Cree IA, Figarella-Branger D, Hawkins C, Ng HK, Pfister SM, Reifenberger G, Soffietti R, von Deimling A, Ellison DW. The 2021 WHO Classification of Tumors of the Central Nervous System: a summary. Neuro Oncol. 2021 Aug 2;23(8):1231-1251. doi: 10.1093/neuonc/noab106. PMID: 34185076; PMCID: PMC8328013.

Marmorstein R, Zhou MM. Writers and readers of histone acetylation: structure, mechanism, and inhibition. Cold Spring Harb Perspect Biol. 2014 Jul 1;6(7):a018762. doi: 10.1101/cshperspect.a018762. PMID: 24984779; PMCID: PMC4067988.

Novak D, Hüser L, Elton JJ, Umansky V, Altevogt P, Utikal J. SOX2 in development and cancer biology. Semin Cancer Biol. 2020 Dec;67(Pt 1):74-82. doi: 10.1016/j.semcancer.2019.08.007. Epub 2019 Aug 11. PMID: 31412296.

Ran FA, Hsu PD, Wright J, Agarwala V, Scott DA, Zhang F. Genome engineering using the CRISPR-Cas9 system. Nat Protoc. 2013 Nov;8(11):2281-2308. doi: 10.1038/nprot.2013.143. Epub 2013 Oct 24. PMID: 24157548; PMCID: PMC3969860.

Shalem O, Sanjana NE, Hartenian E, Shi X, Scott DA, Mikkelson T, Heckl D, Ebert BL, Root DE, Doench JG, Zhang F. Genome-scale CRISPR-Cas9 knockout screening in human cells. Science. 2014 Jan 3;343(6166):84-87. doi: 10.1126/science.1247005. Epub 2013 Dec 12. PMID: 24336571; PMCID: PMC4089965.

Singh SK, Hawkins C, Clarke ID, Squire JA, Bayani J, Hide T, Henkelman RM, Cusimano MD, Dirks PB. Identification of human brain tumour initiating cells. Nature. 2004 Nov 18;432(7015):396-401. doi: 10.1038/nature03128. PMID: 15549107.

Stallcup MR, Poulard C. Gene-Specific Actions of Transcriptional Coregulators Facilitate Physiological Plasticity: Evidence for a Physiological Coregulator Code. Trends Biochem

Sci. 2020 Jun;45(6):497-510. doi: 10.1016/j.tibs.2020.02.006. Epub 2020 Mar 13. PMID: 32413325; PMCID: PMC7230073.

Venugopal C, Hallett R, Vora P, Manoranjan B, Mahendram S, Qazi MA, McFarlane N, Subapanditha M, Nolte SM, Singh M, Bakhshinyan D, Garg N, Vijayakumar T, Lach B, Provias JP, Reddy K, Murty NK, Doble BW, Bhatia M, Hassell JA, Singh SK. Pyrvinium Targets CD133 in Human Glioblastoma Brain Tumor-Initiating Cells. Clin Cancer Res. 2015 Dec 1;21(23):5324-37. doi: 10.1158/1078-0432.CCR-14-3147. Epub 2015 Jul 7. PMID: 26152745.

Vora P, Venugopal C, Salim SK, Tatari N, Bakhshinyan D, Singh M, Seyfrid M, Upreti D, Rentas S, Wong N, Williams R, Qazi MA, Chokshi C, Ding A, Subapanditha M, Savage N, Mahendram S, Ford E, Adile AA, McKenna D, McFarlane N, Huynh V, Wylie RG, Pan J, Bramson J, Hope K, Moffat J, Singh S. The Rational Development of CD133-Targeting Immunotherapies for Glioblastoma. Cell Stem Cell. 2020 Jun 4;26(6):832-844.e6. doi: 10.1016/j.stem.2020.04.008. Epub 2020 May 27. PMID: 32464096.

Yuan H, Marmorstein R. Histone acetyltransferases: Rising ancient counterparts to protein kinases. Biopolymers. 2013 Feb;99(2):98-111. doi: 10.1002/bip.22128. PMID: 23175385; PMCID: PMC4017165.

Chapter 3: Functional Characterization of GPNMB in Glioblastoma Models

Preamble

In this chapter, I present an original manuscript describing functional role of GPNMB in glioblastoma using multi-omic approaches and multiple mouse models revealing novel biology:

Savage, N., Venugopal, C., Mikolajewicz, N., Tatari, N., Chokshi, C., Gwynne, W., Wei, J., Han H., Kislinger, T., Moffat, J., & Singh, S. K. Functional Characterization of GPNMB in Glioblastoma Models. (manuscript in preparation)

Author contributions are as follows for the aforementioned manuscript: Conceptualization: N.S, S.K.S and J.M; Resources: S.K.S, J.M, and T.K; Methodology, Investigation and Validation: N.S, N.T, C.C, W.G, and J.W; Software and formal analysis: N.S, N.M, H.H; Visualization: N.S, N.M, H.H; Writing – original draft preparation: N.S; Writing – review and editing: N.S, C.V, J.M, S.K.S; Project administration and supervision: S.K.S and J.M; Funding acquisition: S.K.S and J.M. All authors read and approved the manuscript.

I present data summarizing our identification of GPNMB as a tumor associated antigen and functional validations to studying its biology in GBM. Using CRISPR in patient derived GBM lines, standard *in vitro* and *in vivo* experiments are employed to determine the role of GPNMB in tumor progression. We use proteomics and immunohistochemistry to examine expression levels and distribution of GPNMB throughout patient tissue blocks with the tumor immune microenvironment intact. Multiplexing data at the protein level with

single-cell RNA-sequencing data to determine the expression levels through different populations of tumors uncovered the restricted expression in tumor cells and myeloid cells. Because the limitation of PDX models is the absence of an immune compartment, this offered the complimentary model of syngeneic models of GBM. We found several hallmark pathways were perturbed in our CRISPR knockout clones, reflecting the reproducible data of our models. We also uncovered new biology of how immune signaling molecules, particularly interferons affects GPNMB.

Abstract

Glioblastoma (GBM) displays extreme heterogeneity and immune suppression leading to a dismal prognosis for patients despite decades of intense research. Glycoprotein nonmetastatic melanoma protein B (GPNMB) has been identified as a clinically relevant target in GBM and shown to be active in the tumor immune microenvironment. We found GPNMB to be upregulated in recurrent tumors and its presence in mesenchymal populations suggests a strong interaction between tumor cells and the supportive niche which can be exploited. Despite GBM being a cancer with a relatively low mutational burden, we show the immunologically cold tumor and immunosuppressive microenvironment is due to an upregulation of interferon response pathways. GPNMB is ultimately upregulated in macrophage populations (a large proportion of bulk GBM tumors) to be a negative regulator of the inflammatory signal of tumor infiltrating lymphocytes. Through a series of models, we show GPNMB to be an important protein in GBM and its hallmark immune landscape.

Introduction

Glioblastoma (GBM) is the most common primary brain tumor in adults, accounting for approximately 15% of intracranial tumors (Louis *et al.* 2021). Once diagnosed, patients undergo aggressive Standard-of-Care consisting of surgical resection, radiation therapy and chemotherapy with the alkylating agent temozolomide (Stupp *et al.* 2005). Despite this, the median patient survival remains less than 15 months post-diagnosis (Stupp *et al.* 2005). Therapy failure is attributed to genotypic and phenotypic variances of tumor populations within and among patients (Meyer *et al.* 2015). Multiple research groups have attempted to categorize patients into manageable subtypes based on genetic characteristics to identify therapeutic vulnerabilities, but a clinically useful system has yet to be established (Phillips *et al.* 2006, Verhaak *et al.* 2010). The Cancer Genome Atlas (TCGA) attempted to classify GBM into four distinct subtypes to better characterize the molecular profiles and predict beneficial treatments for patients (Verhaak *et al.* 2010). However, this classification system was quickly upended when it was revealed through single cell RNA-sequencing that all subtypes are present within a single GBM tumor (Patel *et al.* 2014). This finding reinforced the notion that geographically distinct regions of the tumor can be classified into different subtypes (Sottorvia *et al.* 2013). When the tumor inevitably relapses, the recurrent tumor can be biologically distinct from the primary GBM (Johnson *et al.* 2014, Kim *et al.* 2015). Thus, GBMs are dynamic structures, with subtypes varying spatially and temporally within a tumor.

The heterogeneity of GBM may be attributed to glioblastoma stem cells (GSCs). GSCs can be identified by the expression of CD133 at the membrane surface (henceforth known as “CD133+” cells) (Singh *et al.* 2004). These CD133+ cells have been shown to

possess mechanisms allowing them to withstand conventional therapies and lead to tumor relapse (Bao *et al.* 2006, Liu *et al.* 2006). We have previously shown the administration of therapies targeting CD133 reduces tumor burden and increases survival times in GBM bearing mice (Vora *et al.* 2020). Despite the efficacy of therapies, mice eventually succumbed to tumors. This ultimately means a single therapeutic agent is unlikely to eliminate all GBM cells and additional targets are required to target CD133-nonexpressing (CD133-) GBM cells. Glycoprotein nonmetastatic melanoma protein B (GPNMB) is a transmembrane protein that has been identified as a potential therapeutic target for the treatment of GBM (Kuan *et al.* 2006). It has previously been found to be an unfavorable prognostic marker in gliomas at the protein level (Feng *et al.* 2020). GPNMB has been found to be upregulated in a restricted population of GBM cells which displayed high therapy resistance, increased self-renewal capacity, and mesenchymal gene signatures (Tejero *et al.* 2019).

Inflammation is a complex cascade of cellular and molecular processes the body uses to heal in response to pathogens or physical injury (Saade *et al.* 2021). A variety of cytokines and chemokines in the tumor microenvironment attract immune cells such as macrophages, microglia, and T cells which in turn contribute additional cytokines, chemokines, and growth factors that promote tumor growth (Saade *et al.* 2021). Interferons (IFNs) are a family of cytokines that play a major immunomodulatory function in GBM by activating signaling pathways that upregulate the expression of IFN-stimulated genes (ISGs) (Cheon *et al.* 2014, Zhu *et al.* 2019). Despite the presence of immune cells in the tumor microenvironment, this population contains a high number of myeloid-derived suppressor cells (MDSCs), regulatory T cells (Tregs), and tumor-associated

macrophages (TAMs), which can contribute to the immunosuppressive microenvironment within the tumor (De Leo *et al.* 2021). Understanding their contribution to the complex interplay between inflammation and GBM could underpin novel strategies to therapeutically exploit.

Results

Identifying GPNMB as a Clinically Relevant Target in Glioblastoma.

CD133 is also a known marker of healthy neural stem cells (NSCs) (Uchida *et al.* 2000). To investigate actionable targets specific to CD133- GBM populations, four primary patient GSC lines and four NSC lines were flow sorted into CD133+/- groups and sent for RNAseq. The minimum value required to achieve the best normalization among all samples for all four comparisons (Figure 1A left, Supplementary 1A) was determined to be a transcript counts per million threshold cutoffs of 3.5. Hallmarks of GBM include heightened angiogenesis and metabolic rewiring, but beyond that patients can display vast differences at a molecular level (Torrisi *et al.* 2022). There was no clear separation between the CD133+/- GSC groups in the multidimensional scaling and despite the sample numbers being imbalanced, a list of four genes were identified as significantly upregulated in CD133- GSCs (Figure 1A, right). From this, GPNMB was identified as the most statistically significant differentially expressed gene in CD133- GSC populations ($p=0.04$). GPNMB transcripts in NSCs fell below the threshold cutoff so comparison could not be performed between groups. This led us to theorize GPNMB could be a tumor specific target. TCGA datasets were queried using GEPIA2 (Tang *et al.* 2019) where it showed transcript levels are upregulated in all GBM subtypes compared to normal brain

tissue ($p<0.01$) (Figure 1B). Of note, GPNMB was highest in the mesenchymal subtype (Supplementary 1B).

Despite a low number of significant differentially expressed genes between groups, similarities among groups were present. CD133+ populations of both GSCs and NSCs displayed elevated cell cycle and DNA replication pathways compared to their CD133- counterparts (Supplementary 1C). Tumor specific pathways (elevated in CD133+/- GSC populations compared to NSC populations) included sugar metabolism, predictably being associated with the Warburg effect (Supplementary 1D). In total, 582 of 602 pathways (96.7%) were enriched in the same direction for CD133+ populations compared to CD133- in both GSCs and NSCs. Interestingly, of the 20 pathways that were differed between GSCs and NSCs, only the CD40 pathway was upregulated in GSCs which stood out because of its importance in antigen presenting cells while GBM is considered an immunologically "cold" tumor (Supplementary 1E).

We proceeded to validate GPNMB protein to be present in GSC samples while being absent in NSCs (Figure 1C). Based on literature, SK-MEL-2 and HEK cells were known to have a presence or absence of GPNMB and therefore used as positive and negative controls respectively for optimizing all protocols (Qian *et al.* 2008, Kuan *et al.* 2006). Next, we confirmed the presence of GPNMB in patient derived GBM xenografts using a human specific antibody, validating it as a platform for preclinical development of GPNMB-targeting therapies (Supplementary 2A). By examining paraffin embedded patient derived xenograft (PDX) brains previously treated with CD133-CAR-Ts (Vora *et al.* 2020) GPNMB expressing cells were detected in the residual tumor (Figure 1D). After

confirming the absence of GPNMB in multiple normal adult brain tissues (Figure 1E), it was concluded GPNMB was a tumor associated antigen.

GPNMB Is A Target For Recurrent GBM And Tumor Associated Macrophages

To begin investigating the clinical implications of GPNMB in GBM, CRISPR knockout vectors were generated using sgRNA sequences from the Toronto Knockout Library Version 3 (TKOv3) (Hart *et al.* 2017). AAVS1 was used as a knockout gene in control populations. We found a decrease in GPNMB protein (Figure 2A) correlated with a decrease in GBM proliferation ($p<0.001$, Figure 2B) indicating a role in tumor aggressiveness. Cells were then injected orthotopically into NSG mice where mice in the GPNMB knockout cohort survived significantly longer in all cell lines ($p<0.001$, Figure 2C) consistent with our *in vitro* results that GPNMB leads to a more aggressive phenotype.

To begin investigating the distribution of GPNMB in GBM, we utilized an inhouse RNAseq data of primary derived cell lines in a variety of matched contexts. In primary lines we successfully grew *in vitro* and engrafted in PDX models, GPNMB transcripts were consistently highest in the patient tissue sample where the tumor immune microenvironment was still intact (Figure 2D). Strikingly among the samples available, GPNMB expression was >10x higher in BT972, a matched recurrent GBM in our inventory. Following this we examined a proteomic data set of BT972 compared to its patient matched primary GBM BT594 and found GPNMB to be an upregulated protein in BT972 (Figure 2E). Consistent within our models, strong immunohistochemistry staining of BT972 in our PDX blocks (Figure 2F) matched the increased RNA levels from the RNA data set (Figure 2D). In another patient matched primary-recurrent GBM proteomic data

set, we found GPNMB to be the most upregulated and statistically significant protein at recurrence (Supplementary 2B), but unfortunately could not recommend a treatment for the patient as no ongoing clinical trials were being conducted. Together, this firmly established GPNMB as a clinically relevant target for recurrent GBMs.

In a previously published inhouse data set of 43 patient matched primary-recurrent GBM specimens with the immune microenvironment intact (Tatari *et al.* 2022), proteomic analysis revealed GPNMB to be significantly upregulated in recurrent samples ($p=0.0033$, Figure 2G). GPNMB was detected in all 86 samples and ranked in the top percentile of upregulated proteins at recurrence. The structure of GPNMB includes a hemITAM motif which is a conserved amino acid sequence typically restricted to myeloid lineages to carry out signaling functions such as cytokine production (Xie *et al.* 2019, Bauer *et al.* 2017, Supplementary 2C). It has previously been reported soluble GPNMB in tumors is generally sourced from TAMs which are a major population of cells in a GBM (Liguori *et al.* 2021, Hambardzumyan *et al.* 2016). Further examination of a subset of these samples using IHC confirmed the higher expression of GPNMB in recurrent GBMs compared to matched primaries (Figure 2H). This observation was later confirmed using HALO analysis (Figure 2I). Having previously validated GPNMB as a protein highly expressed in GBM cells, we next wanted to examine it as a potential contributor to the dynamic intercommunication between GBM cells and TAMs.

GPNMB in the Tumor Immune Microenvironment.

We attempted to deconvolute the distribution of GPNMB by examining the tumors using sciRNAseq. Our data reinforced the notion that GPNMB is upregulated and

mutually expressed in myeloid populations and GBM cells while being mostly absent in lymphoid, OPC, neuron and astrocyte populations (Figure 3A). Consistent among our data sets was the presence of GPNMB transcripts being highest among the recurrent GBMs compared to its matched primary GBM, as well as GPNMB transcripts being highest among the recurrent GBM myeloid cells compared to its matched primary GBM myeloid cells (Supplementary 2D).

To begin investigating the functional role of GPNMB in GBM we used GlioVis (Bowman *et al.* 2017) to interrogate publicly available data from TCGA. We conducted gene ontology enrichment analysis of RNAseq data of GBMs (Log2-fold>2, p-value<0.05) where it was revealed the most significant biological process was determined to be regulation of the inflammatory response (Figure 3B). Migration and chemotaxis of leukocytes and myeloid cells were also significantly enriched indicating the strong role GPNMB plays in modulating the tumor immune microenvironment. Paradoxically, GBM is immunologically cold despite exhibiting pro-inflammatory signals (Liu *et al.* 2021, Alanio *et al.* 2022), and greater lymphocyte infiltration correlates with worse patient survival times (Mariniari *et al.* 2020). Among genes to correlate with GPNMB most strongly were the pan-macrophage marker CD68 (R=0.663) and *MSR1*/CD204 (R=0.649), an M2-macrophage marker associated with worse prognosis for GBM patients (Sørensen *et al.* 2018). Macrophages are no longer classified along a single spectrum of M1-M2 polarization but GPNMB more strongly correlated with genes more historically associated with an M2 immunosuppressive phenotype (Figure 3C). Weak to anti-correlative trends between GPNMB and pro-inflammatory cytokines were found (ex. TNF-alpha and iNOS). GPNMB was also found to have a strong correlation with CCL18 (R=0.505), an

increasingly appreciated chemokine at the junction of macrophage polarization, GBM growth, and a proxy for anti-inflammatory cytokines in the environment such as IL-4, IL-10 and IL-14 (Schraufstatter *et al.* 2012, Huang *et al.* 2022, Cavalheiro *et al.* 2022, Ronald *et al.* 2003). Together, GPNMB was determined to be at the critical junction of intercommunication between tumor cells and TAMs and possibly plays a dynamic role in tumor evolution by moderating inflammatory cascades.

We next examined the biology of GPNMB in an immunocompetent model using GL261, a murine glioma commonly used in GBM research, to complement our study. Clones of GL261 deficient for GPNMB protein were generated (Supplementary 3A) and interrogated in a similar fashion to our patient derived GBMs. GL261 displayed similar biology to human samples where clones deficient in GPNMB had a lower proliferation capacity (p-value < 0.0001, Figure 3D) and when injected intracranially into C57BL/6 mice the clones had an increased survival time ($n = 8$, $p = 0.0016$, Figure 3E). At endpoint, the last three surviving mice of each cohort had their fresh brains sectioned to isolate the bulk tumor and flash frozen for sciRNAseq (Figure 3F). Analysis again revealed GPNMB to be most closely associated with the mesenchymal subtype of GBM while GPNMB-KO brains took on a more developmental like phenotype, more closely resembling the NPC, OPC and AC subtypes (Neftel *et al.* 2019). A tight junction between tumor cells and immune cells was found in the wild type cohort while being reduced in the knockouts (Supplementary 3B). GPNMB transcripts were detected in both tumor cells and immune cells of the wild type cohort but absent in both populations of the knockout cohort (Supplementary 3C).

Investigating the Functional Role of GPNMB in GBM.

Multiple receptor signaling pathways were altered in the absence of GPNMB including well defined pathways of GBM tumor progression such as PDGFR and KIT (angiogenesis), TGFβ (pleiotropic), FAK and Integrins (cell adhesion) and Stats (immunity) (Figure 4A). Immune pathways such as innate/adaptive immune activations and leukocyte differentiation/proliferation were also downregulated in GPNMB-KO tumor cells (Figure 4A). Activation of the immune system is a tightly regulated process to prevent excessive inflammation and down regulated through regulatory immune cells to maintain immune tolerance, but chronic inflammation contributes to cancer progression by inhibiting the immune system's ability to identify and attack cancer cells. Of the pathways enriched within wild type cells, a consistent theme emerged of contextual proinflammatory pathways which activate the immune system that eventually lead to immune suppression (Figure 4B). The pathways strongly associated with GPNMB wild type populations included Hallmark TGF-beta, Interferon-gamma, IL6-JAK-STAT3, Interferon-alpha, IL2-STAT5, Inflammatory Response and TNF-alpha Signaling Via NF-kB. Confidence in the identification of these pathways was attributed to GPNMB's association with other previously reported including Notch signaling, TGF-beta and Integrin interactions (Figure 4C). This validated the complimentary roles of our PDX and GL261 models to uncover novel biology.

Co-expression profiling of GPNMB most strongly associated with interferon signaling (Figure 4D). Interferons are a group of signaling proteins that activate several downstream signaling pathways, including the JAK-STAT pathway previously mentioned and interferon regulatory factors (IRFs), which ultimately leads to transcription of

interferon-stimulated genes (ISGs). IRF8 activity was significantly associated with GPNMB expressing populations along with myeloid specific genes such as *TLR4* (Figure 4E), being one of the most strongly downregulated transcription factors in GPNMB knockouts along with STAT5A, IRF2 and STAT1 (Supplementary 3D). IRF8 has been shown to functionally integrate IFN-gamma signals to induce genes involved in macrophage antimicrobial defenses subsequently producing inflammatory cytokines that activate early immune responses (Dror *et al.* 2007). Ultimately, IRF8 regulates GPNMB expression levels by being a directly bound transcription factor at the promoter of GPNMB predicted by TRANSFAC match between the transcription factor and its predicted binding site (Figure 4F, Matys *et al.* 2003) and validated using the CHEA Transcription Factor Binding Site Profiles dataset (Rouillard *et al.* 2016, Lachmann *et al.* 2010).

GPNMB Is Upregulated To Counteract The Proinflammatory Signals of Interferons

GBM cells are known to produce interferons to promote survival in response to DNA damage caused by radiation therapy where acute exposure of GBM cells to high concentrations of type I interferons cause cell cycle arrest and apoptosis, while chronic exposure to lower concentrations provide pro-survival advantages (Cheon *et al.* 2023). We have previously shown that treatment-naïve GBM samples acquire a pattern of tumor-intrinsic immunomodulatory signatures as a response to SoC therapy (Qazi *et al.* 2022).

In PDX mice treated with SoC there was an enrichment of canonical cytokine signaling pathways compared to controls (Figure 5A). Interferon-alpha (Type-I) and Interferon-gamma (Type-II) were strongly enriched, in addition to TNF-alpha, TGF-beta, IL-6 and IL-2 pathways. Tracking samples through SoC regimens revealed a pseudotime

progression along with a hallmark Epithelial–Mesenchymal Transition gene signature associated among the SoC treated cohort (Figure 5B). Along the trajectory as the mesenchymal signature becomes stronger, IFN-gamma and IRF8 expression increases accordingly. In TCGA GBM, IRF8 has a moderate correlation with GPNMB (R=0.48) and is the IRF most closely correlated with GPNMB (Figure 5C). In patient tissue samples, clustered analysis of members in interferon signaling members strongly associated GPNMB with IRF8 and interferon receptor subunits IFNGR2 and IFNLR1 in the mesenchymal subtype of GBM (Figure 5D) and myeloid cells (Figure 5E) in particular. Taken together, GBMs respond to interferon signals and evolve in response to SoC treatments along with immune activation to upregulate GPNMB.

Discussion

Here we employed a series of GBM models to examine the role of GPNMB in tumor intrinsic biology of GBM as well as an active member in the immune microenvironment. We first identified GPNMB to be upregulated in GBM as it was absent in both healthy neural stem cells and the adult human brain. We examined the role of GPNMB in several aspects of GBM progression, including proliferation and tumor development *in vivo* indicating a role in GBM progression. Next, we observed the increased presence of GPNMB in recurrence at the protein level of GBM cells and macrophages. While previous studies have indicated an association with GPNMB in GBM recurrence, this was found at the RNA level and been attributed to immune populations (Xiong *et al.* 2022). We show GPNMB to be upregulated at the protein level of patient

matched samples, with and without the immune microenvironment intact and can be in response to abiotic therapeutic pressures (i.e. Standard of Care).

PDX models of GBM are valuable for their accurate recapitulation of human biology but lack an immune system. To examine the role of GPNMB in the tumor microenvironment, we used syngeneic mouse models harboring GL261 to provide a complimentary system. Similar biology was observed where the absence of GPNMB lead to a less aggressive phenotype. GPNMB was again associated with an immune function, which could be due to its presence in both the GBM cells and macrophage populations. It was recently reported immune evasion is an acquired trait by GBM through an epigenetic immunoediting mechanism (Gangoso *et al.* 2021). Due to immune attack, GBM activated transcription factors display myeloid-affiliated transcriptional program which associated with recruiting tumor-associated macrophages and was common in human mesenchymal GSCs (Gangoso *et al.* 2021). Researchers proposed this to be conducted through IRF8, a myeloid-specific master transcription factor that is typically silent in NSCs. While *IRF8* was the 12th most upregulated gene based on a Log-Fold Change, researchers did not comment on GPNMB to be the top upregulated gene in immune evasive populations.

We show GPNMB to be upregulated in GBM cells due to the inflammatory signature, a dynamic and continually evolving process displayed between GBM cells and immune cells alike. GPNMB could be associated with the inflammatory signature in recurrent GBM for three reasons: 1) GPNMB has been associated with wound healing (Silva *et al.* 2018) and after GBM patients undergo an extensive brain surgery to debulk the tumor the brain ultimately needs to heal the traumatic wounds, 2) GBM is a notoriously

immune-suppressive environment with a large macrophage population and GPNMB could be a mechanism GBM cells hijack to defend against the inflammatory cytotoxic function of T cells (Kobayashi *et al.* 2018), 3) Radiation therapy directly causes DNA damage along with immunomodulatory effects through interferon mechanisms (Zhang *et al.* 2020). We show GPNMB to be correlated with an inflammatory signature because of its immune-suppressive function and a possible explanation for conflicting yet complimentary literature of the past. While it has been shown that the use of interferon therapy as an adjuvant treatment for GBM may be beneficial, success in clinical trials is associated with Type I interferons. IFN-gamma is the sole member of the Type II interferon class and works through independent interferon receptors.

Clinical trials targeting GPNMB in other cancers have proven safe in the past yet unsuccessful. Potential reasons for treatment failure could be due to large time gaps between administering doses, or the heterogeneity within tumors. To date, no clinical trials have been conducted against GPNMB in GBM patients. Together, we show GPNMB to be a potentially valuable target in GBM to effectively eliminate cancer cells and the supportive niche while leaving healthy brain tissue unharmed. Further studies are needed to develop new therapeutic strategies for targeting GPNMB in combination with existing therapies.

Materials and Methods

Culturing Cell Lines

Human GBM samples were acquired from consenting patients, as approved by Hamilton Health Sciences and the McMaster Health Sciences Research Ethics Board. Tumor specimens were processed using previously published protocols (Chokshi *et al.* 2020). GBMs were then cultured in Neurocult Complete (NCC) media, a defined and commercially available serum-free neural stem cell medium (STEMCELL Technologies, Cat.05751), supplemented with human recombinant epidermal growth factor (20ng/mL: STEMCELL Technologies, Cat.78006), basic fibroblast growth factor (20ng/mL; STEMCELL Technologies Cat.78006), heparin (2 µg/mL 0.2% Heparin Sodium Salt in PBS; STEMCELL technologies, Cat.07980), antibiotic-antimycotic (1X; Wisent, Cat# 450-115-EL). Tumorspheres derived from these cultures were expanded on polyornithine-laminin coated plates for adherent growth until sufficient populations were acquired for experimental purposes. Passaging consisted of dissociating a 10cm dish with 1 mL of TrypLE (ThermoFisher Cat. 25200056) for 5 min at 37°C followed by collection with PBS and centrifugation at 300g. Neural stem cells were derived and propagated in a similar fashion, as previously published (Suk 2022, STAR Protocols).

RNAseq Sample Processing and Quality Assurance

Cells were sent for RNA extraction and RNAseq with Illumina HiSeq 2500 V4 SR. For analysis, four sets of comparisons were performed: 1) BT CD133+ vs CD133-; 2) NSC CD133+ vs CD133-; 3) CD133+ NSC vs CD133+ BT; and 4) CD133- NSC vs CD133- BT. Data was filtered using a CPM threshold of 3.5 for all comparisons. Multidimensional

scaling (MDS) plot showed a separation of the samples in the four comparisons. Using a smear plot, the pattern of gene expressions at different levels were examined to check for potential artifacts with no significant artifacts being observed at this CPM cutoff.

Determining Differentially Expressed (DE) Genes and Ranks

The standard method in the EdgeR software, Quasi-likelihood F-test, was used for DE determination in edgeR because we have the minimal number of samples required (minimum 4 samples total and at least 2 per group) and it is more stringent than the classical and likelihood ratio methods. The ranking score for each gene is generated by p-values and fold changes from the analysis with the following formula: sign(logFC) x $-\log_{10}$(p-value) where: sign(logFC) determines the direction of the change with +ve as up-regulation and –ve as down, $-\log_{10}$(p-value) determine the scale of ranking, the lower the p-value, the higher the score. The genes are ordered from top up-regulated to down-regulated ones as .rnk files (SS02 EM Folder). We use this ranking score as input for GSEA analysis.

Gene Set Enrichment Analysis (GSEA)

GSEA was performed for all 4 comparisons using the .rnk files with the gene set: Human_GOBP_AllPathways_with_GO_iea_December_24_2015_symbol.gmt. 1000 permutations were carried out with random seed parameter = 349. The result comparing all the GSEA analysis can be found at SS02 EM Folder in the file Pathway.xlsx. The pathways identified in GSEA1, GSEA2, GSEA3, and GSEA4 are listed in an excel file with the normalized enrichment score (NES) and FDR q-value. It is important to note that

not all the pathways have enrichment values provided by all four GSEA analysis. This is due to the difference in the genes we input for GSEA analysis. It is the standard protocol for RNAseq analysis to filter out genes with low expression and for each comparison, there are different set of genes being filtered out. To make the results of all four GSEA analysis completely comparable, RNAseq data was reanalyzed using only the protein_coding genes without gene expression filter, see section 1.7 for details.

Enrichment Maps (EM)

Because of the high degree of similarity between 1) CD133+ vs CD133- in NSC (GSEA2) and BT (GSEA1); and 2) NSC vs BT in CD133+ (GSEA3) and CD133- (GSEA4), combined Enrichment Maps were generated (A: GSEA1 and GSEA2; B: GSEA3 and GSEA4). Enrichment maps were generated with Jaccard Coefficient of 0.25 (for edges) and FDR q-value cutoff at 0.0001 (for nodes). A link to the original cytoscape file (.cys) used to generate the figure was included in the legend. The .cys file contains one EM with the same setting (FDR q-value and Jaccard Coefficient) and one EM with much less stringent conditions (FDR q-value < 0.1, p-value < 0.05, Jaccard Coefficient > 0.25) to reveal more pathways in the analysis.

Stem-Cell Specific Pathways Differentiating Tumor from Normal

In order to compare results from two separate GSEA analysis, several steps were taken to ensure that all input parameters were identical. We regenerated .rnk files that include all genes and are no longer filtered by CPM cutoffs (which filtered out different genes depending on the expressions among the samples). Instead, all protein_coding genes

were used for normalization and ranking. This led to identical genes (both in number and identity) used in GSEA calculation against the same gene sets (.gmt file) for each analyses and the results contained enrichment scores for exactly the same pathways for direct comparison. To assess the significance of the difference observed in enrichment scores, z-values were calculated using the direction of enrichment and nominal p-values (not calculated by permutation) from GSEA results. Because z-values are theoretically normalized values with levels of change and standard deviation incorporated within, the z-value of the pathway from one analysis can be compared with z-value of the same pathway from another analysis, provided all other parameters are the same. The difference between the z-scores of each pathway can be directly used to calculate statistical significance ($p < 0.05$ is equivalent to $z > 1.644$). Pathways with significant differences ($p < 0.01$) were selected to generate EM. GSEA results (we generated new GSEA1c, GSEA2c, GSEA3c, and GSEA4c) from all four comparisons were combined to identify differentiating pathways.

Online Databses

To incorporate publicly available data sets, the GEPIA2 interface was utilized to compare correlations of individual genes, or genome-wide gene expression profiles between GBM specimens of The Cancer Genome Atlas (TCGA) and normal brain tissue of the Genotype-Tissue Expression (GTEx) portal as previously described (Tang et al., 2017).

Generating Gene Knockout Constructs

Guide RNAs (sgRNAs) targeting AAVS1 (GGGGCCACTAGGGACAGGAT) and GPNMB (KO-A: AATGATGGTACAGACCTCCG, KO-B: AGGAATCCTACTCAGCTCCA) were obtained from the TKOv3 library (Hart *et al* 2017) and cloned into lentiCRISPRv2 constructs (Addgene Cat.52961). Successful ligations were validated using Sanger sequencing and each construct was packaged independently into lentiviruses using second-generation packaging constructs. Briefly, HEK293T cells were seeded at 10×10^6 cells per T75 flask and incubated overnight in high-glucose DMEM media with 2 mM L-glutamine and 1 mM sodium pyruvate (ThermoFisher Cat.11995065), supplemented with 1% non-essential amino acid solution (ThermoFisher Cat.11140050) and 10% fetal bovine serum (Gibco Cat.12483020). The following day, the HEK293T media was replaced with viral harvesting media consisting of HEK media supplemented with 10 mM HEPES (ThermoFisher, Cat#: 15630080) and 1 mM sodium butyrate (Sigma–Aldrich, Cat#: 303410).

Transfection was conducted with a mixture of psPAX2 (8.0 ug; Addgene #12260), pMDG.2 (3.0 ug; Addgene #12259), TKOv3 plasmid library (8.0 ug) and polyethylenimine (PEI, 57ug) (Sigma–Aldrich, Cat.408719) in 1.3 mL of Opti-MEM. After incubating the mixture for 15 min at room temperature, the PEI/DNA mixture was carefully added to the T75 flasks in dropwise fashion. Viral supernatants were collected 48 hours after transfection and then concentrated using ultracentrifugation (20,000 rpm for 2 hours at 4 °C) before being snap frozen and stored at − 80 °C.

Cell Proliferation Assay

Single cells were plated in a 96-well plate at a density of 1,000 cells/200 µL per well and incubated at 37°C and 5% CO^2 for five days. 20 µL of Presto Blue (ThermoFisher, Cat.A13262), a fluorescent cell metabolism indicator, was added to each well four hours prior to reading out the assy. Fluorescence was measured using a FLUOstar Omega Fluorescence 556 Microplate reader (BMG LABTECH) with excitation and emission wavelengths of 544nm and 590nm respectively. Readings were then analyzed using Omega analysis software. Proliferation was calculated for each well by subtracting the average RFI of blank wells from the RFI of individual wells. Mean RFI was plotted for each well being tested as a side-by-side comparison of proliferation.

Western Blots

Cells pellets were lysed in RIPA buffer (50mM Tris HCl pH 8.0, 150mM NaCl, 1% NP-40, 0.5% sodium deoxycholate, and 0.1% SDS) containing HALT™ Protease and Phosphatase Inhibitor Cocktail (ThermoFisher Cat.78440) and placed on an active nutator in 4°C for 1 hour. Once complete, centrifugation took place at 14,000rcf at 4°C for 10 minutes. Supernatant was collected and protein concentration was determined using the Bradford method (BioRad). 30µg total protein was loaded in all lanes, and proteins were resolved on 4%–12% Novex Bis-Tris gradient gels (Invitrogen) at 100V for 60 minutes and transferred to Immobilon-P PVDF membranes (Millipore) at 200mA for 120 minutes. Membranes were blocked in TBS-T containing 5% BSA for 30 minutes at room temperature followed by the addition of primary antibodies to be incubated at 4^{o}C on a rocker at slow speeds. The following morning, membranes were washed repeatedly with

TBS-T followed by incubation with secondary antibodies in TBS-T containing 5% BSA for 60 minutes. After repeated washes in TBS-T membranes were imaged. Antibody-bound proteins were visualized using LICOR Odyssey DLx.

Antibodies were purchased and used at the following concentrations: Human GPNMB (Cell Signaling Technologies, E4D7P Cat.38313), Mouse GPNMB (Abcam, EPR18226-147, Cat.ab188222), Beta-Actin (Cell Signaling Technologies, 13E5 Cat.4970, 1:5000), anti-Mouse IgG Secondary (LICOR, 926-68070, 1:10,000), anti-Rabbit IgG Secondary (LICOR, 926-32211, 1:10,000).

Animal Studies and Tumor Analysis

Animal studies were performed in accordance with guidelines outlined by Animal Use Protocols of McMaster University Central Animal Facility. Intracranial injections were conducted in 6-8 week old NOD/SCID gamma (NSG) or C57BL/6 mice as previously described (Chokshi *et al.* 2021) using GBM4 and GBM8 ($1x10^5$ cells per mouse) or with MBT06 and ($1x10^6$ cells per mouse). Briefly, a small burr hole was drilled 2mm behind the coronal suture and 3mm to the right of the sagittal suture. Cells suspended in 10 µL PBS were injected intracranially using a Hamilton syringe (Hamilton, Cat#7635-01) into the right frontal lobes. Animals were sacrificed at humane endpoint followed by perfusions using 10% formalin and collected brains were sliced into 2mm thick sections with a brain-slicing matrix for paraffin embedding and H&E staining. Images were captured using an Aperio Slide Scanner (Leica Biosystems) and analyzed using ImageScope v11.1.2.760 software (Aperio). Survival studies utilized the number of days post-surgery and input for Kaplan-Meier analysis.

Immunohistochemistry (IHC)

GPNMB IHC was performed on Patient Derived Xenograft (PDX) brain tissues, patient tumor samples, or Normal Human Brain Tissue MicroArray (Novus Biologics, Cat.NBP2-78062). Antigen retrieval was performed using Epitope Retrieval Buffer (ER2) (Leica, Cat#AR9640-Leica) for 20 minutes at 100°C. Antibodies were diluted in Powervision IHC Super Blocker (Leica, Cat#PV6122) and stained for 15 minutes. GPNMB antibody (Cell Signaling Technologies, E4D7P Cat.38313) was diluted in TBS buffer with 1% BSA (1:500) and stained overnight at 4 °C. Slides were treated with a peroxidase block, developed with DAB and counterstained with hematoxylin all contained in the Leica Bond Polymer Refine Detection Kit (Leica, Cat#DS9800). Slides were then covered with Permount. The digitization of the immunohistochemically stained TMA histology slides was performed using the Olympus® VS120 Slide Scanner. Data was acquired through the HALO® Image Analysis Platform by Indica Labs with quantitative analysis being performed using HALO® Multiplex IHC module in combination with HALO® TMA module.

References

Alanio C, Binder ZA, Chang RB, Nasrallah MP, Delman D, Li JH, Tang OY, Zhang LY, Zhang JV, Wherry EJ, O'Rourke DM, Beatty GL. Immunologic Features in De Novo and Recurrent Glioblastoma Are Associated with Survival Outcomes. Cancer Immunol Res. 2022 Jul 1;10(7):800-810. doi: 10.1158/2326-6066.CIR-21-1050. PMID: 35507919; PMCID: PMC9250610.

Bao S, Wu Q, McLendon RE, Hao Y, Shi Q, Hjelmeland AB, Dewhirst MW, Bigner DD, Rich JN. Glioma stem cells promote radioresistance by preferential activation of the DNA damage response. Nature. 2006 Dec 7;444(7120):756-60. doi: 10.1038/nature05236. Epub 2006 Oct 18. PMID: 17051156.

Bauer B, Steinle A. HemITAM: A single tyrosine motif that packs a punch. Sci Signal. 2017 Dec 5;10(508):eaan3676. doi: 10.1126/scisignal.aan3676. PMID: 29208681.

Bowman RL, Wang Q, Carro A, Verhaak RG, Squatrito M. GlioVis data portal for visualization and analysis of brain tumor expression datasets. Neuro Oncol. 2017 Jan;19(1):139-141. doi: 10.1093/neuonc/now247. Epub 2016 Nov 9. PMID: 28031383; PMCID: PMC5193031.

Cavalheiro VJ, Campos ACP, Lima LGCA, Roça CT, Docema MFL, Lancellotti CLP, Martinez RCR, Pagano RL, Chammas R, Teixeira MJ, Maldaun MVC, Neville IS. Unraveling the peripheral and local role of inflammatory cytokines in glioblastoma

survival. Cytokine. 2023 Jan;161:156059. doi: 10.1016/j.cyto.2022.156059. Epub 2022 Oct 19. PMID: 36272241.

Cheon H, Borden EC, Stark GR. Interferons and their stimulated genes in the tumor microenvironment. Semin Oncol. 2014 Apr;41(2):156-73. doi: 10.1053/j.seminoncol.2014.02.002. Epub 2014 Feb 14. PMID: 24787290; PMCID: PMC4118773.

Chokshi CR, Savage N, Venugopal C, Singh SK. A Patient-Derived Xenograft Model of Glioblastoma. STAR Protoc. 2020 Nov 21;1(3):100179. doi: 10.1016/j.xpro.2020.100179. PMID: 33377073; PMCID: PMC7757408.

De Leo A, Ugolini A, Veglia F. Myeloid Cells in Glioblastoma Microenvironment. Cells. 2020 Dec 24;10(1):18. doi: 10.3390/cells10010018. PMID: 33374253; PMCID: PMC7824606.

Dror N, Alter-Koltunoff M, Azriel A, Amariglio N, Jacob-Hirsch J, Zeligson S, Morgenstern A, Tamura T, Hauser H, Rechavi G, Ozato K, Levi BZ. Identification of IRF-8 and IRF-1 target genes in activated macrophages. Mol Immunol. 2007 Jan;44(4):338-46. doi: 10.1016/j.molimm.2006.02.026. Epub 2006 Apr 4. PMID: 16597464.

Feng X, Zhang L, Ke S, Liu T, Hao L, Zhao P, Tu W, Cang S. High expression of GPNMB indicates an unfavorable prognosis in glioma: Combination of data from the GEO and

CGGA databases and validation in tissue microarray. Oncol Lett. 2020 Sep;20(3):2356-2368. doi: 10.3892/ol.2020.11787. Epub 2020 Jun 26. PMID: 32782553; PMCID: PMC7400985.

Gangoso E, Southgate B, Bradley L, Rus S, Galvez-Cancino F, McGivern N, Güç E, Kapourani CA, Byron A, Ferguson KM, Alfazema N, Morrison G, Grant V, Blin C, Sou I, Marques-Torrejon MA, Conde L, Parrinello S, Herrero J, Beck S, Brandner S, Brennan PM, Bertone P, Pollard JW, Quezada SA, Sproul D, Frame MC, Serrels A, Pollard SM. Glioblastomas acquire myeloid-affiliated transcriptional programs via epigenetic immunoediting to elicit immune evasion. Cell. 2021 Apr 29;184(9):2454-2470.e26. doi: 10.1016/j.cell.2021.03.023. Epub 2021 Apr 14. PMID: 33857425; PMCID: PMC8099351.

Hambardzumyan D, Gutmann DH, Kettenmann H. The role of microglia and macrophages in glioma maintenance and progression. Nat Neurosci. 2016 Jan;19(1):20-7. doi: 10.1038/nn.4185. PMID: 26713745; PMCID: PMC4876023.

Hart T, Tong AHY, Chan K, Van Leeuwen J, Seetharaman A, Aregger M, Chandrashekhar M, Hustedt N, Seth S, Noonan A, Habsid A, Sizova O, Nedyalkova L, Climie R, Tworzyanski L, Lawson K, Sartori MA, Alibeh S, Tieu D, Masud S, Mero P, Weiss A, Brown KR, Usaj M, Billmann M, Rahman M, Constanzo M, Myers CL, Andrews BJ, Boone C, Durocher D, Moffat J. Evaluation and Design of Genome-Wide CRISPR/SpCas9 Knockout Screens. G3 (Bethesda). 2017 Aug 7;7(8):2719-2727. doi: 10.1534/g3.117.041277. PMID: 28655737; PMCID: PMC5555476

Huang Y, Motta E, Nanvuma C, Kuhrt LD, Yuan Y, Xia P, Lubas M, Zhu S, Schnauss M, Qazi N, Hu F, Zhang H, Lei T, Synowitz M, Flüh C, Kettenmann H. Microglia/macrophage-derived human CCL18 promotes glioma progression via CCR8-ACP5 axis analyzed in humanized slice model. Cell Rep. 2022 Apr 12;39(2):110670. doi: 10.1016/j.celrep.2022.110670. PMID: 35417708.

Johnson BE, Mazor T, Hong C, Barnes M, Aihara K, McLean CY, Fouse SD, Yamamoto S, Ueda H, Tatsuno K, Asthana S, Jalbert LE, Nelson SJ, Bollen AW, Gustafson WC, Charron E, Weiss WA, Smirnov IV, Song JS, Olshen AB, Cha S, Zhao Y, Moore RA, Mungall AJ, Jones SJM, Hirst M, Marra MA, Saito N, Aburatani H, Mukasa A, Berger MS, Chang SM, Taylor BS, Costello JF. Mutational analysis reveals the origin and therapy-driven evolution of recurrent glioma. Science. 2014 Jan 10;343(6167):189-193. doi: 10.1126/science.1239947. Epub 2013 Dec 12. PMID: 24336570; PMCID: PMC3998672.

Kim H, Zheng S, Amini SS, Virk SM, Mikkelsen T, Brat DJ, Grimsby J, Sougnez C, Muller F, Hu J, Sloan AE, Cohen ML, Van Meir EG, Scarpace L, Laird PW, Weinstein JN, Lander ES, Gabriel S, Getz G, Meyerson M, Chin L, Barnholtz-Sloan JS, Verhaak RG. Whole-genome and multisector exome sequencing of primary and post-treatment glioblastoma reveals patterns of tumor evolution. Genome Res. 2015 Mar;25(3):316-27. doi: 10.1101/gr.180612.114. Epub 2015 Feb 3. PMID: 25650244; PMCID: PMC4352879.

Kobayashi M, Chung JS, Beg M, Arriaga Y, Verma U, Courtney K, Mansour J, Haley B, Khan S, Horiuchi Y, Ramani V, Harker D, Gopal P, Araghizadeh F, Cruz PD Jr, Ariizumi K. Blocking Monocytic Myeloid-Derived Suppressor Cell Function via Anti-DC-HIL/GPNMB Antibody Restores the In Vitro Integrity of T Cells from Cancer Patients. Clin Cancer Res. 2019 Jan 15;25(2):828-838. doi: 10.1158/1078-0432.CCR-18-0330. Epub 2018 Jul 26. PMID: 30049749; PMCID: PMC7315386.

Kuan CT, Wakiya K, Dowell JM, Herndon JE 2nd, Reardon DA, Graner MW, Riggins GJ, Wikstrand CJ, Bigner DD. Glycoprotein nonmetastatic melanoma protein B, a potential molecular therapeutic target in patients with glioblastoma multiforme. Clin Cancer Res. 2006 Apr 1;12(7 Pt 1):1970-82. doi: 10.1158/1078-0432.CCR-05-2797. PMID: 16609006.

Lachmann A, Xu H, Krishnan J, Berger SI, Mazloom AR, Ma'ayan A. ChEA: transcription factor regulation inferred from integrating genome-wide ChIP-X experiments. Bioinformatics. 2010 Oct 1;26(19):2438-44. doi: 10.1093/bioinformatics/btq466. Epub 2010 Aug 13. PMID: 20709693; PMCID: PMC2944209.

Liguori M, Digifico E, Vacchini A, Avigni R, Colombo FS, Borroni EM, Farina FM, Milanesi S, Castagna A, Mannarino L, Craparotta I, Marchini S, Erba E, Panini N, Tamborini M, Rimoldi V, Allavena P, Belgiovine C. The soluble glycoprotein NMB (GPNMB) produced by macrophages induces cancer stemness and metastasis via CD44 and IL-33. Cell Mol Immunol. 2021 Mar;18(3):711-722. doi: 10.1038/s41423-020-0501-0. Epub 2020 Jul 29. PMID: 32728200; PMCID: PMC8027814.

Liu G, Yuan X, Zeng Z, Tunici P, Ng H, Abdulkadir IR, Lu L, Irvin D, Black KL, Yu JS. Analysis of gene expression and chemoresistance of CD133+ cancer stem cells in glioblastoma. Mol Cancer. 2006 Dec 2;5:67. doi: 10.1186/1476-4598-5-67. PMID: 17140455; PMCID: PMC1697823.

Liu H, Sun Y, Zhang Q, Jin W, Gordon RE, Zhang Y, Wang J, Sun C, Wang ZJ, Qi X, Zhang J, Huang B, Gui Q, Yuan H, Chen L, Ma X, Fang C, Liu YQ, Yu X, Feng S. Pro-inflammatory and proliferative microglia drive progression of glioblastoma. Cell Rep. 2021 Sep 14;36(11):109718. doi: 10.1016/j.celrep.2021.109718. PMID: 34525361.

Louis DN, Perry A, Wesseling P, Brat DJ, Cree IA, Figarella-Branger D, Hawkins C, Ng HK, Pfister SM, Reifenberger G, Soffietti R, von Deimling A, Ellison DW. The 2021 WHO Classification of Tumors of the Central Nervous System: a summary. Neuro Oncol. 2021 Aug 2;23(8):1231-1251. doi: 10.1093/neuonc/noab106. PMID: 34185076; PMCID: PMC8328013.

Marinari E, Allard M, Gustave R, Widmer V, Philippin G, Merkler D, Tsantoulis P, Dutoit V, Dietrich PY. Inflammation and lymphocyte infiltration are associated with shorter survival in patients with high-grade glioma. Oncoimmunology. 2020 Jun 21;9(1):1779990. doi: 10.1080/2162402X.2020.1779990. PMID: 32923142; PMCID: PMC7458651.

Matys V, Fricke E, Geffers R, Gössling E, Haubrock M, Hehl R, Hornischer K, Karas D, Kel AE, Kel-Margoulis OV, Kloos DU, Land S, Lewicki-Potapov B, Michael H, Münch R, Reuter I, Rotert S, Saxel H, Scheer M, Thiele S, Wingender E. TRANSFAC: transcriptional regulation, from patterns to profiles. Nucleic Acids Res. 2003 Jan 1;31(1):374-8. doi: 10.1093/nar/gkg108. PMID: 12520026; PMCID: PMC165555.

Meyer M, Reimand J, Lan X, Head R, Zhu X, Kushida M, Bayani J, Pressey JC, Lionel AC, Clarke ID, Cusimano M, Squire JA, Scherer SW, Bernstein M, Woodin MA, Bader GD, Dirks PB. Single cell-derived clonal analysis of human glioblastoma links functional and genomic heterogeneity. Proc Natl Acad Sci U S A. 2015 Jan 20;112(3):851-6. doi: 10.1073/pnas.1320611111. Epub 2015 Jan 5. PMID: 25561528; PMCID: PMC4311802.

Neftel C, Laffy J, Filbin MG, Hara T, Shore ME, Rahme GJ, Richman AR, Silverbush D, Shaw ML, Hebert CM, Dewitt J, Gritsch S, Perez EM, Gonzalez Castro LN, Lan X, Druck N, Rodman C, Dionne D, Kaplan A, Bertalan MS, Small J, Pelton K, Becker S, Bonal D, Nguyen QD, Servis RL, Fung JM, Mylvaganam R, Mayr L, Gojo J, Haberler C, Geyeregger R, Czech T, Slavc I, Nahed BV, Curry WT, Carter BS, Wakimoto H, Brastianos PK, Batchelor TT, Stemmer-Rachamimov A, Martinez-Lage M, Frosch MP, Stamenkovic I, Riggi N, Rheinbay E, Monje M, Rozenblatt-Rosen O, Cahill DP, Patel AP, Hunter T, Verma IM, Ligon KL, Louis DN, Regev A, Bernstein BE, Tirosh I, Suvà ML. An Integrative Model of Cellular States, Plasticity, and Genetics for Glioblastoma. Cell. 2019 Aug 8;178(4):835-849.e21. doi: 10.1016/j.cell.2019.06.024. Epub 2019 Jul 18. PMID: 31327527; PMCID: PMC6703186.

Patel AP, Tirosh I, Trombetta JJ, Shalek AK, Gillespie SM, Wakimoto H, Cahill DP, Nahed BV, Curry WT, Martuza RL, Louis DN, Rozenblatt-Rosen O, Suvà ML, Regev A, Bernstein BE. Single-cell RNA-seq highlights intratumoral heterogeneity in primary glioblastoma. Science. 2014 Jun 20;344(6190):1396-401. doi: 10.1126/science.1254257. Epub 2014 Jun 12. PMID: 24925914; PMCID: PMC4123637.

Phillips HS, Kharbanda S, Chen R, Forrest WF, Soriano RH, Wu TD, Misra A, Nigro JM, Colman H, Soroceanu L, Williams PM, Modrusan Z, Feuerstein BG, Aldape K. Molecular subclasses of high-grade glioma predict prognosis, delineate a pattern of disease progression, and resemble stages in neurogenesis. Cancer Cell. 2006 Mar;9(3):157-73. doi: 10.1016/j.ccr.2006.02.019. PMID: 16530701.

Qian X, Mills E, Torgov M, LaRochelle WJ, Jeffers M. Pharmacologically enhanced expression of GPNMB increases the sensitivity of melanoma cells to the CR011-vcMMAE antibody-drug conjugate. Mol Oncol. 2008 Jun;2(1):81-93. doi: 10.1016/j.molonc.2008.02.002. Epub 2008 Feb 16. PMID: 19383330; PMCID: PMC5527796.

Rabin, Ronald L. “CC, C, and CX3C Chemokines.” ScienceDirect, Academic Press, 1 Jan. 2003, www.sciencedirect.com/science/article/pii/B0123411033000449. Accessed 11 Mar. 2023.

Rouillard AD, Gundersen GW, Fernandez NF, Wang Z, Monteiro CD, McDermott MG, Ma'ayan A. The harmonizome: a collection of processed datasets gathered to serve and mine knowledge about genes and proteins. Database (Oxford). 2016 Jul 3;2016:baw100. doi: 10.1093/database/baw100. PMID: 27374120; PMCID: PMC4930834.

Saade M, Araujo de Souza G, Scavone C, Kinoshita PF. The Role of GPNMB in Inflammation. Front Immunol. 2021 May 12;12:674739. doi: 10.3389/fimmu.2021.674739. PMID: 34054862; PMCID: PMC8149902.

Schraufstatter IU, Zhao M, Khaldoyanidi SK, Discipio RG. The chemokine CCL18 causes maturation of cultured monocytes to macrophages in the M2 spectrum. Immunology. 2012 Apr;135(4):287-98. doi: 10.1111/j.1365-2567.2011.03541.x. PMID: 22117697; PMCID: PMC3372745.

Silva WN, Prazeres PHDM, Paiva AE, Lousado L, Turquetti AOM, Barreto RSN, de Alvarenga EC, Miglino MA, Gonçalves R, Mintz A, Birbrair A. Macrophage-derived GPNMB accelerates skin healing. Exp Dermatol. 2018 Jun;27(6):630-635. doi: 10.1111/exd.13524. Epub 2018 Apr 30. PMID: 29505115; PMCID: PMC6013359.

Singh SK, Hawkins C, Clarke ID, Squire JA, Bayani J, Hide T, Henkelman RM, Cusimano MD, Dirks PB. Identification of human brain tumour initiating cells. Nature. 2004 Nov 18;432(7015):396-401. doi: 10.1038/nature03128. PMID: 15549107.

Sørensen MD, Dahlrot RH, Boldt HB, Hansen S, Kristensen BW. Tumor-associated microglia/macrophages predict poor prognosis in high-grade gliomas and correlate with an aggressive tumor subtype. Neuropathol Appl Neurobiol. 2018 Feb;44(2):185-206. doi: 10.1111/nan.12428. Epub 2017 Sep 5. PMID: 28767130.

Sottoriva A, Spiteri I, Piccirillo SG, Touloumis A, Collins VP, Marioni JC, Curtis C, Watts C, Tavaré S. Intratumor heterogeneity in human glioblastoma reflects cancer evolutionary dynamics. Proc Natl Acad Sci U S A. 2013 Mar 5;110(10):4009-14. doi: 10.1073/pnas.1219747110. Epub 2013 Feb 14. PMID: 23412337; PMCID: PMC3593922.

Stupp R, Mason WP, van den Bent MJ, Weller M, Fisher B, Taphoorn MJ, Belanger K, Brandes AA, Marosi C, Bogdahn U, Curschmann J, Janzer RC, Ludwin SK, Gorlia T, Allgeier A, Lacombe D, Cairncross JG, Eisenhauer E, Mirimanoff RO; European Organisation for Research and Treatment of Cancer Brain Tumor and Radiotherapy Groups; National Cancer Institute of Canada Clinical Trials Group. Radiotherapy plus concomitant and adjuvant temozolomide for glioblastoma. N Engl J Med. 2005 Mar 10;352(10):987-96. doi: 10.1056/NEJMoa043330. PMID: 15758009.

Tang Z, Kang B, Li C, Chen T, Zhang Z. GEPIA2: an enhanced web server for large-scale expression profiling and interactive analysis. Nucleic Acids Res. 2019 Jul 2;47(W1):W556-W560. doi: 10.1093/nar/gkz430. PMID: 31114875; PMCID: PMC6602440.

Tatari N, Khan S, Livingstone J, Zhai K, Mckenna D, Ignatchenko V, Chokshi C, Gwynne WD, Singh M, Revill S, Mikolajewicz N, Zhu C, Chan J, Hawkins C, Lu JQ, Provias JP, Ask K, Morrissy S, Brown S, Weiss T, Weller M, Han H, Greenspoon JN, Moffat J, Venugopal C, Boutros PC, Singh SK, Kislinger T. The proteomic landscape of glioblastoma recurrence reveals novel and targetable immunoregulatory drivers. Acta Neuropathol. 2022 Dec;144(6):1127-1142. doi: 10.1007/s00401-022-02506-4. Epub 2022 Sep 30. PMID: 36178522.

Tejero R, Huang Y, Katsyv I, Kluge M, Lin JY, Tome-Garcia J, Daviaud N, Wang Y, Zhang B, Tsankova NM, Friedel CC, Zou H, Friedel RH. Gene signatures of quiescent glioblastoma cells reveal mesenchymal shift and interactions with niche microenvironment. EBioMedicine. 2019 Apr;42:252-269. doi: 10.1016/j.ebiom.2019.03.064. Epub 2019 Apr 3. PMID: 30952620; PMCID: PMC6491796.

Torrisi F, Alberghina C, D'Aprile S, Pavone AM, Longhitano L, Giallongo S, Tibullo D, Di Rosa M, Zappalà A, Cammarata FP, Russo G, Ippolito M, Cuttone G, Li Volti G, Vicario N, Parenti R. The Hallmarks of Glioblastoma: Heterogeneity, Intercellular Crosstalk and Molecular Signature of Invasiveness and Progression. Biomedicines. 2022 Mar 30;10(4):806. doi: 10.3390/biomedicines10040806. PMID: 35453557; PMCID: PMC9031586.

Uchida N, Buck DW, He D, Reitsma MJ, Masek M, Phan TV, Tsukamoto AS, Gage FH, Weissman IL. Direct isolation of human central nervous system stem cells. Proc Natl Acad Sci U S A. 2000 Dec 19;97(26):14720-5. doi: 10.1073/pnas.97.26.14720. PMID: 11121071; PMCID: PMC18985.

Verhaak RG, Hoadley KA, Purdom E, Wang V, Qi Y, Wilkerson MD, Miller CR, Ding L, Golub T, Mesirov JP, Alexe G, Lawrence M, O'Kelly M, Tamayo P, Weir BA, Gabriel S, Winckler W, Gupta S, Jakkula L, Feiler HS, Hodgson JG, James CD, Sarkaria JN, Brennan C, Kahn A, Spellman PT, Wilson RK, Speed TP, Gray JW, Meyerson M, Getz G, Perou CM, Hayes DN; Cancer Genome Atlas Research Network. Integrated genomic analysis identifies clinically relevant subtypes of glioblastoma characterized by abnormalities in PDGFRA, IDH1, EGFR, and NF1. Cancer Cell. 2010 Jan 19;17(1):98-110. doi: 10.1016/j.ccr.2009.12.020. PMID: 20129251; PMCID: PMC2818769.

Vora P, Venugopal C, Salim SK, Tatari N, Bakhshinyan D, Singh M, Seyfrid M, Upreti D, Rentas S, Wong N, Williams R, Qazi MA, Chokshi C, Ding A, Subapanditha M, Savage N, Mahendram S, Ford E, Adile AA, McKenna D, McFarlane N, Huynh V, Wylie RG, Pan J, Bramson J, Hope K, Moffat J, Singh S. The Rational Development of CD133-Targeting Immunotherapies for Glioblastoma. Cell Stem Cell. 2020 Jun 4;26(6):832-844.e6. doi: 10.1016/j.stem.2020.04.008. Epub 2020 May 27. PMID: 32464096.

Xie R, Okita Y, Ichikawa Y, Fikry MA, Huynh Dam KT, Tran STP, Kato M. Role of the kringle-like domain in glycoprotein NMB for its tumorigenic potential. Cancer Sci. 2019

Jul;110(7):2237-2246. doi: 10.1111/cas.14076. Epub 2019 Jun 26. PMID: 31127873; PMCID: PMC6609797.

Xiong A, Zhang J, Chen Y, Zhang Y, Yang F. Integrated single-cell transcriptomic analyses reveal that GPNMB-high macrophages promote PN-MES transition and impede T cell activation in GBM. EBioMedicine. 2022 Sep;83:104239. doi: 10.1016/j.ebiom.2022.104239. Epub 2022 Aug 30. PMID: 36054938; PMCID: PMC9437813.

Zhang F, Manna S, Pop LM, Chen ZJ, Fu YX, Hannan R. Type I Interferon Response in Radiation-Induced Anti-Tumor Immunity. Semin Radiat Oncol. 2020 Apr;30(2):129-138. doi: 10.1016/j.semradonc.2019.12.009. PMID: 32381292.

Zhu C, Zou C, Guan G, Guo Q, Yan Z, Liu T, Shen S, Xu X, Chen C, Lin Z, Cheng W, Wu A. Development and validation of an interferon signature predicting prognosis and treatment response for glioblastoma. Oncoimmunology. 2019 Jun 12;8(9):e1621677. doi: 10.1080/2162402X.2019.1621677. PMID: 31428519; PMCID: PMC6685507.

Chapter 4: Therapeutic Targeting of GPNMB in Glioblastoma Models

Preamble

In this chapter, I present an original manuscript describing therapeutic targeting of GPNMB in glioblastoma using CAR-Ts in multiple mouse models generating a new immunotherapy for possible clinical development:

Savage, N., Zemp, F., Venugopal, C., Shaikh, V., Zhai, K., Chafe, S., Maich, M., Anand, A., Moffat, J., Mahoney, D., & Singh, S. K. Therapeutic Targeting of GPNMB in Glioblastoma Models. (manuscript in preparation)

Author contributions are as follows for the aforementioned manuscript: Conceptualization: N.S, S.K.S, D.M, and J.M;Resources: S.K.S, D.M, and J.M; Methodology, Investigation and Validation: N.S, F.Z, V.S, K.Z, W.M, and A.A; Software and formal analysis: N.S; Visualization: N.S, F.Z, and S.C; Writing – original draft preparation: N.S; Writing – review and editing: N.S, F.Z, C.V, J.M, D.M, S.K.S; Project administration and supervision: S.K.S, D.M, and J.M; Funding acquisition: S.K.S and J.M. All authors read and approved the manuscript.

I present data for the localization and abundance of GPNMB on plasma membranes of GBM cells to be targetable by immunotherapies, and the absence of GPNMB in normal tissues throughout the body proposing the using of CAR-Ts as a safe modality. Standard *in vitro* assays are employed to validate the functional activation and cytotoxic killing by CAR-Ts in a series of cell lines before progressing to evaluate efficacy

in vivo. While the study was ultimately successful in PDX models, building on our previous findings that GPNMB is upregulated in MDSCs, humanized mouse models were employed to determine the efficacy against tumor progression and on the tumor immune microenvironment.

Abstract

Glioblastoma (GBM) is an aggressive and uniformly fatal brain tumor with little clinical advancement of effective therapies for the past several decades. The heterogeneity present within GBM ultimately means multiple therapies will need to be administered to eradicate all populations effectively. Glycoprotein nonmetastatic melanoma protein B (GPNMB) has previously been identified as a targetable marker for antibodies in GBM but to date no human clinical trials have been conducted. The rapid advancement of immunotherapies, particularly genetically enhanced T cells (CAR-Ts) provides an opportunity to overcome the immunosuppressive microenvironment of GBM. We show GPNMB to be absent in normal tissue throughout the body, only exhibiting GPNMB protein in GBM cells and tumor associated macrophages. We then test the efficacy of a novel CAR-T against GPNMB in a series of mouse models and later combine it with our previously published CD133-targeting CAR-T to provide better coverage against GBM cells. Together, rational therapeutic combinations may offer potential relief to clinical patients by targeting the tumor supporting niche in addition to the tumor itself.

Introduction

While classical pharmacology has largely failed to provide benefits to brain cancer patients due to the semipermeable blood-brain barrier, rapid advances involving immunotherapies may provide solutions (Chokshi *et al.* 2021). Chimeric antigen receptor T cells (CAR-Ts) are genetically modified T-cells designed to target molecules specific to cancers while leaving normal tissues unharmed (Chokshi *et al.* 2021). CAR-T clinical trials for GBM have proven to be efficacious, but extreme heterogeneity within and among GBM patients likely means more than one target will be needed to eradicate the tumors entirely (Brown *et al.* 2015, Brown *et al.* 2016, O'Rourke *et al.* 2017, Liu *et al.* 2023). We have previously shown CD133 to be an effective CAR-T target in GBM models (Vora *et al.* 2020). However, CD133 expression by cells is interconvertible, meaning CD133- cells reacquire expression as it is essential in maintaining stem cell populations (Brescia *et al.* 2013). CD133+/- subpopulations have distinct transcriptomes which have been exploited before to target CD133+ cells (Venugopal *et al.* 2015). With CD133 being such a dynamic surface marker, the heterogeneity within tumours, differences among glioblastoma patients, and CD133- cells capable of gaining expression, a dual knockout method targeting CD133+/- subpopulations simultaneously would be advantageous over current therapeutic practices.

Glycoprotein nonmetastatic melanoma protein B (GPNMB) is a transmembrane glycoprotein that has emerged in several cancers including GBM to be an exploitable target by immunotherapies (Kopp *et al.* 2019, Ott *et al.* 2019, Yardley *et al.* 2015, Kuan *et al.* 2006). GPNMB expression has been associated with a more aggressive phenotype and studies have shown that targeting GPNMB with monoclonal antibodies reduces tumor

sizes in animal models of GBM, suggesting that it is a promising target (Kuan *et al.* 2006, Kuan *et al.* 2010).

Glembatumumab Vedotin, GV, is an antibody-drug conjugate against GPNMB and has been used in clinical trials of multiple cancers with minimal toxicity concerns (Kopp *et al.* 2019, Ott *et al.* 2019, Yardley *et al.* 2015, Kuan *et al.* 2006). GBM is known to be highly immunosuppressive which prevents immune cells from effectively attacking the tumor (Pearson *et al.* 2020). This is a complex process with multiple dimensions contributing to a lack of improvement for patients. Conflicting reports attribute the failure of immune checkpoint inhibitors in clinical trials to a lack of immune checkpoints present within the tumor or an absence of cytotoxic T cells at the tumor site (Omuro *et al.* 2018, McGranahan *et al.* 2016). Macrophages constitute a large population of cells in a bulk GBM tumor and contribute to immunosuppression (Morantz *et al.* 1979). Because macrophages have been credited with releasing soluble GPNMB into the microenvironment which can inhibit T cell activity, we investigate the potential of GPNMB as a valuable immunotherapy target to eradicate GBM cells and their supportive niche (Chung *et al.* 2009, Kobayashi *et al.* 2019).

Results

Validating Safety and Feasibility of a CAR-T Against GPNMB

We have previously shown GPNMB to be a viable target in GBM using due to its absence in normal brain tissue of fully grown adults. To prove CAR-Ts could be a safe modality, we first used a normal tissue microarray containing 23 normal tissue samples from throughout the body including vital organs such as the liver, stomach, kidney and colon (Figure 1A). Samples were stained using a human specific GPNMB antibody optimized using PDX blocks known to have a presence or absence of GPNMB as positive and negative controls respectively (Supplementary 1). Nearly complete absence of staining provided strong rationale CAR-Ts could cause minimal systemic toxicity. Any positive staining in the skin tissue or thymus tissue was attributed to known preferential localization of GPNMB to organelle membranes of melanosomes and lysosomes in skin (Tomihari *et al.* 2009) or internally within monocytes in the absence of microbial infections (Ripoll *et al.* 2007).

To validate GPNMB was present at the surface of GBM cells, GPNMB knockout clones of SK-MEL-2 (a high expressing positive control, Tse *et al.* 2006) were first generated and confirmed by western blot (Figure 1B). Commercially available anti-GPNMB antibody (R&D Systems, AF2550) has previously been validated for its utility in western blots and flow cytometry (Xie *et al.* 2019). An antibody titration was then performed on SK-MEL-2 which generated a curve successfully detecting surface expression in a dose dependent manner while a control isotype failed to generate signal (Figure 1C). Varying surface expression levels of GPNMB was then confirmed against multiple GBM lines providing targetability by immunotherapies (Figure 1D).

Developing a GPNMB CAR-T Against GBM

A second-generation CAR-T was developed to target GPNMB+ cells (Figure 2A). The CAR is composed of an extracellular domain which binds to GPNMB using the same binder sequence of GV, the fully human IgG2 antibody used in clinical trials. The intracellular domain contains the co-stimulatory domain CD28 and CD3-zeta to activate the T cell to kill the GPNMB-expressing (GPNMB+) cell. To examine efficacy of the GPNMB CAR-Ts, a CD19 CAR-T was used in conjunction as a control in standard *in vitro* assays. GFP in the CAR plasmid was used to confirm successful integration of the CAR-lentivirus into T cells and showed high transduction efficiency of both constructs (Figure 2B). CAR-Ts were expanded *ex vivo* for up to 14 days before testing efficacy. GPNMB CAR-Ts showed cytotoxic killing in a dose and time dependent manner in multiple GBM lines (Figure 2C, $p<0.01$). A visual swarming by GPNMB CAR-Ts against GBM cells was observed compared to unengaged CD19 CAR-Ts (Figure 4D). Cytotoxicity was then validated 24 hours after exposure by measuring levels of early-stage and mid-stage activation markers CD69 and CD25 respectively (Figure 2E). CD69 expression on PBMCs activated *in vitro* correlates with proliferative T cell responses (Maino *et al.* 1995, Prince *et al.* 1997, Cibrián *et al.* 2017). Sustained CD25 expression in CAR-Ts is predictive of robust anti-tumor functionality in antigen-stimulated CAR-Ts (Chang *et al.* 2015) but could also be attributed to long term exposure of IL-2 supplemented in cell media or to potential mismatch HLA-types of GBM cells and healthy donor PBMCs. The absence of CD69 in control CAR-Ts indicates antigen specific activation of GPNMB CAR-Ts.

To further validate efficacy of the GPNMB CAR-T against GBM samples, sustained proliferation was measured and determined to be significantly higher in GPNMB CAR-Ts against multiples GBMs after 3 days (Figure 2F, $p<0.01$). Secreted tumor necrosis factor (TNF-alpha) and interferon-gamma (IFN-gamma) were measured by ELISA where significantly stronger TNF-a and IFN-gamma responses were detected in the supernatant of GPNMB CAR-Ts relative to CD19 CAR-Ts when co-cultured with GBM (Figure 2G and 2H, $p<0.05$).

Testing GPNMB CAR-Ts in PDX Models

Using NSG mice to harbor patient derived GBM samples orthotopically, cells containing a Luciferase reporter gene were injected intracranially. Tumor sizes were measured on Day 6 via bioluminescence signal for mice to be divided evenly into cohorts, then injected with CAR-Ts on Day 7 (n = 6) (Figure 3A). Mice received a single dose of $1x10^6$ CAR-Ts intracranially and tumor sizes were measured weekly (Figure 3B). Tumor growth in the GPNMB CAR-T cohorts were significantly impaired compared to CD19 CAR-T controls and mice which received GPNMB CAR-Ts also exhibited significantly longer survival times indicating this to be an efficacious therapy *in vivo* (Figure 3C). All results were reproducible as a monotherapy against GPNMB+ GBM PDX models (Figures 3D).

Examining residual tumors of mice at endpoint for GPNMB did result in positive staining albeit with a less intense signal compared to CD19 CAR-T treated mice (Figure 3E). We attributed this to either antigen density below physiological threshold for CAR-Ts to engage, or increased GPNMB expression due to IFN-gamma in the microenvironment

after CAR-Ts had potentially exhausted. To ensure GPNMB+ cells were eliminated prior to exhaustion, mice were designated to be injected with GBMs and again treated with CAR-Ts but fresh brains were collected for flow cytometry ten days after treatment. Successfully, no GPNMB was detected at the surface of GBM cells in GPNMB CAR-T treated mice (Figure 3F). Expression of CD133 remained similar between CAR-T modalities indicating it was not being affected *in vivo* and remains a mutually distinct population in GBM to be targeted in a polytherapeutic approach.

Rational Combinations of CAR-Ts Targeting GBM Subpopulations

The hierarchy, distribution, and plasticity of GBM cells through tumor evolution *in vivo* is complex and beyond the breadth of this paper, but it was evident *in vitro* that mutually exclusive populations of GPNMB+ and CD133+ exists in addition to double positive populations could be targeted by our CAR-T constructs (Figure 4A). Therefore, we thought it was reasonable to suspect administering both CAR-T modalities could greatly improve treatment efficacy compared to a single CAR-T treatment. Previous experimental protocols were replicated with an additional regimen to administer a second dose of CAR-Ts after initial tumor responses was measured to improve survival outcomes (Figure 4B). Each round of injections consisted of $1x10^6$ CAR-Ts delivered intracranially, with Arm 4 consisting of $5x10^5$ CAR-Ts of each construct pooled into one injection. Tumor sizes were again measured weekly via bioluminescence signal (Figure 4C). Tumor growth of all treatment arms impaired tumor growth compared to CD19 CAR-T controls (Figure 4D). Mice receiving CD133 CAR-Ts showed a more beneficial response compared to GPNMB CAR-Ts suspected due to increased antigen presence *in vivo* (Figure 3F). Arm

4 showed a heightened response, significantly improving tumor control by Day 20 compared to controls and both monotherapies. Reduced tumor burden directly translated to improved survival times (Figure 4E). In addition to combined administration of CAR-Ts in Arm 4, additional arms were included in the study to determine if metronomic administration improved tumor control or survival times (Supplementary 3A-G). Ultimately, trends were present in sequentially administered therapies but did not meet statistical significance.

GPNMB as a Target to Eliminate Tumor Associated Macrophages

A major limitation to PDX models of GBM is the absence of an immune system but potentially attacking the GPNMB+ immunosuppressive niche could modulate the tumor microenvironment. Theoretically this could support the host immune system to penetrate and attack cancer cells in a similar manner to immune checkpoint inhibitors. In addition to its expression in GBM cells, GPNMB is also expressed in tumor promoting macrophages which play a crucial role in the immune response to GBM. Because of this, GPNMB CAR-Ts were tested against macrophages to determine if GPNMB can be a target against the tumor microenvironment in addition to the tumor itself.

Presence of GPNMB was first confirmed in the monocyte-macrophage lineage with an increased abundance towards M2 polarization (Figure 5A). Macrophage polarization was conducted using previously published protocols (Shi *et al.* 2017). To determine GPNMB would be accessible at the plasma membrane for CAR-Ts, flow cytometry was again employed and confirmed presence at the surface of M2-like macrophages while being absent in unprimed macrophages or monocytes (Figure 5B). Similarly to GBM

cytotoxic activity, GPNMB CAR-Ts increasingly displayed macrophage killing ability as effector concentrations increased or exposure time was prolonged (Figure 5C).

After patients undergo initial treatments for GBM the tumor inevitably recurs, and clinical options are limited. Additional treatments should always be considered on a case-by-case basis with a multidisciplinary team of healthcare providers, including neurosurgeons, medical oncologists, radiation oncologists, and neurologists if a personalized treatment option is to be developed. To test the feasibility of GPNMB CAR-Ts effectively targeting recurrent GBM, we validated the expression of GPNMB in a patient derived line which had previously been exposed to standard-of-care (BT972). Validation was conducted as previously described using western blots (Figure 5D). After confirming the presence of GPNMB in established PDX brains (Figure 5E) and expression at the surface of GBM cells for CAR-Ts to target (Figure 1D) a humanized mouse model was employed to determine a wholistic approach to targeting GPNMB in established tumors.

Tumor sizes in NOG-EXL mice were measured on Day 6 via bioluminescence and $1x10^6$ CAR-Ts were injected on Day 7 as previously described. Untransduced T cells were used as controls for this experiment instead of CD19 CAR-Ts to A) administer an equal number of total T cells between cohorts and B) leave the CD19+ B-lymphocyte population intact for tumor analysis. Weekly monitoring commenced and when it was observed one week after treatment that only 1 of 6 mice responded to treatment (Supplementary 3) it was determined a second round of CAR-Ts were to be administered. The lack of response could be attributed to a variety of reasons including poor CAR-T viability the day of injections, the humanized immune system rejecting the adoptive cell

therapy, or other underdetermined differences in biology of a new mouse strain and/or recurrent GBM. To overcome these potential pitfalls the second round of injections were increased to $3x10^6$ CAR-Ts per mouse to also account for increased tumor sizes. Of the control mice, 2 of 6 mice experienced stable tumor progression week-over-week before growth continued with 1 of 6 mice reaching humane endpoint before the fourth IVIS time point. Comparatively, 4 of 6 mice in the GPNMB CAR-T experienced dramatic tumor reduction week-over-week including the 2 mice with the largest tumors. Interestingly, the only mouse to experience response to treatment in the initial CAR-T injections did not benefit from the second round of treatment. One mouse remained unresponsive throughout treatments. Ultimately, significant therapeutic efficacy was achieved using GPNMB CAR-Ts against an established recurrent GBM model.

Discussion

GPNMB has been shown to be a viable target for monoclonal antibody drug therapies. We show GPNMB to be absent throughout the body, opening the way for CAR-T modalities to be administered systemically to patients. In summary, we present a novel method to target GPNMB+ glioblastoma cells in a series of glioblastoma models, proving the specificity, activation, and efficacy of CAR-Ts. We conclude that our CAR-T modality presents a viable strategy to target a clinically relevant population of GBM cells and could be expanded to other cancer types to include melanoma, breast cancer, osteosarcomas and potentially patients with metastatic cancers who are not provided any other means of treatment.

A CAR-T modality could greatly improve on existing therapies against GPNMB expressing tumors because of the persistence of CAR-Ts compared to antibodies. While the current version provides strong rationale for future development, its construction as a second-generation construct limits itself to the host of advancements made by next-generation CARs to improve persistence, efficacy and safety features.

In addition to the feasibility of GPNMB as a target in isolation, we prove the viability of GPNMB as a rational data driven co-target alongside CD133. While the combined treatments were effective in a preclinical model, improvements could be made by developing a Tandem CAR-T where the presence of either antigen is sufficient to initiate cytotoxic killing. Tandem CAR-Ts would greatly increase coverage of tumor killing by effectively doubling the number of available CAR-Ts compared to our current method. Also, different combinations of other antigens could increase tumor coverage while retaining safety, such as EGFRvIII for patients who express EGFRvIII but could lack GPNMB expression. With this method, the tumor could still be targeted alongside the TAMs.

In conclusion, GPNMB is a promising target for immunotherapy research for GBM as well as other cancers. Uncovering its role in the development and progression of cancer has opened new avenues for the treatment of cancer. The development of GPNMB-targeted immunotherapy is a complex and challenging process, but the results of recent clinical trials are encouraging and have provided a strong foundation for continued development. The story of GPNMB is a testament to the power of targeting the immune system in the treatment of cancer and the potential of immunotherapy research to change the lives of patients.

Materials and Methods

Flow Cytometry

Cells were dissociated using TrypLE (ThermoFisher Cat.12605010), resuspended in PBS containing 2mM EDTA (ThermoFisher Cat.AM9260G), and stained with 5ug GPNMB antibodies (R&D Systems, Cat.AF2550) or Normal Goat IgG Control (R&D Systems, Cat.AB-108-C) on ice for 20 minutes before being washed. After washing, Goat anti-Rabbit IgG (H+L) Cross-Adsorbed Secondary Antibody FITC was added at a 1:10,000 dilution and incubated on ice another 20 minutes. After washing, cell were run on a CytoFLEX flow cytometer (Beckman Coulter) with dead cells being excluded by 7AAD viability dye (1:100; Beckman Coulter Cat.A07704). Compensation was performed using mouse IgG CompBeads (BD Biosciences, Cat.552843).

Generation of Chimeric Antigen Receptor – T Cells

CAR constructs were packaged individually into lentivirus using second-generation packaging constructs. Briefly, HEK293T cells were seeded into T-75 cm2 flasks at a density of 10 million cells per flask and cultured in high-glucose DMEM with 2mM L-glutamine and 1mM sodium pyruvate supplemented with 1% non-essential amino acid solution and 10% fetal bovine serum. The following day, media was replaced with viral harvesting media (HEK culture media supplemented with 10mM HEPES and 1mM sodium butyrate). CAR plasmid 8.75µg, psPAX (8.75µg, Addgene Cat.12260) and pMD2.G (1.75µg, Addgene Cat.12259) were mixed with 58 µg polyethylenimin (PEI) in 1.3mL of Opti-MEM. After indubating for 15 minutes at room temperature, the PEI/DNA mixture was carefully added into the T75 flasks in a dropwise manner. Viral supernatants

were collected 72 hours after transfection and concentrated using ultracentrifugation (20,000 rpm for 2 hours at 4°C). Samples were resuspended in 100µL of XSFM and stored at −80°C until required.

Peripheral blood mononuclear cells (PBMCs) were collected from consenting healthy blood donors and grown in XSFM media (Irvine Scientific, Cat.91141). T cells were activated using Transact (Miltenyi Biotec, Cat.130-111-160) in 24-well plates supplemented with 100U/mL rhIL-2 (Peprotech, Cat.200-02). The following day, T cells were transduced with lentivirus and expanded into fresh media (XSFM media supplemented with 100U/mL rhIL-2) as required for up to 14 days until experimentation, or frozen for storage. Transduction efficiency was determined by GFP expression in T cells, analyzed using a CytoFLEX flow cytometer (Beckman Coulter). Dead cells were excluded using 7AAD the viability dye (1:100; Beckman Coulter, Cat.A07704).

Cytotoxicity Assay

Luciferase-expressing GBM cell lines (Target cells) were generated and plated at a concentration of 10^4 cells per well in 96-well plates containing 100uL of NCC media. CAR-T (Effector) cells were then added in 100uL at 0:1, 1:1, 2:1, and 5:1 Effector-to-Target (E:T) ratios and incubated at 37°C for 24 hours. Control wells were incubated without CAR-Ts to measure spontaneous lysis or treated with 1% Nonidet P-40 (NP40, Thermofisher, Cat#98379) to measure maximal lysis. At 6- and 24-hour time points D-firefly luciferin potassium salt (100 mg/mL) was added to each well ten minutes before readout. Measurements were conducted with a luminometer (Omega) for ten seconds and calculated as relative luminescence units (RLU).

Percent S*pecific* L*ysis* = 100 x [(S$pontaneous$ L$ysis\ RLU$ − T$est\ RLU$)]/[(S$pontaneous$ L$ysis\ RLU$ − L$ysis$ C$ontrol\ RLU$)]

CAR-T Activation

Activation assays were established similar to cytotoxicity assays using wild type GBM cells as target cells. CAR-Ts were co-cultured with target cells at a 1:1 ratio for 24 hours before being collected, centrifuged and washed. T cells were then stained for CD3 with PE-Cy7-conjugated mouse-anti-human CD3 antibody (BD Biosciences, Cat.563423), and GFP+/CD3+ cells were analyzed for activation markers CD25 (BD Biosciences Cat.555432) and CD69 (BD Biosciences, Cat.555533) by flow cytometry using a CytoFLEX flow cytometer (Beckman Coulter). Dead cells were excluded using 7AAD the viability dye (1:100; Beckman Coulter Cat.A07704). Compensation was performed using mouse IgG CompBeads (BD Biosciences, Cat#552843).

CAR-T Proliferation

CAR-T cells were co-cultured with target cells at a 1:1 ratio for 24 hours. Cells were then collected and GFP+/CD3+ cells were plated at a density of 1,000 cells/200 µL per well and incubated at 37°C and 5% CO^2 for three days. A fluorescent cell metabolism indicator, was then added to each well four hours prior to reading out the assy. Fluorescence was measured using a FLUOstar Omega Fluorescence 556 Microplate reader (BMG LABTECH) with excitation and emission wavelengths of 544nm and 590nm respectively. Readings were then analyzed using Omega analysis software.

CAR-T Cytokine Production

CAR-T cells were co-cultured with target cells at a 1:1 ratio for 24 hours. Supernatants were collected and stored at -80°C until required. DuoSet ELISA kits for human IFN-gamma (R&D Systems, Cat.DY285B) and human TNF-alpha (R&D Systems Cat.DY210) were used for quantification of cytokines, according to manufacturer's descriptions.

Animal Studies and Tumor Analysis

Animal studies were performed in accordance with guidelines outlined by Animal Use Protocols of McMaster University Central Animal Facility. Intracranial injections were conducted in 6-8 week old NOD/SCID gamma (NSG) mice as previously described (Chokshi *et al.* 2021) using GBM4 and GBM8 ($1x10^5$ cells per mouse). Briefly, a small burr hole was drilled 2mm behind the coronal suture and 3mm to the right of the sagittal suture. Cells suspended in 10 µL PBS were injected intracranially using a Hamilton syringe (Hamilton, Cat#7635-01) into the right frontal lobes. Animals were sacrificed at humane endpoint followed by perfusions using 10% formalin and collected brains were sliced into 2mm thick sections with a brain-slicing matrix for paraffin embedding and H&E staining. Images were captured using an Aperio Slide Scanner (Leica Biosystems) and analyzed using ImageScope v11.1.2.760 software (Aperio). Survival studies utilized the number of days post-surgery and input for Kaplan-Meier analysis. NOG-EXL (Taconic, NOD.Cg-*Prkdc*^{scid} *Il2rg*^{tm1Sug} Tg(SV40/HTLV-IL3,CSF2)10-7Jic/JicTac, Cat.13395-F) mice were purchased for humanized studies and injected as previously outlined.

References

Brakel BA, Chokshi CR, Salim SK, Venugopal C, Singh S. In vitro evaluation of CAR-T cells in patient-derived glioblastoma models. STAR Protoc. 2021 Oct 29;2(4):100920. doi: 10.1016/j.xpro.2021.100920. PMID: 34761232; PMCID: PMC8567433.

Brescia P, Ortensi B, Fornasari L, Levi D, Broggi G, Pelicci G. CD133 is essential for glioblastoma stem cell maintenance. Stem Cells. 2013 May;31(5):857-69. doi: 10.1002/stem.1317. PMID: 23307586.

Brown CE, Badie B, Barish ME, Weng L, Ostberg JR, Chang WC, Naranjo A, Starr R, Wagner J, Wright C, Zhai Y, Bading JR, Ressler JA, Portnow J, D'Apuzzo M, Forman SJ, Jensen MC. Bioactivity and Safety of IL13Rα2-Redirected Chimeric Antigen Receptor CD8+ T Cells in Patients with Recurrent Glioblastoma. Clin Cancer Res. 2015 Sep 15;21(18):4062-72. doi: 10.1158/1078-0432.CCR-15-0428. Epub 2015 Jun 9. PMID: 26059190; PMCID: PMC4632968.

Brown CE, Alizadeh D, Starr R, Weng L, Wagner JR, Naranjo A, Ostberg JR, Blanchard MS, Kilpatrick J, Simpson J, Kurien A, Priceman SJ, Wang X, Harshbarger TL, D'Apuzzo M, Ressler JA, Jensen MC, Barish ME, Chen M, Portnow J, Forman SJ, Badie B. Regression of Glioblastoma after Chimeric Antigen Receptor T-Cell Therapy. N Engl J Med. 2016 Dec 29;375(26):2561-9. doi: 10.1056/NEJMoa1610497. PMID: 28029927; PMCID: PMC5390684.

Chang ZL, Silver PA, Chen YY. Identification and selective expansion of functionally superior T cells expressing chimeric antigen receptors. J Transl Med. 2015 May 20;13:161. doi: 10.1186/s12967-015-0519-8. PMID: 25990251; PMCID: PMC4457995.

Chokshi CR, Brakel BA, Tatari N, Savage N, Salim SK, Venugopal C, Singh SK. Advances in Immunotherapy for Adult Glioblastoma. Cancers (Basel). 2021 Jul 7;13(14):3400. doi: 10.3390/cancers13143400. PMID: 34298615; PMCID: PMC8305609.

Chung JS, Bonkobara M, Tomihari M, Cruz PD Jr, Ariizumi K. The DC-HIL/syndecan-4 pathway inhibits human allogeneic T-cell responses. Eur J Immunol. 2009 Apr;39(4):965-74. doi: 10.1002/eji.200838990. PMID: 19350579; PMCID: PMC2766302.

Cibrián D, Sánchez-Madrid F. CD69: from activation marker to metabolic gatekeeper. Eur J Immunol. 2017 Jun;47(6):946-953. doi: 10.1002/eji.201646837. PMID: 28475283; PMCID: PMC6485631.

Kobayashi M, Chung JS, Beg M, Arriaga Y, Verma U, Courtney K, Mansour J, Haley B, Khan S, Horiuchi Y, Ramani V, Harker D, Gopal P, Araghizadeh F, Cruz PD Jr, Ariizumi K. Blocking Monocytic Myeloid-Derived Suppressor Cell Function via Anti-DC-HIL/GPNMB Antibody Restores the In Vitro Integrity of T Cells from Cancer Patients. Clin Cancer Res. 2019 Jan 15;25(2):828-838. doi: 10.1158/1078-0432.CCR-18-0330. Epub 2018 Jul 26. PMID: 30049749; PMCID: PMC7315386.

Kopp LM, Malempati S, Krailo M, Gao Y, Buxton A, Weigel BJ, Hawthorne T, Crowley E, Moscow JA, Reid JM, Villalobos V, Randall RL, Gorlick R, Janeway KA. Phase II trial of the glycoprotein non-metastatic B-targeted antibody-drug conjugate, glembatumumab vedotin (CDX-011), in recurrent osteosarcoma AOST1521: A report from the Children's Oncology Group. Eur J Cancer. 2019 Nov;121:177-183. doi: 10.1016/j.ejca.2019.08.015. Epub 2019 Oct 3. PMID: 31586757; PMCID: PMC6952063.

Kuan CT, Wakiya K, Dowell JM, Herndon JE 2nd, Reardon DA, Graner MW, Riggins GJ, Wikstrand CJ, Bigner DD. Glycoprotein nonmetastatic melanoma protein B, a potential molecular therapeutic target in patients with glioblastoma multiforme. Clin Cancer Res. 2006 Apr 1;12(7 Pt 1):1970-82. doi: 10.1158/1078-0432.CCR-05-2797. PMID: 16609006.

Kuan CT, Wakiya K, Keir ST, Li J, Herndon JE 2nd, Pastan I, Bigner DD. Affinity-matured anti-glycoprotein NMB recombinant immunotoxins targeting malignant gliomas and melanomas. Int J Cancer. 2011 Jul 1;129(1):111-21. doi: 10.1002/ijc.25645. Epub 2010 Nov 3. PMID: 20824708; PMCID: PMC3024457.

Liu Z, Zhou J, Yang X, Liu Y, Zou C, Lv W, Chen C, Cheng KK, Chen T, Chang LJ, Wu D, Mao J. Safety and antitumor activity of GD2-Specific 4SCAR-T cells in patients with glioblastoma. Mol Cancer. 2023 Jan 9;22(1):3. doi: 10.1186/s12943-022-01711-9. PMID: 36617554; PMCID: PMC9827625.

Maino VC, Suni MA, Ruitenberg JJ. Rapid flow cytometric method for measuring lymphocyte subset activation. Cytometry. 1995 Jun 1;20(2):127-33. doi: 10.1002/cyto.990200205. PMID: 7664623.

Maric G, Annis MG, MacDonald PA, Russo C, Perkins D, Siwak DR, Mills GB, Siegel PM. GPNMB augments Wnt-1 mediated breast tumor initiation and growth by enhancing PI3K/AKT/mTOR pathway signaling and β-catenin activity. Oncogene. 2019 Jun;38(26):5294-5307. doi: 10.1038/s41388-019-0793-7. Epub 2019 Mar 26. PMID: 30914799.

McGranahan N, Furness AJ, Rosenthal R, Ramskov S, Lyngaa R, Saini SK, Jamal-Hanjani M, Wilson GA, Birkbak NJ, Hiley CT, Watkins TB, Shafi S, Murugaesu N, Mitter R, Akarca AU, Linares J, Marafioti T, Henry JY, Van Allen EM, Miao D, Schilling B, Schadendorf D, Garraway LA, Makarov V, Rizvi NA, Snyder A, Hellmann MD, Merghoub T, Wolchok JD, Shukla SA, Wu CJ, Peggs KS, Chan TA, Hadrup SR, Quezada SA, Swanton C. Clonal neoantigens elicit T cell immunoreactivity and sensitivity to immune checkpoint blockade. Science. 2016 Mar 25;351(6280):1463-9. doi: 10.1126/science.aaf1490. Epub 2016 Mar 3. PMID: 26940869; PMCID: PMC4984254.

O'Rourke DM, Nasrallah MP, Desai A, Melenhorst JJ, Mansfield K, Morrissette JJD, Martinez-Lage M, Brem S, Maloney E, Shen A, Isaacs R, Mohan S, Plesa G, Lacey SF, Navenot JM, Zheng Z, Levine BL, Okada H, June CH, Brogdon JL, Maus MV. A single dose of peripherally infused EGFRvIII-directed CAR T cells mediates antigen loss and

induces adaptive resistance in patients with recurrent glioblastoma. Sci Transl Med. 2017 Jul 19;9(399):eaaa0984. doi: 10.1126/scitranslmed.aaa0984. PMID: 28724573; PMCID: PMC5762203.

Omuro A, Vlahovic G, Lim M, Sahebjam S, Baehring J, Cloughesy T, Voloschin A, Ramkissoon SH, Ligon KL, Latek R, Zwirtes R, Strauss L, Paliwal P, Harbison CT, Reardon DA, Sampson JH. Nivolumab with or without ipilimumab in patients with recurrent glioblastoma: results from exploratory phase I cohorts of CheckMate 143. Neuro Oncol. 2018 Apr 9;20(5):674-686. doi: 10.1093/neuonc/nox208. PMID: 29106665; PMCID: PMC5892140.

Ott PA, Pavlick AC, Johnson DB, Hart LL, Infante JR, Luke JJ, Lutzky J, Rothschild NE, Spitler LE, Cowey CL, Alizadeh AR, Salama AK, He Y, Hawthorne TR, Bagley RG, Zhang J, Turner CD, Hamid O. A phase 2 study of glembatumumab vedotin, an antibody-drug conjugate targeting glycoprotein NMB, in patients with advanced melanoma. Cancer. 2019 Apr 1;125(7):1113-1123. doi: 10.1002/cncr.31892. Epub 2019 Jan 28. PMID: 30690710.

Pearson JRD, Cuzzubbo S, McArthur S, Durrant LG, Adhikaree J, Tinsley CJ, Pockley AG, McArdle SEB. Immune Escape in Glioblastoma Multiforme and the Adaptation of Immunotherapies for Treatment. Front Immunol. 2020 Oct 15;11:582106. doi: 10.3389/fimmu.2020.582106. PMID: 33178210; PMCID: PMC7594513.

Prince HE, Lapé-Nixon M. CD69 expression reliably predicts the anti-CD3-induced proliferative response of lymphocytes from human immunodeficiency virus type 1-infected patients. Clin Diagn Lab Immunol. 1997 Mar;4(2):217-22. doi: 10.1128/cdli.4.2.217-222.1997. PMID: 9067659; PMCID: PMC170505.

Ripoll VM, Irvine KM, Ravasi T, Sweet MJ, Hume DA. Gpnmb is induced in macrophages by IFN-gamma and lipopolysaccharide and acts as a feedback regulator of proinflammatory responses. J Immunol. 2007 May 15;178(10):6557-66. doi: 10.4049/jimmunol.178.10.6557. PMID: 17475886.

Shi Y, Ping YF, Zhou W, He ZC, Chen C, Bian BS, Zhang L, Chen L, Lan X, Zhang XC, Zhou K, Liu Q, Long H, Fu TW, Zhang XN, Cao MF, Huang Z, Fang X, Wang X, Feng H, Yao XH, Yu SC, Cui YH, Zhang X, Rich JN, Bao S, Bian XW. Tumour-associated macrophages secrete pleiotrophin to promote PTPRZ1 signalling in glioblastoma stem cells for tumour growth. Nat Commun. 2017 Jun 1;8:15080. doi: 10.1038/ncomms15080. PMID: 28569747; PMCID: PMC5461490.

Tomihari M, Hwang SH, Chung JS, Cruz PD Jr, Ariizumi K. Gpnmb is a melanosome-associated glycoprotein that contributes to melanocyte/keratinocyte adhesion in a RGD-dependent fashion. Exp Dermatol. 2009 Jul;18(7):586-95. doi: 10.1111/j.1600-0625.2008.00830.x. Epub 2009 Mar 6. PMID: 19320736; PMCID: PMC2774115.

Venugopal C, Hallett R, Vora P, Manoranjan B, Mahendram S, Qazi MA, McFarlane N, Subapanditha M, Nolte SM, Singh M, Bakhshinyan D, Garg N, Vijayakumar T, Lach B, Provias JP, Reddy K, Murty NK, Doble BW, Bhatia M, Hassell JA, Singh SK. Pyrvinium Targets CD133 in Human Glioblastoma Brain Tumor-Initiating Cells. Clin Cancer Res. 2015 Dec 1;21(23):5324-37. doi: 10.1158/1078-0432.CCR-14-3147. Epub 2015 Jul 7. PMID: 26152745.

Vora P, Venugopal C, Salim SK, Tatari N, Bakhshinyan D, Singh M, Seyfrid M, Upreti D, Rentas S, Wong N, Williams R, Qazi MA, Chokshi C, Ding A, Subapanditha M, Savage N, Mahendram S, Ford E, Adile AA, McKenna D, McFarlane N, Huynh V, Wylie RG, Pan J, Bramson J, Hope K, Moffat J, Singh S. The Rational Development of CD133-Targeting Immunotherapies for Glioblastoma. Cell Stem Cell. 2020 Jun 4;26(6):832-844.e6. doi: 10.1016/j.stem.2020.04.008. Epub 2020 May 27. PMID: 32464096.

Yardley DA, Weaver R, Melisko ME, Saleh MN, Arena FP, Forero A, Cigler T, Stopeck A, Citrin D, Oliff I, Bechhold R, Loutfi R, Garcia AA, Cruickshank S, Crowley E, Green J, Hawthorne T, Yellin MJ, Davis TA, Vahdat LT. EMERGE: A Randomized Phase II Study of the Antibody-Drug Conjugate Glembatumumab Vedotin in Advanced Glycoprotein NMB-Expressing Breast Cancer. J Clin Oncol. 2015 May 10;33(14):1609-19. doi: 10.1200/JCO.2014.56.2959. Epub 2015 Apr 6. PMID: 25847941.

Xie R, Okita Y, Ichikawa Y, Fikry MA, Huynh Dam KT, Tran STP, Kato M. Role of the kringle-like domain in glycoprotein NMB for its tumorigenic potential. Cancer Sci. 2019

Jul;110(7):2237-2246. doi: 10.1111/cas.14076. Epub 2019 Jun 26. PMID: 31127873; PMCID: PMC6609797.

Chapter 5: Discussion

Cancer is a complex disease that affects millions of people globally and has been the subject of extensive research for generations. Over the years, significant advancements have been made leading to improved treatments and a better understanding of the underlying mechanisms of the disease. Despite these achievements, cancer remains a significant health burden with many challenges remaining to be overcome. At present, cancer research is focused on several key areas, including the development of more powerful diagnostic tools, understanding of the genetic and molecular drivers of cancer, and exploring innovative treatment options. The use of liquid biopsies for example, which involves analyzing blood samples is becoming increasingly common and has the potential to revolutionize the way brain tumours are diagnosed rather than requiring highly invasive surgeries.

GBM is an aggressive type of brain cancer that has a poor prognosis and limited treatment options. Despite the significant advances made in the research of other malignancies, little improvement has been made for patients with GBM. One significant area of research is the study of the genetic and molecular drivers. Researchers are using more advanced technologies such as genomics, epigenetics, and transcriptomics to gain a better understanding of the genetic changes that occur in cancer cells. In GBM the use of targeted therapies is being designed to exploit specific genetic changes that occur rather than affecting all cells in the brain indiscriminately, as traditional chemotherapy does. Precision medicine is a personalized approach to cancer treatment that considers an individual's unique genetic makeup and the specific genetic changes that have occurred in their tumor. Currently, there are several targeted therapies in development

for GBM such as drugs to inhibit blood supply or drugs that inhibit specific signaling pathways.

Currently most immunotherapies target immune checkpoints using antibodies to effectively "unmask" cancer cells and allow the immune system to attack them. In preclinical studies, immunotherapies have been effective against GBM, and it is likely some of these treatments could be incorporated into standard of care in the future as they become more sophisticated and personalized. Precision medicine is becoming more widespread in cancer research and will continue to do so as genetic tests become cheaper and computers becomes more powerful to analyze larger data sets. This knowledge will help researchers develop new and improved immunotherapies that are being developed to become off-the-shelf products.

Chapter 2

In Chapter 2, I explored novel biology of GSCs to uncover genetic regulators of CD133 and stemness. CRISPR screens are relatively new tools allowing researchers to identify the function of specific genes in biological processes. Stemness is a complex process with several signaling pathways involved. Here, I was able to rapidly generate a large data set to identify several genes important in GSCs and validate the importance of a subset of genes. Some genes (such as *KEAP1* and *SOX2*) have been extensively studied in GBM while others (*TADA1* and *TADA2B*) lack comprehensive examination in healthy or cancerous contexts altogether. Using patient derived GBM samples in a stem cell enriching media in this context for the first time provided an extensive data set for what contributes to tumor progression and can be exploited in the future for translational medicine.

One striking similarity between NSCs and GSCs is their regulation by signaling pathways that control cell proliferation, survival, and differentiation. The overlapping features of NSCs and GSCs have important implications for the development of new treatments for GBM. This could result in a more effective and less toxic treatment for brain cancers. SOX2 is an important transcription factor in the brain and studies have shown that alterations in SOX2 can have significant effects on brain development and function. For example, overexpression of SOX2 in the adult brain has been shown to increase the production of new neurons, which may have therapeutic potential for the treatment of neurological disorders. Finding the balance between healthy stem cells and cancerous stem cells will be critical for developing regenerative medicines.

For this reason I conducted the first CUT&RUN in GBM to examine SOX2 interactions with DNA across the genome. CUT&RUN is an improvement over ChIP-seq because of higher detection of DNA sequences due to lower background noise. The reduced sample requirements are invaluable for rare specimens such as primary brain tumors. Our main hypothesis was proven that SOX2 has a direct interaction with *PROM1* to regulate CD133 expression in GBM. The finding is the first direct link whereas previous studies only showed correlative associations. Because detection of the SOX2-*PROM1* interaction occurred *in situ*, this is a powerful contribution to deconvoluting biological processes regulating stemness. In addition to this, this interaction provides another insight into the biology of CD133 where signaling mechanisms and potential ligands have long remained elusive to the scientific community. This CUT&RUN data set was generated to validate *PROM1* regulation via SOX2 in GBM but will serve as a discovery

platform for future scientists to distinguish differences of other markers regulated by SOX2.

Chapter 3

A major challenge to treating GBM is the highly invasive nature of cells, which makes it near impossible to remove the tumor through surgery. It is likely in the future that new surgical techniques will be developed to better resect the tumor and improve patient outcomes, but there remains a significant need for new and effective treatments alongside this. One of the most rapid advancements in cancer research in recent decades has been the development of cell therapies. The biggest challenge developing cell therapies such as CAR-Ts is identifying the specific targets that the immune system can attack in cancer cells while leaving normal tissue unharmed. This is of particular concern in brain tumors because of the incredibly delicate nature of the brain.

In Chapter 3, I examined the biology of an understudied protein in GBM to study how it contributes to tumor progression and why it is expressed. As previously mentioned, NSCs and GSCs share several signaling pathways. RNA-seq is another high-throughput technique we employed to analyze the expression and abundance of RNA in our primary cell lines. By contrasting the signaling pathways and genes that are not shared between NSCs and GSCs we identified GPNMB as a tumor associated antigen. This is a major contribution to the field of GBM because most of the previous publications relied on mouse models, RNA only or induction of GPNMB at the protein level to interrogate its biology. The identification of GPNMB as a protein expressed within GBM cells themselves, particularly when and how it is upregulated at recurrence after first line treatment for patients failed is an invaluable insight to develop new therapies in the future.

In Chapter 4, I built on the rationale of GPNMB being a valuable target for immunotherapies and tested a novel CAR-T in a series of contexts. Previous attempts to target GPNMB have been limited to ADCs. By showing the absence of GPNMB throughout the body we provided strong rationale for a systemic cell therapy being a viable option for patients. Genetically engineering T cells to target and destroy cells which express GPNMB at the surface could provide a more durable treatment option because of the omnipresence of the CAR-Ts.

While GPNMB CAR-Ts were effective at reducing tumor burden and prolonging mouse survival time in our PDX models, mice eventually succumbed to this disease. The heterogeneity displayed by GBM ultimately means a single therapy is unlikely to be effective in the clinic so rational co-targeting strategies must be employed. Again, we succeeded in combining GPNMB CAR-Ts with our previously published CD133 to target mutually exclusive populations and more comprehensively target the tumor. While our data was proof-of-concept using a pooled approach, bi-specific and tandem CAR constructs could also greatly improve our approach in the future. Cell therapy is a rapidly evolving field with the potential to revolutionize the way we treat a variety of diseases and conditions.

In addition, modulating the TIME has been an intense area of focus, particularly modifying TAM functions. Inhibiting CD47 and CD73 have proven to be effective methods of enhancing anti-tumor responses in immunocompetent models. Because it has been shown GPNMB more closely associated with TAMs compared to M1 or M2 polarizations, we validated the presence of GPNMB at the surface of macrophages and making them susceptible to our CAR-T. Since our binder sequence of the CAR-T is not compatible with

the mouse ortholog of GPNMB, we utilized humanized mouse models to test whether CAR-Ts could A) overcome an immunosuppressive microenvironment to kill tumor cells and B) kill TAMs. In theory, this could be an effective method to not only reduce the size of the bulk tumor, but also eliminate a large proportion of the immunosuppressive niche to enhance anti-tumor responses of other immune cells of the host. While we successfully achieved the former stated goal, data is pending for the latter and will be available for future discussions.

Future Directions

CAR-NKs (chimeric antigen receptor natural killer cells) are a promising advancement in the realm of cellular therapies and could be beneficial for GBM patients. CAR-NKs are like CAR-Ts, but genetically incorporate the CAR construct to NK cells. One advantage of CAR-NKs over CAR-Ts is their ability to target multiple cancer cells simultaneously unlike traditional CAR-Ts, which often only target a single specific protein on cancer cells. CAR-NKs have shown promising results in preclinical studies for their ability to effectively target cancer stem cells which prevented the growth and spread of the disease. In addition to their versatility and effectiveness, CAR-NKs also have a relatively low toxicity profile compared to CAR-Ts. However, there remain challenges to overcome before these are applied on a large scale such as safety concerns of off-tumor toxicity, or simply manufacturing large enough quantities of cells at an economical cost.

In conclusion, the future of GBM research holds great promise, with many exciting developments on the horizon. From new surgical techniques and immunotherapies to targeted therapies and diagnostic tools, the future of GBM research is bright. As

technology continues to advance, researchers will have the tools they need to make even greater strides in the fight against this disease, bringing us closer to a world where GBM is no longer a threat to human health.

Concluding Remarks

In my thesis, I present a modern perspective of glioblastoma research, my contributions to the field and possible avenues for future scientists in my position to explore. Not only was I fortunate enough to use multiple incredibly powerful high throughput techniques to generate data I was fortunate enough to be surrounded by wonderful scientists to help make sense of it all. While asking questions and solving puzzles has been a past time of mine since I've been able to do either, my biggest fear was having all my work sit on a shelf the rest of my life unused. While that remains a possibility and time will tell, I could not be prouder of the hypotheses I have been able to test in my time and I fully believe these insights will make meaningful impacts in the lives of patients if I am fortunate enough for someone after me to take the baton and build on these foundations.

References

Ahmad H, Fadul CE, Schiff D, Purow B. Checkpoint inhibitor failure in hypermutated and mismatch repair-mutated recurrent high-grade gliomas. Neurooncol Pract. 2019 Dec;6(6):424-427. doi: 10.1093/nop/npz016. Epub 2019 Apr 7. PMID: 31832212; PMCID: PMC6899050.

Alonso MM, Diez-Valle R, Manterola L, Rubio A, Liu D, Cortes-Santiago N, Urquiza L, Jauregi P, Lopez de Munain A, Sampron N, Aramburu A, Tejada-Solís S, Vicente C, Odero MD, Bandrés E, García-Foncillas J, Idoate MA, Lang FF, Fueyo J, Gomez-Manzano C. Genetic and epigenetic modifications of Sox2 contribute to the invasive phenotype of malignant gliomas. PLoS One. 2011;6(11):e26740. doi: 10.1371/journal.pone.0026740. Epub 2011 Nov 1. PMID: 22069467; PMCID: PMC3206066.

Aponte PM, Caicedo A. Stemness in Cancer: Stem Cells, Cancer Stem Cells, and Their Microenvironment. Stem Cells Int. 2017;2017:5619472. doi: 10.1155/2017/5619472. Epub 2017 Apr 4. PMID: 28473858; PMCID: PMC5394399.

Avilion AA, Nicolis SK, Pevny LH, Perez L, Vivian N, Lovell-Badge R. Multipotent cell lineages in early mouse development depend on SOX2 function. Genes Dev. 2003 Jan 1;17(1):126-40. doi: 10.1101/gad.224503. PMID: 12514105; PMCID: PMC195970.

Bannister AJ, Kouzarides T. Regulation of chromatin by histone modifications. Cell Res. 2011 Mar;21(3):381-95. doi: 10.1038/cr.2011.22. Epub 2011 Feb 15. PMID: 21321607; PMCID: PMC3193420.

Bao S, Wu Q, McLendon RE, Hao Y, Shi Q, Hjelmeland AB, Dewhirst MW, Bigner DD, Rich JN. Glioma stem cells promote radioresistance by preferential activation of the DNA damage response. Nature. 2006 Dec 7;444(7120):756-60. doi: 10.1038/nature05236. Epub 2006 Oct 18. PMID: 17051156.

Batra SK, Castelino-Prabhu S, Wikstrand CJ, Zhu X, Humphrey PA, Friedman HS, Bigner DD. Epidermal growth factor ligand-independent, unregulated, cell-transforming potential of a naturally occurring human mutant EGFRvIII gene. Cell Growth Differ. 1995 Oct;6(10):1251-9. PMID: 8845302.

Bayik D, Zhou Y, Park C, Hong C, Vail D, Silver DJ, Lauko A, Roversi G, Watson DC, Lo A, Alban TJ, McGraw M, Sorensen M, Grabowski MM, Otvos B, Vogelbaum MA, Horbinski C, Kristensen BW, Khalil AM, Hwang TH, Ahluwalia MS, Cheng F, Lathia JD. Myeloid-Derived Suppressor Cell Subsets Drive Glioblastoma Growth in a Sex-Specific Manner. Cancer Discov. 2020 Aug;10(8):1210-1225. doi: 10.1158/2159-8290.CD-19-1355. Epub 2020 Apr 16. PMID: 32300059; PMCID: PMC7415660.

Benmebarek MR, Karches CH, Cadilha BL, Lesch S, Endres S, Kobold S. Killing Mechanisms of Chimeric Antigen Receptor (CAR) T Cells. Int J Mol Sci. 2019 Mar 14;20(6):1283. doi: 10.3390/ijms20061283. PMID: 30875739; PMCID: PMC6470706.

Berdeja JG, Madduri D, Usmani SZ, Jakubowiak A, Agha M, Cohen AD, Stewart AK, Hari P, Htut M, Lesokhin A, Deol A, Munshi NC, O'Donnell E, Avigan D, Singh I, Zudaire E, Yeh TM, Allred AJ, Olyslager Y, Banerjee A, Jackson CC, Goldberg JD, Schecter JM, Deraedt W, Zhuang SH, Infante J, Geng D, Wu X, Carrasco-Alfonso MJ, Akram M, Hossain F, Rizvi S, Fan F, Lin Y, Martin T, Jagannath S. Ciltacabtagene autoleucel, a B-cell maturation antigen-directed chimeric antigen receptor T-cell therapy in patients with relapsed or refractory multiple myeloma (CARTITUDE-1): a phase 1b/2 open-label study. Lancet. 2021 Jul 24;398(10297):314-324. doi: 10.1016/S0140-6736(21)00933-8. Epub 2021 Jun 24. Erratum in: Lancet. 2021 Oct 2;398(10307):1216. PMID: 34175021.

Biasoli D, Kahn SA, Cornélio TA, Furtado M, Campanati L, Chneiweiss H, Moura-Neto V, Borges HL. Retinoblastoma protein regulates the crosstalk between autophagy and apoptosis, and favors glioblastoma resistance to etoposide. Cell Death Dis. 2013 Aug 15;4(8):e767. doi: 10.1038/cddis.2013.283. PMID: 23949216; PMCID: PMC3763445.

Biondini M, Kiepas A, El-Houjeiri L, Annis MG, Hsu BE, Fortier AM, Morin G, Martina JA, Sirois I, Aguilar-Mahecha A, Gruosso T, McGuirk S, Rose AAN, Tokat UM, Johnson RM, Sahin O, Bareke E, St-Pierre J, Park M, Basik M, Majewski J, Puertollano R, Pause A, Huang S, Keler T, Siegel PM. HSP90 inhibitors induce GPNMB cell-surface

expression by modulating lysosomal positioning and sensitize breast cancer cells to glembatumumab vedotin. Oncogene. 2022 Mar;41(12):1701-1717. doi: 10.1038/s41388-022-02206-z. Epub 2022 Feb 2. PMID: 35110681.

Bock, C., Datlinger, P., Chardon, F. et al. High-content CRISPR screening. Nat Rev Methods Primers 2, 8 (2022). https://doi.org/10.1038/s43586-021-00093-4

Boettcher M, McManus MT. Choosing the Right Tool for the Job: RNAi, TALEN, or CRISPR. Mol Cell. 2015 May 21;58(4):575-85. doi: 10.1016/j.molcel.2015.04.028. PMID: 26000843; PMCID: PMC4441801.

Bond AM, Ming GL, Song H. Ontogeny of adult neural stem cells in the mammalian brain. Curr Top Dev Biol. 2021;142:67-98. doi: 10.1016/bs.ctdb.2020.11.002. Epub 2020 Dec 17. PMID: 33706926; PMCID: PMC8363052.

Bonifacino JS, Traub LM. Signals for sorting of transmembrane proteins to endosomes and lysosomes. Annu Rev Biochem. 2003;72:395-447. doi: 10.1146/annurev.biochem.72.121801.161800. Epub 2003 Mar 6. PMID: 12651740.

Bonnet D, Dick JE. Human acute myeloid leukemia is organized as a hierarchy that originates from a primitive hematopoietic cell. Nat Med. 1997 Jul;3(7):730-7. doi: 10.1038/nm0797-730. PMID: 9212098.

Brown CE, Badie B, Barish ME, Weng L, Ostberg JR, Chang WC, Naranjo A, Starr R, Wagner J, Wright C, Zhai Y, Bading JR, Ressler JA, Portnow J, D'Apuzzo M, Forman SJ, Jensen MC. Bioactivity and Safety of IL13Rα2-Redirected Chimeric Antigen Receptor CD8+ T Cells in Patients with Recurrent Glioblastoma. Clin Cancer Res. 2015 Sep 15;21(18):4062-72. doi: 10.1158/1078-0432.CCR-15-0428. Epub 2015 Jun 9. PMID: 26059190; PMCID: PMC4632968.

Brown CE, Alizadeh D, Starr R, Weng L, Wagner JR, Naranjo A, Ostberg JR, Blanchard MS, Kilpatrick J, Simpson J, Kurien A, Priceman SJ, Wang X, Harshbarger TL, D'Apuzzo M, Ressler JA, Jensen MC, Barish ME, Chen M, Portnow J, Forman SJ, Badie B. Regression of Glioblastoma after Chimeric Antigen Receptor T-Cell Therapy. N Engl J Med. 2016 Dec 29;375(26):2561-9. doi: 10.1056/NEJMoa1610497. PMID: 28029927; PMCID: PMC5390684.

Bulstrode H, Johnstone E, Marques-Torrejon MA, Ferguson KM, Bressan RB, Blin C, Grant V, Gogolok S, Gangoso E, Gagrica S, Ender C, Fotaki V, Sproul D, Bertone P, Pollard SM. Elevated FOXG1 and SOX2 in glioblastoma enforces neural stem cell identity through transcriptional control of cell cycle and epigenetic regulators. Genes Dev. 2017 Apr 15;31(8):757-773. doi: 10.1101/gad.293027.116. Epub 2017 May 2. PMID: 28465359; PMCID: PMC5435889.

Cai J, Weiss ML, Rao MS. In search of "stemness". Exp Hematol. 2004 Jul;32(7):585-98. doi: 10.1016/j.exphem.2004.03.013. PMID: 15246154; PMCID: PMC3279197.

Cai C, Tang D, Han Y, Shen E, Abdihamid O, Guo C, Shen H, Zeng S. A comprehensive analysis of the fatal toxic effects associated with CD19 CAR-T cell therapy. Aging (Albany NY). 2020 Sep 24;12(18):18741-18753. doi: 10.18632/aging.104058. Epub 2020 Sep 24. PMID: 32973124; PMCID: PMC7585129.

Cancer Genome Atlas Research Network. Comprehensive genomic characterization defines human glioblastoma genes and core pathways. Nature. 2008 Oct 23;455(7216):1061-8. doi: 10.1038/nature07385. Epub 2008 Sep 4. Erratum in: Nature. 2013 Feb 28;494(7438):506. PMID: 18772890; PMCID: PMC2671642.

Cao Y. Regulation of germ layer formation by pluripotency factors during embryogenesis. Cell Biosci. 2013 Mar 11;3(1):15. doi: 10.1186/2045-3701-3-15. PMID: 23497659; PMCID: PMC3602094.

Carson KA, Grossman SA, Fisher JD, Shaw EG. Prognostic factors for survival in adult patients with recurrent glioma enrolled onto the new approaches to brain tumor therapy CNS consortium phase I and II clinical trials. J Clin Oncol. 2007 Jun 20;25(18):2601-6. doi: 10.1200/JCO.2006.08.1661. PMID: 17577040; PMCID: PMC4118746.

Chai E, Zhang L, Li C. LOX-1+ PMN-MDSC enhances immune suppression which promotes glioblastoma multiforme progression. Cancer Manag Res. 2019 Aug

2;11:7307-7315. doi: 10.2147/CMAR.S210545. PMID: 31447588; PMCID: PMC6683959.

Chen J, Sun HW, Yang YY, Chen HT, Yu XJ, Wu WC, Xu YT, Jin LL, Wu XJ, Xu J, Zheng L. Reprogramming immunosuppressive myeloid cells by activated T cells promotes the response to anti-PD-1 therapy in colorectal cancer. Signal Transduct Target Ther. 2021 Jan 8;6(1):4. doi: 10.1038/s41392-020-00377-3. PMID: 33414378; PMCID: PMC7791142.

Chung JS, Ramani V, Kobayashi M, Fattah F, Popat V, Zhang S, Cruz PD Jr, Gerber DE, Ariizumi K. DC-HIL/Gpnmb Is a Negative Regulator of Tumor Response to Immune Checkpoint Inhibitors. Clin Cancer Res. 2020 Mar 15;26(6):1449-1459. doi: 10.1158/1078-0432.CCR-19-2360. Epub 2019 Dec 10. PMID: 31822499.

Chung JS, Dougherty I, Cruz PD Jr, Ariizumi K. Syndecan-4 mediates the coinhibitory function of DC-HIL on T cell activation. J Immunol. 2007 Nov 1;179(9):5778-84. doi: 10.4049/jimmunol.179.9.5778. PMID: 17947650.

Cloughesy TF, Mochizuki AY, Orpilla JR, Hugo W, Lee AH, Davidson TB, Wang AC, Ellingson BM, Rytlewski JA, Sanders CM, Kawaguchi ES, Du L, Li G, Yong WH, Gaffey SC, Cohen AL, Mellinghoff IK, Lee EQ, Reardon DA, O'Brien BJ, Butowski NA, Nghiemphu PL, Clarke JL, Arrillaga-Romany IC, Colman H, Kaley TJ, de Groot JF, Liau LM, Wen PY, Prins RM. Neoadjuvant anti-PD-1 immunotherapy promotes a survival

benefit with intratumoral and systemic immune responses in recurrent glioblastoma. Nat Med. 2019 Mar;25(3):477-486. doi: 10.1038/s41591-018-0337-7. Epub 2019 Feb 11. PMID: 30742122; PMCID: PMC6408961.

D'Alessio A, Proietti G, Sica G, Scicchitano BM. Pathological and Molecular Features of Glioblastoma and Its Peritumoral Tissue. Cancers (Basel). 2019 Apr 3;11(4):469. doi: 10.3390/cancers11040469. PMID: 30987226; PMCID: PMC6521241.

Dapash M, Hou D, Castro B, Lee-Chang C, Lesniak MS. The Interplay between Glioblastoma and Its Microenvironment. Cells. 2021 Aug 31;10(9):2257. doi: 10.3390/cells10092257. PMID: 34571905; PMCID: PMC8469987.

Davis JB, Krishna SS, Abi Jomaa R, Duong CT, Espina V, Liotta LA, Mueller C. A new model isolates glioblastoma clonal interactions and reveals unexpected modes for regulating motility, proliferation, and drug resistance. Sci Rep. 2019 Nov 22;9(1):17380. doi: 10.1038/s41598-019-53850-7. PMID: 31758030; PMCID: PMC6874607.

Dodonova SO, Zhu F, Dienemann C, Taipale J, Cramer P. Nucleosome-bound SOX2 and SOX11 structures elucidate pioneer factor function. Nature. 2020 Apr;580(7805):669-672. doi: 10.1038/s41586-020-2195-y. Epub 2020 Apr 22. PMID: 32350470.

Du Z, Lovly CM. Mechanisms of receptor tyrosine kinase activation in cancer. Mol Cancer. 2018 Feb 19;17(1):58. doi: 10.1186/s12943-018-0782-4. PMID: 29455648; PMCID: PMC5817791.

Duan D, Wang K, Wei C, Feng D, Liu Y, He Q, Xu X, Wang C, Zhao S, Lv L, Long J, Lin D, Zhao A, Fang B, Jiang J, Tang S, Gao J. The BCMA-Targeted Fourth-Generation CAR-T Cells Secreting IL-7 and CCL19 for Therapy of Refractory/Recurrent Multiple Myeloma. Front Immunol. 2021 Mar 5;12:609421. doi: 10.3389/fimmu.2021.609421. PMID: 33767695; PMCID: PMC7985831.

Dubinski D, Wölfer J, Hasselblatt M, Schneider-Hohendorf T, Bogdahn U, Stummer W, Wiendl H, Grauer OM. CD4+ T effector memory cell dysfunction is associated with the accumulation of granulocytic myeloid-derived suppressor cells in glioblastoma patients. Neuro Oncol. 2016 Jun;18(6):807-18. doi: 10.1093/neuonc/nov280. Epub 2015 Nov 17. PMID: 26578623; PMCID: PMC4864257.

Elshazzly M, Lopez MJ, Reddy V, Caban O. Embryology, Central Nervous System. 2022 Apr 5. In: StatPearls [Internet]. Treasure Island (FL): StatPearls Publishing; 2023 Jan–. PMID: 30252280.

Eshhar Z, Waks T, Gross G, Schindler DG. Specific activation and targeting of cytotoxic lymphocytes through chimeric single chains consisting of antibody-binding domains and the gamma or zeta subunits of the immunoglobulin and T-cell receptors. Proc Natl Acad

Sci U S A. 1993 Jan 15;90(2):720-4. doi: 10.1073/pnas.90.2.720. PMID: 8421711; PMCID: PMC45737.

Feng X, Zhang L, Ke S, Liu T, Hao L, Zhao P, Tu W, Cang S. High expression of GPNMB indicates an unfavorable prognosis in glioma: Combination of data from the GEO and CGGA databases and validation in tissue microarray. Oncol Lett. 2020 Sep;20(3):2356-2368. doi: 10.3892/ol.2020.11787. Epub 2020 Jun 26. PMID: 32782553; PMCID: PMC7400985.

Fennell DA, Ewings S, Ottensmeier C, Califano R, Hanna GG, Hill K, Danson S, Steele N, Nye M, Johnson L, Lord J, Middleton C, Szlosarek P, Chan S, Gaba A, Darlison L, Wells-Jordan P, Richards C, Poile C, Lester JF, Griffiths G; CONFIRM trial investigators. Nivolumab versus placebo in patients with relapsed malignant mesothelioma (CONFIRM): a multicentre, double-blind, randomised, phase 3 trial. Lancet Oncol. 2021 Nov;22(11):1530-1540. doi: 10.1016/S1470-2045(21)00471-X. Epub 2021 Oct 14. PMID: 34656227; PMCID: PMC8560642.

Ferletta M, Caglayan D, Mokvist L, Jiang Y, Kastemar M, Uhrbom L, Westermark B. Forced expression of Sox21 inhibits Sox2 and induces apoptosis in human glioma cells. Int J Cancer. 2011 Jul 1;129(1):45-60. doi: 10.1002/ijc.25647. Epub 2010 Nov 9. PMID: 20824710.

Fu W, Wang W, Li H, Jiao Y, Huo R, Yan Z, Wang J, Wang S, Wang J, Chen D, Cao Y, Zhao J. Single-Cell Atlas Reveals Complexity of the Immunosuppressive Microenvironment of Initial and Recurrent Glioblastoma. Front Immunol. 2020 May 7;11:835. doi: 10.3389/fimmu.2020.00835. PMID: 32457755; PMCID: PMC7221162.

Gangemi RM, Griffero F, Marubbi D, Perera M, Capra MC, Malatesta P, Ravetti GL, Zona GL, Daga A, Corte G. SOX2 silencing in glioblastoma tumor-initiating cells causes stop of proliferation and loss of tumorigenicity. Stem Cells. 2009 Jan;27(1):40-8. doi: 10.1634/stemcells.2008-0493. PMID: 18948646.

Garros-Regulez L, Aldaz P, Arrizabalaga O, Moncho-Amor V, Carrasco-Garcia E, Manterola L, Moreno-Cugnon L, Barrena C, Villanua J, Ruiz I, Pollard S, Lovell-Badge R, Sampron N, Garcia I, Matheu A. mTOR inhibition decreases SOX2-SOX9 mediated glioma stem cell activity and temozolomide resistance. Expert Opin Ther Targets. 2016;20(4):393-405. doi: 10.1517/14728222.2016.1151002. PMID: 26878385; PMCID: PMC4898154.

Glumac PM, LeBeau AM. The role of CD133 in cancer: a concise review. Clin Transl Med. 2018 Jul 9;7(1):18. doi: 10.1186/s40169-018-0198-1. PMID: 29984391; PMCID: PMC6035906.

Gomez-Manzano C, Fueyo J, Kyritsis AP, McDonnell TJ, Steck PA, Levin VA, Yung WK. Characterization of p53 and p21 functional interactions in glioma cells en route to

apoptosis. J Natl Cancer Inst. 1997 Jul 16;89(14):1036-44. doi: 10.1093/jnci/89.14.1036. PMID: 9230885.

González-Tablas Pimenta M, Otero Á, Arandia Guzman DA, Pascual-Argente D, Ruíz Martín L, Sousa-Casasnovas P, García-Martin A, Roa Montes de Oca JC, Villaseñor-Ledezma J, Torres Carretero L, Almeida M, Ortiz J, Nieto A, Orfao A, Tabernero MD. Tumor cell and immune cell profiles in primary human glioblastoma: Impact on patient outcome. Brain Pathol. 2021 Mar;31(2):365-380. doi: 10.1111/bpa.12927. Epub 2021 Feb 13. PMID: 33314398; PMCID: PMC8018082.

Guerra-Rebollo, M., Garrido, C., Sánchez-Cid, L. et al. Targeting of replicating CD133 and OCT4/SOX2 expressing glioma stem cells selects a cell population that reinitiates tumors upon release of therapeutic pressure. Sci Rep 9, 9549 (2019). https://doi.org/10.1038/s41598-019-46014-0

Guo X, Xue H, Shao Q, Wang J, Guo X, Chen X, Zhang J, Xu S, Li T, Zhang P, Gao X, Qiu W, Liu Q, Li G. Hypoxia promotes glioma-associated macrophage infiltration via periostin and subsequent M2 polarization by upregulating TGF-beta and M-CSFR. Oncotarget. 2016 Dec 6;7(49):80521-80542. doi: 10.18632/oncotarget.11825. PMID: 27602954; PMCID: PMC5348338.

Gurdon JB, Bourillot PY. Morphogen gradient interpretation. Nature. 2001 Oct 25;413(6858):797-803. doi: 10.1038/35101500. PMID: 11677596.

Han S, Zhang C, Li Q, Dong J, Liu Y, Huang Y, Jiang T, Wu A. Tumour-infiltrating CD4(+) and CD8(+) lymphocytes as predictors of clinical outcome in glioma. Br J Cancer. 2014 May 13;110(10):2560-8. doi: 10.1038/bjc.2014.162. Epub 2014 Apr 1. PMID: 24691423; PMCID: PMC4021514.

Heinrich C, Bergami M, Gascón S, Lepier A, Viganò F, Dimou L, Sutor B, Berninger B, Götz M. Sox2-mediated conversion of NG2 glia into induced neurons in the injured adult cerebral cortex. Stem Cell Reports. 2014 Dec 9;3(6):1000-14. doi: 10.1016/j.stemcr.2014.10.007. Epub 2014 Nov 20. PMID: 25458895; PMCID: PMC4264057.

Heppner GH, Miller BE. Tumor heterogeneity: biological implications and therapeutic consequences. Cancer Metastasis Rev. 1983;2(1):5-23. doi: 10.1007/BF00046903. PMID: 6616442.

Hombach A, Wieczarkowiecz A, Marquardt T, Heuser C, Usai L, Pohl C, Seliger B, Abken H. Tumor-specific T cell activation by recombinant immunoreceptors: CD3 zeta signaling and CD28 costimulation are simultaneously required for efficient IL-2 secretion and can be integrated into one combined CD28/CD3 zeta signaling receptor molecule. J Immunol. 2001 Dec 1;167(11):6123-31. doi: 10.4049/jimmunol.167.11.6123. Erratum in: J Immunol. 2004 Jul 1;173(1):695. PMID: 11714771.

Huang PW, Chang JW. Immune checkpoint inhibitors win the 2018 Nobel Prize. Biomed J. 2019 Oct;42(5):299-306. doi: 10.1016/j.bj.2019.09.002. Epub 2019 Nov 5. PMID: 31783990; PMCID: PMC6889239.

Incekara F, Smits M, van der Voort SR, Dubbink HJ, Atmodimedjo PN, Kros JM, Vincent AJPE, van den Bent M. The Association Between the Extent of Glioblastoma Resection and Survival in Light of MGMT Promoter Methylation in 326 Patients With Newly Diagnosed IDH-Wildtype Glioblastoma. Front Oncol. 2020 Jul 10;10:1087. doi: 10.3389/fonc.2020.01087. PMID: 32766140; PMCID: PMC7381265.

Jinek M, Chylinski K, Fonfara I, Hauer M, Doudna JA, Charpentier E. A programmable dual-RNA-guided DNA endonuclease in adaptive bacterial immunity. Science. 2012 Aug 17;337(6096):816-21. doi: 10.1126/science.1225829. Epub 2012 Jun 28. PMID: 22745249; PMCID: PMC6286148.

Johnson BE, Mazor T, Hong C, Barnes M, Aihara K, McLean CY, Fouse SD, Yamamoto S, Ueda H, Tatsuno K, Asthana S, Jalbert LE, Nelson SJ, Bollen AW, Gustafson WC, Charron E, Weiss WA, Smirnov IV, Song JS, Olshen AB, Cha S, Zhao Y, Moore RA, Mungall AJ, Jones SJM, Hirst M, Marra MA, Saito N, Aburatani H, Mukasa A, Berger MS, Chang SM, Taylor BS, Costello JF. Mutational analysis reveals the origin and therapy-driven evolution of recurrent glioma. Science. 2014 Jan 10;343(6167):189-193. doi: 10.1126/science.1239947. Epub 2013 Dec 12. PMID: 24336570; PMCID: PMC3998672.

Keir CH, Vahdat LT. The use of an antibody drug conjugate, glembatumumab vedotin (CDX-011), for the treatment of breast cancer. Expert Opin Biol Ther. 2012 Feb;12(2):259-63. doi: 10.1517/14712598.2012.642357. Epub 2012 Jan 9. PMID: 22229970.

Kim H, Zheng S, Amini SS, Virk SM, Mikkelsen T, Brat DJ, Grimsby J, Sougnez C, Muller F, Hu J, Sloan AE, Cohen ML, Van Meir EG, Scarpace L, Laird PW, Weinstein JN, Lander ES, Gabriel S, Getz G, Meyerson M, Chin L, Barnholtz-Sloan JS, Verhaak RG. Whole-genome and multisector exome sequencing of primary and post-treatment glioblastoma reveals patterns of tumor evolution. Genome Res. 2015 Mar;25(3):316-27. doi: 10.1101/gr.180612.114. Epub 2015 Feb 3. PMID: 25650244; PMCID: PMC4352879.

Kobayashi M, Chung JS, Beg M, Arriaga Y, Verma U, Courtney K, Mansour J, Haley B, Khan S, Horiuchi Y, Ramani V, Harker D, Gopal P, Araghizadeh F, Cruz PD Jr, Ariizumi K. Blocking Monocytic Myeloid-Derived Suppressor Cell Function via Anti-DC-HIL/GPNMB Antibody Restores the In Vitro Integrity of T Cells from Cancer Patients. Clin Cancer Res. 2019 Jan 15;25(2):828-838. doi: 10.1158/1078-0432.CCR-18-0330. Epub 2018 Jul 26. PMID: 30049749; PMCID: PMC7315386.

Kolenda J, Jensen SS, Aaberg-Jessen C, Christensen K, Andersen C, Brünner N, Kristensen BW. Effects of hypoxia on expression of a panel of stem cell and

chemoresistance markers in glioblastoma-derived spheroids. J Neurooncol. 2011 May;103(1):43-58. doi: 10.1007/s11060-010-0357-8. Epub 2010 Sep 11. PMID: 20835751.

Kopp JL, Ormsbee BD, Desler M, Rizzino A. Small increases in the level of Sox2 trigger the differentiation of mouse embryonic stem cells. Stem Cells. 2008 Apr;26(4):903-11. doi: 10.1634/stemcells.2007-0951. Epub 2008 Jan 31. PMID: 18238855.

Kopp LM, Malempati S, Krailo M, Gao Y, Buxton A, Weigel BJ, Hawthorne T, Crowley E, Moscow JA, Reid JM, Villalobos V, Randall RL, Gorlick R, Janeway KA. Phase II trial of the glycoprotein non-metastatic B-targeted antibody-drug conjugate, glembatumumab vedotin (CDX-011), in recurrent osteosarcoma AOST1521: A report from the Children's Oncology Group. Eur J Cancer. 2019 Nov;121:177-183. doi: 10.1016/j.ejca.2019.08.015. Epub 2019 Oct 3. PMID: 31586757; PMCID: PMC6952063.

Lakshmanachetty S, Cruz-Cruz J, Hoffmeyer E, Cole AP, Mitra SS. New Insights into the Multifaceted Role of Myeloid-Derived Suppressor Cells (MDSCs) in High-Grade Gliomas: From Metabolic Reprograming, Immunosuppression, and Therapeutic Resistance to Current Strategies for Targeting MDSCs. Cells. 2021 Apr 14;10(4):893. doi: 10.3390/cells10040893. PMID: 33919732; PMCID: PMC8070707.

Larjavaara S, Mäntylä R, Salminen T, Haapasalo H, Raitanen J, Jääskeläinen J, Auvinen A. Incidence of gliomas by anatomic location. Neuro Oncol. 2007 Jul;9(3):319-

25. doi: 10.1215/15228517-2007-016. Epub 2007 May 23. PMID: 17522333; PMCID: PMC1907421.

Le Borgne R, Planque N, Martin P, Dewitte F, Saule S, Hoflack B. The AP-3-dependent targeting of the melanosomal glycoprotein QNR-71 requires a di-leucine-based sorting signal. J Cell Sci. 2001 Aug;114(Pt 15):2831-41. doi: 10.1242/jcs.114.15.2831. PMID: 11683416.

Lee AH, Sun L, Mochizuki AY, Reynoso JG, Orpilla J, Chow F, Kienzler JC, Everson RG, Nathanson DA, Bensinger SJ, Liau LM, Cloughesy T, Hugo W, Prins RM. Neoadjuvant PD-1 blockade induces T cell and cDC1 activation but fails to overcome the immunosuppressive tumor associated macrophages in recurrent glioblastoma. Nat Commun. 2021 Nov 26;12(1):6938. doi: 10.1038/s41467-021-26940-2. PMID: 34836966; PMCID: PMC8626557.

Lin D, Wang M, Chen Y, Gong J, Chen L, Shi X, Lan F, Chen Z, Xiong T, Sun H, Wan S. Trends in Intracranial Glioma Incidence and Mortality in the United States, 1975-2018. Front Oncol. 2021 Nov 1;11:748061. doi: 10.3389/fonc.2021.748061. PMID: 34790574; PMCID: PMC8591029.

Lin R, Cai J, Nathan C, Wei X, Schleidt S, Rosenwasser R, Iacovitti L. Neurogenesis is enhanced by stroke in multiple new stem cell niches along the ventricular system at

sites of high BBB permeability. Neurobiol Dis. 2015 Feb;74:229-39. doi: 10.1016/j.nbd.2014.11.016. Epub 2014 Dec 5. PMID: 25484283.

Liu G, Yuan X, Zeng Z, Tunici P, Ng H, Abdulkadir IR, Lu L, Irvin D, Black KL, Yu JS. Analysis of gene expression and chemoresistance of CD133+ cancer stem cells in glioblastoma. Mol Cancer. 2006 Dec 2;5:67. doi: 10.1186/1476-4598-5-67. PMID: 17140455; PMCID: PMC1697823.

Liu Z, Meng Q, Bartek J Jr, Poiret T, Persson O, Rane L, Rangelova E, Illies C, Peredo IH, Luo X, Rao MV, Robertson RA, Dodoo E, Maeurer M. Tumor-infiltrating lymphocytes (TILs) from patients with glioma. Oncoimmunology. 2016 Nov 29;6(2):e1252894. doi: 10.1080/2162402X.2016.1252894. PMID: 28344863; PMCID: PMC5353900.

Liu Z, Zhou J, Yang X, Liu Y, Zou C, Lv W, Chen C, Cheng KK, Chen T, Chang LJ, Wu D, Mao J. Safety and antitumor activity of GD2-Specific 4SCAR-T cells in patients with glioblastoma. Mol Cancer. 2023 Jan 9;22(1):3. doi: 10.1186/s12943-022-01711-9. PMID: 36617554; PMCID: PMC9827625.

Lohr J, Ratliff T, Huppertz A, Ge Y, Dictus C, Ahmadi R, Grau S, Hiraoka N, Eckstein V, Ecker RC, Korff T, von Deimling A, Unterberg A, Beckhove P, Herold-Mende C. Effector T-cell infiltration positively impacts survival of glioblastoma patients and is impaired by tumor-derived TGF-β. Clin Cancer Res. 2011 Jul 1;17(13):4296-308. doi: 10.1158/1078-0432.CCR-10-2557. Epub 2011 Apr 8. PMID: 21478334.

Louis DN, Perry A, Wesseling P, Brat DJ, Cree IA, Figarella-Branger D, Hawkins C, Ng HK, Pfister SM, Reifenberger G, Soffietti R, von Deimling A, Ellison DW. The 2021 WHO Classification of Tumors of the Central Nervous System: a summary. Neuro Oncol. 2021 Aug 2;23(8):1231-1251. doi: 10.1093/neuonc/noab106. PMID: 34185076; PMCID: PMC8328013.

Louis DN, Perry A, Wesseling P, Brat DJ, Cree IA, Figarella-Branger D, Hawkins C, Ng HK, Pfister SM, Reifenberger G, Soffietti R, von Deimling A, Ellison DW. The 2021 WHO Classification of Tumors of the Central Nervous System: a summary. Neuro Oncol. 2021 Aug 2;23(8):1231-1251. doi: 10.1093/neuonc/noab106. PMID: 34185076; PMCID: PMC8328013.

Lv K, Chen Z, Zhang X, Zhang Q, Liu L. Selective enrichment of CD133+/SOX2+ glioblastoma stem cells via adherent culture. Oncol Lett. 2018 Oct;16(4):4567-4576. doi: 10.3892/ol.2018.9154. Epub 2018 Jul 17. PMID: 30197675; PMCID: PMC6126346.

Maddison K, Graves MC, Bowden NA, Fay M, Vilain RE, Faulkner S, Tooney PA. Low tumour-infiltrating lymphocyte density in primary and recurrent glioblastoma. Oncotarget. 2021 Oct 12;12(21):2177-2187. doi: 10.18632/oncotarget.28069. PMID: 34676050; PMCID: PMC8522837.

Mantovani F, Collavin L, Del Sal G. Mutant p53 as a guardian of the cancer cell. Cell Death Differ. 2019 Jan;26(2):199-212. doi: 10.1038/s41418-018-0246-9. Epub 2018 Dec 11. PMID: 30538286; PMCID: PMC6329812.

Marqués-Torrejón MÁ, Porlan E, Banito A, Gómez-Ibarlucea E, Lopez-Contreras AJ, Fernández-Capetillo O, Vidal A, Gil J, Torres J, Fariñas I. Cyclin-dependent kinase inhibitor p21 controls adult neural stem cell expansion by regulating Sox2 gene expression. Cell Stem Cell. 2013 Jan 3;12(1):88-100. doi: 10.1016/j.stem.2012.12.001. Epub 2012 Dec 20. PMID: 23260487; PMCID: PMC3714747.

Miraglia S, Godfrey W, Yin AH, Atkins K, Warnke R, Holden JT, Bray RA, Waller EK, Buck DW. A novel five-transmembrane hematopoietic stem cell antigen: isolation, characterization, and molecular cloning. Blood. 1997 Dec 15;90(12):5013-21. PMID: 9389721.

Neftel C, Laffy J, Filbin MG, Hara T, Shore ME, Rahme GJ, Richman AR, Silverbush D, Shaw ML, Hebert CM, Dewitt J, Gritsch S, Perez EM, Gonzalez Castro LN, Lan X, Druck N, Rodman C, Dionne D, Kaplan A, Bertalan MS, Small J, Pelton K, Becker S, Bonal D, Nguyen QD, Servis RL, Fung JM, Mylvaganam R, Mayr L, Gojo J, Haberler C, Geyeregger R, Czech T, Slavc I, Nahed BV, Curry WT, Carter BS, Wakimoto H, Brastianos PK, Batchelor TT, Stemmer-Rachamimov A, Martinez-Lage M, Frosch MP, Stamenkovic I, Riggi N, Rheinbay E, Monje M, Rozenblatt-Rosen O, Cahill DP, Patel AP, Hunter T, Verma IM, Ligon KL, Louis DN, Regev A, Bernstein BE, Tirosh I, Suvà

ML. An Integrative Model of Cellular States, Plasticity, and Genetics for Glioblastoma. Cell. 2019 Aug 8;178(4):835-849.e21. doi: 10.1016/j.cell.2019.06.024. Epub 2019 Jul 18. PMID: 31327527; PMCID: PMC6703186.

Nicolas S, Abdellatef S, Haddad MA, Fakhoury I, El-Sibai M. Hypoxia and EGF Stimulation Regulate VEGF Expression in Human Glioblastoma Multiforme (GBM) Cells by Differential Regulation of the PI3K/Rho-GTPase and MAPK Pathways. Cells. 2019 Nov 6;8(11):1397. doi: 10.3390/cells8111397. PMID: 31698752; PMCID: PMC6912653.

Nguyen LT, Saibil SD, Sotov V, Le MX, Khoja L, Ghazarian D, Bonilla L, Majeed H, Hogg D, Joshua AM, Crump M, Franke N, Spreafico A, Hansen A, Al-Habeeb A, Leong W, Easson A, Reedijk M, Goldstein DP, McCready D, Yasufuku K, Waddell T, Cypel M, Pierre A, Zhang B, Boross-Harmer S, Cipollone J, Nelles M, Scheid E, Fyrsta M, Lo CS, Nie J, Yam JY, Yen PH, Gray D, Motta V, Elford AR, DeLuca S, Wang L, Effendi S, Ellenchery R, Hirano N, Ohashi PS, Butler MO. Phase II clinical trial of adoptive cell therapy for patients with metastatic melanoma with autologous tumor-infiltrating lymphocytes and low-dose interleukin-2. Cancer Immunol Immunother. 2019 May;68(5):773-785. doi: 10.1007/s00262-019-02307-x. Epub 2019 Feb 11. PMID: 30747243.

O'Rourke DM, Nasrallah MP, Desai A, Melenhorst JJ, Mansfield K, Morrissette JJD, Martinez-Lage M, Brem S, Maloney E, Shen A, Isaacs R, Mohan S, Plesa G, Lacey SF, Navenot JM, Zheng Z, Levine BL, Okada H, June CH, Brogdon JL, Maus MV. A single

dose of peripherally infused EGFRvIII-directed CAR T cells mediates antigen loss and induces adaptive resistance in patients with recurrent glioblastoma. Sci Transl Med. 2017 Jul 19;9(399):eaaa0984. doi: 10.1126/scitranslmed.aaa0984. PMID: 28724573; PMCID: PMC5762203.

Orecchioni M, Ghosheh Y, Pramod AB, Ley K. Macrophage Polarization: Different Gene Signatures in M1(LPS+) vs. Classically and M2(LPS-) vs. Alternatively Activated Macrophages. Front Immunol. 2019 May 24;10:1084. doi: 10.3389/fimmu.2019.01084. Erratum in: Front Immunol. 2020 Feb 25;11:234. PMID: 31178859; PMCID: PMC6543837.

Ott PA, Pavlick AC, Johnson DB, Hart LL, Infante JR, Luke JJ, Lutzky J, Rothschild NE, Spitler LE, Cowey CL, Alizadeh AR, Salama AK, He Y, Hawthorne TR, Bagley RG, Zhang J, Turner CD, Hamid O. A phase 2 study of glembatumumab vedotin, an antibody-drug conjugate targeting glycoprotein NMB, in patients with advanced melanoma. Cancer. 2019 Apr 1;125(7):1113-1123. doi: 10.1002/cncr.31892. Epub 2019 Jan 28. PMID: 30690710.

Pan LQ, Zhao WB, Lai J, Ding D, Wei XY, Li YY, Liu WH, Yang XY, Xu YC, Chen SQ. Hetero-modification of TRAIL trimer for improved drug delivery and in vivo antitumor activities. Sci Rep. 2015 Oct 8;5:14872. doi: 10.1038/srep14872. PMID: 26445897; PMCID: PMC4597189.

Park JH, Lee HK. Current Understanding of Hypoxia in Glioblastoma Multiforme and Its Response to Immunotherapy. Cancers (Basel). 2022 Feb 24;14(5):1176. doi: 10.3390/cancers14051176. PMID: 35267480; PMCID: PMC8909860.

Park JH, Kim HJ, Kim CW, Kim HC, Jung Y, Lee HS, Lee Y, Ju YS, Oh JE, Park SH, Lee JH, Lee SK, Lee HK. Tumor hypoxia represses γδ T cell-mediated antitumor immunity against brain tumors. Nat Immunol. 2021 Mar;22(3):336-346. doi: 10.1038/s41590-020-00860-7. Epub 2021 Feb 11. PMID: 33574616.

Patel AP, Tirosh I, Trombetta JJ, Shalek AK, Gillespie SM, Wakimoto H, Cahill DP, Nahed BV, Curry WT, Martuza RL, Louis DN, Rozenblatt-Rosen O, Suvà ML, Regev A, Bernstein BE. Single-cell RNA-seq highlights intratumoral heterogeneity in primary glioblastoma. Science. 2014 Jun 20;344(6190):1396-401. doi: 10.1126/science.1254257. Epub 2014 Jun 12. PMID: 24925914; PMCID: PMC4123637.

Peh GS, Lang RJ, Pera MF, Hawes SM. CD133 expression by neural progenitors derived from human embryonic stem cells and its use for their prospective isolation. Stem Cells Dev. 2009 Mar;18(2):269-82. doi: 10.1089/scd.2008.0124. PMID: 18651819.

Peng P, Lou Y, Wang S, Wang J, Zhang Z, Du P, Zheng J, Liu P, Xu LX. Activated NK cells reprogram MDSCs via NKG2D-NKG2DL and IFN-γ to modulate antitumor T-cell response after cryo-thermal therapy. J Immunother Cancer. 2022 Dec;10(12):e005769. doi: 10.1136/jitc-2022-005769. PMID: 36521929; PMCID: PMC9756281.

Peng W, Liu C, Xu C, Lou Y, Chen J, Yang Y, Yagita H, Overwijk WW, Lizée G, Radvanyi L, Hwu P. PD-1 blockade enhances T-cell migration to tumors by elevating IFN-γ inducible chemokines. Cancer Res. 2012 Oct 15;72(20):5209-18. doi: 10.1158/0008-5472.CAN-12-1187. Epub 2012 Aug 20. PMID: 22915761; PMCID: PMC3476734.

Phillips HS, Kharbanda S, Chen R, Forrest WF, Soriano RH, Wu TD, Misra A, Nigro JM, Colman H, Soroceanu L, Williams PM, Modrusan Z, Feuerstein BG, Aldape K. Molecular subclasses of high-grade glioma predict prognosis, delineate a pattern of disease progression, and resemble stages in neurogenesis. Cancer Cell. 2006 Mar;9(3):157-73. doi: 10.1016/j.ccr.2006.02.019. PMID: 16530701.

Pickar-Oliver A, Gersbach CA. The next generation of CRISPR-Cas technologies and applications. Nat Rev Mol Cell Biol. 2019 Aug;20(8):490-507. doi: 10.1038/s41580-019-0131-5. PMID: 31147612; PMCID: PMC7079207.

Poliwoda S, Noor N, Downs E, Schaaf A, Cantwell A, Ganti L, Kaye AD, Mosel LI, Carroll CB, Viswanath O, Urits I. Stem cells: a comprehensive review of origins and emerging clinical roles in medical practice. Orthop Rev (Pavia). 2022 Aug 25;14(3):37498. doi: 10.52965/001c.37498. PMID: 36034728; PMCID: PMC9404248.

Qazi MA, Salim SK, Brown KR, Mikolajewicz N, Savage N, Han H, Subapanditha MK, Bakhshinyan D, Nixon A, Vora P, Desmond K, Chokshi C, Singh M, Khoo A, Macklin A,

Khan S, Tatari N, Winegarden N, Richards L, Pugh T, Bock N, Mansouri A, Venugopal C, Kislinger T, Goyal S, Moffat J, Singh SK. Characterization of the minimal residual disease state reveals distinct evolutionary trajectories of human glioblastoma. Cell Rep. 2022 Sep 27;40(13):111420. doi: 10.1016/j.celrep.2022.111420. PMID: 36170831.

Ran FA, Hsu PD, Wright J, Agarwala V, Scott DA, Zhang F. Genome engineering using the CRISPR-Cas9 system. Nat Protoc. 2013 Nov;8(11):2281-2308. doi: 10.1038/nprot.2013.143. Epub 2013 Oct 24. PMID: 24157548; PMCID: PMC3969860.

Ravi VM, Neidert N, Will P, Joseph K, Maier JP, Kückelhaus J, Vollmer L, Goeldner JM, Behringer SP, Scherer F, Boerries M, Follo M, Weiss T, Delev D, Kernbach J, Franco P, Schallner N, Dierks C, Carro MS, Hofmann UG, Fung C, Sankowski R, Prinz M, Beck J, Salié H, Bengsch B, Schnell O, Heiland DH. T-cell dysfunction in the glioblastoma microenvironment is mediated by myeloid cells releasing interleukin-10. Nat Commun. 2022 Feb 17;13(1):925. doi: 10.1038/s41467-022-28523-1. PMID: 35177622; PMCID: PMC8854421.

Reardon DA, Brandes AA, Omuro A, Mulholland P, Lim M, Wick A, Baehring J, Ahluwalia MS, Roth P, Bähr O, Phuphanich S, Sepulveda JM, De Souza P, Sahebjam S, Carleton M, Tatsuoka K, Taitt C, Zwirtes R, Sampson J, Weller M. Effect of Nivolumab vs Bevacizumab in Patients With Recurrent Glioblastoma: The CheckMate 143 Phase 3 Randomized Clinical Trial. JAMA Oncol. 2020 Jul 1;6(7):1003-1010. doi: 10.1001/jamaoncol.2020.1024. PMID: 32437507; PMCID: PMC7243167.

Reya T, Morrison SJ, Clarke MF, Weissman IL. Stem cells, cancer, and cancer stem cells. Nature. 2001 Nov 1;414(6859):105-11. doi: 10.1038/35102167. PMID: 11689955.

Rich JN, Shi Q, Hjelmeland M, Cummings TJ, Kuan CT, Bigner DD, Counter CM, Wang XF. Bone-related genes expressed in advanced malignancies induce invasion and metastasis in a genetically defined human cancer model. J Biol Chem. 2003 May 2;278(18):15951-7. doi: 10.1074/jbc.M211498200. Epub 2003 Feb 17. PMID: 12590137.

Schepers GE, Teasdale RD, Koopman P. Twenty pairs of sox: extent, homology, and nomenclature of the mouse and human sox transcription factor gene families. Dev Cell. 2002 Aug;3(2):167-70. doi: 10.1016/s1534-5807(02)00223-x. PMID: 12194848.

Schmitz M, Temme A, Senner V, Ebner R, Schwind S, Stevanovic S, Wehner R, Schackert G, Schackert HK, Fussel M, Bachmann M, Rieber EP, Weigle B. Identification of SOX2 as a novel glioma-associated antigen and potential target for T cell-based immunotherapy. Br J Cancer. 2007 Apr 23;96(8):1293-301. doi: 10.1038/sj.bjc.6603696. Epub 2007 Mar 20. Erratum in: Br J Cancer. 2007 Jun 18;96(12):1928. PMID: 17375044; PMCID: PMC2360145.

Schuster SJ, Bishop MR, Tam CS, Waller EK, Borchmann P, McGuirk JP, Jäger U, Jaglowski S, Andreadis C, Westin JR, Fleury I, Bachanova V, Foley SR, Ho PJ, Mielke S, Magenau JM, Holte H, Pantano S, Pacaud LB, Awasthi R, Chu J, Anak Ö, Salles G,

Maziarz RT; JULIET Investigators. Tisagenlecleucel in Adult Relapsed or Refractory Diffuse Large B-Cell Lymphoma. N Engl J Med. 2019 Jan 3;380(1):45-56. doi: 10.1056/NEJMoa1804980. Epub 2018 Dec 1. PMID: 30501490.

Shalem O, Sanjana NE, Hartenian E, Shi X, Scott DA, Mikkelson T, Heckl D, Ebert BL, Root DE, Doench JG, Zhang F. Genome-scale CRISPR-Cas9 knockout screening in human cells. Science. 2014 Jan 3;343(6166):84-87. doi: 10.1126/science.1247005. Epub 2013 Dec 12. PMID: 24336571; PMCID: PMC4089965.

Sherriff J, Tamangani J, Senthil L, Cruickshank G, Spooner D, Jones B, Brookes C, Sanghera P. Patterns of relapse in glioblastoma multiforme following concomitant chemoradiotherapy with temozolomide. Br J Radiol. 2013 Feb;86(1022):20120414. doi: 10.1259/bjr.20120414. PMID: 23385995; PMCID: PMC3608050.

Singh SK, Hawkins C, Clarke ID, Squire JA, Bayani J, Hide T, Henkelman RM, Cusimano MD, Dirks PB. Identification of human brain tumour initiating cells. Nature. 2004 Nov 18;432(7015):396-401. doi: 10.1038/nature03128. PMID: 15549107.

Solinas G, Schiarea S, Liguori M, Fabbri M, Pesce S, Zammataro L, Pasqualini F, Nebuloni M, Chiabrando C, Mantovani A, Allavena P. Tumor-conditioned macrophages secrete migration-stimulating factor: a new marker for M2-polarization, influencing tumor cell motility. J Immunol. 2010 Jul 1;185(1):642-52. doi: 10.4049/jimmunol.1000413. Epub 2010 Jun 7. PMID: 20530259.

Song WS, Yang YP, Huang CS, Lu KH, Liu WH, Wu WW, Lee YY, Lo WL, Lee SD, Chen YW, Huang PI, Chen MT. Sox2, a stemness gene, regulates tumor-initiating and drug-resistant properties in CD133-positive glioblastoma stem cells. J Chin Med Assoc. 2016 Oct;79(10):538-45. doi: 10.1016/j.jcma.2016.03.010. Epub 2016 Aug 13. PMID: 27530866.

Sönmez C, Wölfer J, Holling M, Brokinkel B, Stummer W, Wiendl H, Thomas C, Schulte-Mecklenbeck A, Grauer OM. Blockade of inhibitory killer cell immunoglobulin-like receptors and IL-2 triggering reverses the functional hypoactivity of tumor-derived NK-cells in glioblastomas. Sci Rep. 2022 Apr 26;12(1):6769. doi: 10.1038/s41598-022-10680-4. PMID: 35474089; PMCID: PMC9042843.

Sottoriva A, Spiteri I, Piccirillo SG, Touloumis A, Collins VP, Marioni JC, Curtis C, Watts C, Tavaré S. Intratumor heterogeneity in human glioblastoma reflects cancer evolutionary dynamics. Proc Natl Acad Sci U S A. 2013 Mar 5;110(10):4009-14. doi: 10.1073/pnas.1219747110. Epub 2013 Feb 14. PMID: 23412337; PMCID: PMC3593922.

Squibb B-M, Bristol-myers squibb announces phase 3 CheckMate 498 study did not meet primary endpoint of overall survival with opdivo (nivolumab) plus radiation in patients with newly diagnosed MGMT-unmethylated glioblastoma multiforme. 2019. May 9. Accessed 2019 November15.

Squibb B-M Bristol-myers squibb provides update on phase 3 opdivo (nivolumab) CheckMate −548 trial in patients with newly diagnosed MGMT-methylated glioblastoma multiforme. 2019. September 5. Accessed 2018 November9.

Stupp R, Hegi ME, Mason WP, van den Bent MJ, Taphoorn MJ, Janzer RC, Ludwin SK, Allgeier A, Fisher B, Belanger K, Hau P, Brandes AA, Gijtenbeek J, Marosi C, Vecht CJ, Mokhtari K, Wesseling P, Villa S, Eisenhauer E, Gorlia T, Weller M, Lacombe D, Cairncross JG, Mirimanoff RO; European Organisation for Research and Treatment of Cancer Brain Tumour and Radiation Oncology Groups; National Cancer Institute of Canada Clinical Trials Group. Effects of radiotherapy with concomitant and adjuvant temozolomide versus radiotherapy alone on survival in glioblastoma in a randomised phase III study: 5-year analysis of the EORTC-NCIC trial. Lancet Oncol. 2009 May;10(5):459-66. doi: 10.1016/S1470-2045(09)70025-7. Epub 2009 Mar 9. PMID: 19269895.

Stupp R, Mason WP, van den Bent MJ, Weller M, Fisher B, Taphoorn MJ, Belanger K, Brandes AA, Marosi C, Bogdahn U, Curschmann J, Janzer RC, Ludwin SK, Gorlia T, Allgeier A, Lacombe D, Cairncross JG, Eisenhauer E, Mirimanoff RO; European Organisation for Research and Treatment of Cancer Brain Tumor and Radiotherapy Groups; National Cancer Institute of Canada Clinical Trials Group. Radiotherapy plus concomitant and adjuvant temozolomide for glioblastoma. N Engl J Med. 2005 Mar 10;352(10):987-96. doi: 10.1056/NEJMoa043330. PMID: 15758009.

Szulzewsky F, Pelz A, Feng X, Synowitz M, Markovic D, Langmann T, Holtman IR, Wang X, Eggen BJ, Boddeke HW, Hambardzumyan D, Wolf SA, Kettenmann H. Glioma-associated microglia/macrophages display an expression profile different from M1 and M2 polarization and highly express Gpnmb and Spp1. PLoS One. 2015 Feb 6;10(2):e0116644. doi: 10.1371/journal.pone.0116644. PMID: 25658639; PMCID: PMC4320099.

Subklewe M. BiTEs better than CAR T cells. Blood Adv. 2021 Jan 26;5(2):607-612. doi: 10.1182/bloodadvances.2020001792. PMID: 33496755; PMCID: PMC7839370.

Taya M, Hammes SR. Glycoprotein Non-Metastatic Melanoma Protein B (GPNMB) and Cancer: A Novel Potential Therapeutic Target. Steroids. 2018 May;133:102-107. doi: 10.1016/j.steroids.2017.10.013. Epub 2017 Oct 31. PMID: 29097143; PMCID: PMC6166407.

Tran B, Rosenthal MA. Survival comparison between glioblastoma multiforme and other incurable cancers. J Clin Neurosci. 2010 Apr;17(4):417-21. doi: 10.1016/j.jocn.2009.09.004. Epub 2010 Feb 18. PMID: 20167494.

Takahashi K, Yamanaka S. Induction of pluripotent stem cells from mouse embryonic and adult fibroblast cultures by defined factors. Cell. 2006 Aug 25;126(4):663-76. doi: 10.1016/j.cell.2006.07.024. Epub 2006 Aug 10. PMID: 16904174.

Takahashi K, Tanabe K, Ohnuki M, Narita M, Ichisaka T, Tomoda K, Yamanaka S. Induction of pluripotent stem cells from adult human fibroblasts by defined factors. Cell. 2007 Nov 30;131(5):861-72. doi: 10.1016/j.cell.2007.11.019. PMID: 18035408.

Tamura K, Aoyagi M, Ando N, Ogishima T, Wakimoto H, Yamamoto M, Ohno K. Expansion of CD133-positive glioma cells in recurrent de novo glioblastomas after radiotherapy and chemotherapy. J Neurosurg. 2013 Nov;119(5):1145-55. doi: 10.3171/2013.7.JNS122417. Epub 2013 Aug 30. PMID: 23991844.

Tatari N, Zhang X, Chafe SC, McKenna D, Lawson KA, Subapanditha M, Shaikh MV, Seyfrid M, Savage N, Venugopal C, Moffat J, Singh SK. Dual Antigen T Cell Engagers Targeting CA9 as an Effective Immunotherapeutic Modality for Targeting CA9 in Solid Tumors. Front Immunol. 2022 Jul 6;13:905768. doi: 10.3389/fimmu.2022.905768. PMID: 35874663; PMCID: PMC9296860.

Tomasik J, Jasiński M, Basak GW. Next generations of CAR-T cells - new therapeutic opportunities in hematology? Front Immunol. 2022 Oct 28;13:1034707. doi: 10.3389/fimmu.2022.1034707. PMID: 36389658; PMCID: PMC9650233.

Topalian SL, Sznol M, McDermott DF, Kluger HM, Carvajal RD, Sharfman WH, Brahmer JR, Lawrence DP, Atkins MB, Powderly JD, Leming PD, Lipson EJ, Puzanov I, Smith DC, Taube JM, Wigginton JM, Kollia GD, Gupta A, Pardoll DM, Sosman JA, Hodi FS. Survival, durable tumor remission, and long-term safety in patients with advanced

melanoma receiving nivolumab. J Clin Oncol. 2014 Apr 1;32(10):1020-30. doi: 10.1200/JCO.2013.53.0105. Epub 2014 Mar 3. Corrected and republished in: J Clin Oncol. 2023 Feb 10;41(5):943-954. PMID: 24590637; PMCID: PMC4811023.

Tse KF, Jeffers M, Pollack VA, McCabe DA, Shadish ML, Khramtsov NV, Hackett CS, Shenoy SG, Kuang B, Boldog FL, MacDougall JR, Rastelli L, Herrmann J, Gallo M, Gazit-Bornstein G, Senter PD, Meyer DL, Lichenstein HS, LaRochelle WJ. CR011, a fully human monoclonal antibody-auristatin E conjugate, for the treatment of melanoma. Clin Cancer Res. 2006 Feb 15;12(4):1373-82. doi: 10.1158/1078-0432.CCR-05-2018. PMID: 16489096.

Venugopal C, Hallett R, Vora P, Manoranjan B, Mahendram S, Qazi MA, McFarlane N, Subapanditha M, Nolte SM, Singh M, Bakhshinyan D, Garg N, Vijayakumar T, Lach B, Provias JP, Reddy K, Murty NK, Doble BW, Bhatia M, Hassell JA, Singh SK. Pyrvinium Targets CD133 in Human Glioblastoma Brain Tumor-Initiating Cells. Clin Cancer Res. 2015 Dec 1;21(23):5324-37. doi: 10.1158/1078-0432.CCR-14-3147. Epub 2015 Jul 7. PMID: 26152745.

Verhaak RG, Hoadley KA, Purdom E, Wang V, Qi Y, Wilkerson MD, Miller CR, Ding L, Golub T, Mesirov JP, Alexe G, Lawrence M, O'Kelly M, Tamayo P, Weir BA, Gabriel S, Winckler W, Gupta S, Jakkula L, Feiler HS, Hodgson JG, James CD, Sarkaria JN, Brennan C, Kahn A, Spellman PT, Wilson RK, Speed TP, Gray JW, Meyerson M, Getz G, Perou CM, Hayes DN; Cancer Genome Atlas Research Network. Integrated genomic

analysis identifies clinically relevant subtypes of glioblastoma characterized by abnormalities in PDGFRA, IDH1, EGFR, and NF1. Cancer Cell. 2010 Jan 19;17(1):98-110. doi: 10.1016/j.ccr.2009.12.020. PMID: 20129251; PMCID: PMC2818769.

Wang Y, Chen M, Wu Z, Tong C, Dai H, Guo Y, Liu Y, Huang J, Lv H, Luo C, Feng KC, Yang QM, Li XL, Han W. CD133-directed CAR T cells for advanced metastasis malignancies: A phase I trial. Oncoimmunology. 2018 May 7;7(7):e1440169. doi: 10.1080/2162402X.2018.1440169. PMID: 29900044; PMCID: PMC5993480.

Wang Q, Hu B, Hu X, Kim H, Squatrito M, Scarpace L, deCarvalho AC, Lyu S, Li P, Li Y, Barthel F, Cho HJ, Lin YH, Satani N, Martinez-Ledesma E, Zheng S, Chang E, Sauvé CG, Olar A, Lan ZD, Finocchiaro G, Phillips JJ, Berger MS, Gabrusiewicz KR, Wang G, Eskilsson E, Hu J, Mikkelsen T, DePinho RA, Muller F, Heimberger AB, Sulman EP, Nam DH, Verhaak RGW. Tumor Evolution of Glioma-Intrinsic Gene Expression Subtypes Associates with Immunological Changes in the Microenvironment. Cancer Cell. 2017 Jul 10;32(1):42-56.e6. doi: 10.1016/j.ccell.2017.06.003. Erratum in: Cancer Cell. 2018 Jan 8;33(1):152. PMID: 28697342; PMCID: PMC5599156.

Wang S, Xia P, Ye B, Huang G, Liu J, Fan Z. Transient activation of autophagy via Sox2-mediated suppression of mTOR is an important early step in reprogramming to pluripotency. Cell Stem Cell. 2013 Nov 7;13(5):617-25. doi: 10.1016/j.stem.2013.10.005. PMID: 24209762.

Wang J, Xu SL, Duan JJ, Yi L, Guo YF, Shi Y, Li L, Yang ZY, Liao XM, Cai J, Zhang YQ, Xiao HL, Yin L, Wu H, Zhang JN, Lv SQ, Yang QK, Yang XJ, Jiang T, Zhang X, Bian XW, Yu SC. Invasion of white matter tracts by glioma stem cells is regulated by a NOTCH1-SOX2 positive-feedback loop. Nat Neurosci. 2019 Jan;22(1):91-105. doi: 10.1038/s41593-018-0285-z. Epub 2018 Dec 17. Erratum in: Nat Neurosci. 2019 May;22(5):840. PMID: 30559479.

Wang Z, Zhong H, Liang X, Ni S. Targeting tumor-associated macrophages for the immunotherapy of glioblastoma: Navigating the clinical and translational landscape. Front Immunol. 2022 Oct 13;13:1024921. doi: 10.3389/fimmu.2022.1024921. PMID: 36311702; PMCID: PMC9606568.

Wegner M. All purpose Sox: The many roles of Sox proteins in gene expression. Int J Biochem Cell Biol. 2010 Mar;42(3):381-90. doi: 10.1016/j.biocel.2009.07.006. Epub 2009 Jul 22. PMID: 19631281.

Wesolowski JR, Rajdev P, Mukherji SK. Temozolomide (Temodar). AJNR Am J Neuroradiol. 2010 Sep;31(8):1383-4. doi: 10.3174/ajnr.A2170. Epub 2010 Jun 10. PMID: 20538821; PMCID: PMC7966084.

Wiedenheft B, Sternberg SH, Doudna JA. RNA-guided genetic silencing systems in bacteria and archaea. Nature. 2012 Feb 15;482(7385):331-8. doi: 10.1038/nature10886. PMID: 22337052.

Wu H, Sun YE. Epigenetic regulation of stem cell differentiation. Pediatr Res. 2006 Apr;59(4 Pt 2):21R-5R. doi: 10.1203/01.pdr.0000203565.76028.2a. PMID: 16549544.

Xiong A, Zhang J, Chen Y, Zhang Y, Yang F. Integrated single-cell transcriptomic analyses reveal that GPNMB-high macrophages promote PN-MES transition and impede T cell activation in GBM. EBioMedicine. 2022 Sep;83:104239. doi: 10.1016/j.ebiom.2022.104239. Epub 2022 Aug 30. PMID: 36054938; PMCID: PMC9437813.

Yang T, Kong Z, Ma W. PD-1/PD-L1 immune checkpoint inhibitors in glioblastoma: clinical studies, challenges and potential. Hum Vaccin Immunother. 2021 Feb 1;17(2):546-553. doi: 10.1080/21645515.2020.1782692. Epub 2020 Jul 9. PMID: 32643507; PMCID: PMC7899692.

Yardley DA, Weaver R, Melisko ME, Saleh MN, Arena FP, Forero A, Cigler T, Stopeck A, Citrin D, Oliff I, Bechhold R, Loutfi R, Garcia AA, Cruickshank S, Crowley E, Green J, Hawthorne T, Yellin MJ, Davis TA, Vahdat LT. EMERGE: A Randomized Phase II Study of the Antibody-Drug Conjugate Glembatumumab Vedotin in Advanced Glycoprotein NMB-Expressing Breast Cancer. J Clin Oncol. 2015 May 10;33(14):1609-19. doi: 10.1200/JCO.2014.56.2959. Epub 2015 Apr 6. PMID: 25847941.

Yiangou L, Ross ADB, Goh KJ, Vallier L. Human Pluripotent Stem Cell-Derived Endoderm for Modeling Development and Clinical Applications. Cell Stem Cell. 2018 Apr 5;22(4):485-499. doi: 10.1016/j.stem.2018.03.016. PMID: 29625066.

Yin AH, Miraglia S, Zanjani ED, Almeida-Porada G, Ogawa M, Leary AG, Olweus J, Kearney J, Buck DW. AC133, a novel marker for human hematopoietic stem and progenitor cells. Blood. 1997 Dec 15;90(12):5002-12. PMID: 9389720.

Yin J, Valin KL, Dixon ML, Leavenworth JW. The Role of Microglia and Macrophages in CNS Homeostasis, Autoimmunity, and Cancer. J Immunol Res. 2017;2017:5150678. doi: 10.1155/2017/5150678. Epub 2017 Dec 19. PMID: 29410971; PMCID: PMC5749282.

Yu J, Vodyanik MA, Smuga-Otto K, Antosiewicz-Bourget J, Frane JL, Tian S, Nie J, Jonsdottir GA, Ruotti V, Stewart R, Slukvin II, Thomson JA. Induced pluripotent stem cell lines derived from human somatic cells. Science. 2007 Dec 21;318(5858):1917-20. doi: 10.1126/science.1151526. Epub 2007 Nov 20. PMID: 18029452.

Zacharakis N, Chinnasamy H, Black M, Xu H, Lu YC, Zheng Z, Pasetto A, Langhan M, Shelton T, Prickett T, Gartner J, Jia L, Trebska-McGowan K, Somerville RP, Robbins PF, Rosenberg SA, Goff SL, Feldman SA. Immune recognition of somatic mutations leading to complete durable regression in metastatic breast cancer. Nat Med. 2018

Jun;24(6):724-730. doi: 10.1038/s41591-018-0040-8. Epub 2018 Jun 4. PMID: 29867227; PMCID: PMC6348479.

Zakrzewski W, Dobrzyński M, Szymonowicz M, Rybak Z. Stem cells: past, present, and future. Stem Cell Res Ther. 2019 Feb 26;10(1):68. doi: 10.1186/s13287-019-1165-5. PMID: 30808416; PMCID: PMC6390367.

Zhai J, Xiao Z, Wang Y, Wang H. Human embryonic development: from peri-implantation to gastrulation. Trends Cell Biol. 2022 Jan;32(1):18-29. doi: 10.1016/j.tcb.2021.07.008. Epub 2021 Aug 17. PMID: 34417090.

Zhang J, Stevens MF, Bradshaw TD. Temozolomide: mechanisms of action, repair and resistance. Curr Mol Pharmacol. 2012 Jan;5(1):102-14. doi: 10.2174/1874467211205010102. PMID: 22122467.

Zhenjiang L, Meng Q, Persson O, Jiri B, Poiret T, Rane L, Rangelova EB, Dodoo E, Maeurer M. Rapid expansion of TILs from patients with glioma and recognition of autologous tumor. J Immunother Cancer. 2014 Nov 6;2(Suppl 3):P27. doi: 10.1186/2051-1426-2-S3-P27. PMCID: PMC4288617.

Chapter 2 Figure Captions

Figure 1. Genome-wide screen on patient derived glioblastoma stem cells.

A) Characterization of CD133 surface levels in patient derived GSC samples.

B) Secondary sphere assay of GSC samples sorted in CD133+/- populations to assess in vitro sphere formation.

C) Proliferation assay of GSC samples sorted in CD133+/- populations to assess proliferative capacity in comparative subpopulations.

D) Schematic of experimental plan for the identification of genetic interactions in BT935. GSCs transduced with TKOv3 were expanded for 12 doublings to be sorted into the top/bottom 5th percentiles of CD133 surface expression.

E) Graphical representation of fitness effects (log2 fold-change, LFC) for reference core essential and non-essential gene sets defined in Hart et al., 2017.

F) Precision-recall curves for the three CRISPR experimental populations using the reference core essential gene set defined in Hart et al., 2017.

Figure 2. Data mining biological processes for top ranked genetic interactions of CD133 in the BT935 CRISPR Screen.

A) Rank correlation of normalized sgRNA read count between experimental populations of the BT935 CRISPR Screen.

B) DrugZ scores for all ranked genes comparing AC133-high to AC133-low GSC populations.

C) CD133 positive and negative interactions. A scatter plot illustrating the fitness effect

(LFC) of all genes highlighting which exhibited a significant genetic interaction. Negative (blue) and positive (yellow) CD133 genetic interactions are shown. Node size represents DrugZ score of genes.

D) Gene Ontology (GO) enrichment of biological processes among genes that exhibited a significant genetic interaction with CD133. The p-values of biological processes are represented by the greyscale color legend (right).

E) String database analysis of interaction networks formed by the top 50 ranked negative genetic interactors of CD133 surface expression. Color coding of interactions: red, Glioma Stem Cells; green, Embryonic Stem Cells; blue, Transferase Complex.

Figure 3. Investigating Functional Role of Hits in CD133 Regulation and Stemness.

A) Characterization of CD133 surface levels in patient derived GSC samples after knockouts of candidate genes in duplicate.

B) Measurements of Mean Fluorescence Intensity of CD133 surface levels in patient derived GSC samples after knockouts of candidate genes in duplicate.

C) Protein quantification and normalization (right) to control AAVS1 after knockouts of candidate genes in duplicate.

D) Self-renewal capacity readout of GSC samples after knockouts of candidate genes in duplicate.

E) Proliferative capacity readout of GSC samples after knockouts of candidate genes in duplicate.

Figure 4. Validating the dysregulation of SOX2 binding in GSCs.

A) RNA expression levels of SOX2 in GBM tissues (red, TCGA) compared to normal brain tissue (grey, GTEx).

B) Western blot validating reduction of CD133 across GSC cell lines in SOX2 CRISPR knockouts and target specific antibody for CUT&RUN.

C) CUT&RUN schematic to identify DNA interactions with SOX2. Visualizing the high level overview of permeabilizing live cells for SOX2 primary antibody incubation, DNA cleavage and nucleotide extraction for sequencing.

D) IGV profile of PROM1 visualizing genomic binding of SOX2 within the first intron.

Supplementary 1. Biological replicates of validation experiments examining top ranked genetic interactions with CD133.

A) Bulk RNA transcript levels of top ranked genetic interactions in GBM. Blue-scale color intensity represents higher transcripts per million.

B) Bulk RNA transcript levels of SOX2 across cancer types and representative matched normal tissues.

C) Characterization of CD133 surface levels in patient derived GSC samples after knockouts of candidate genes in duplicate (BT954 left, MBT103 right).

D) Measurements of Mean Fluorescence Intensity of CD133 surface levels in patient derived GSC samples after knockouts of candidate genes in duplicate (BT954 left, MBT103 right).

E) Protein quantification and normalization (right) to control AAVS1 after knockouts of candidate genes in duplicate (BT954 left, MBT103 right).

F) Self-renewal capacity readout of GSC samples after knockouts of candidate genes in duplicate (BT954 left, MBT103 right).

G) Proliferative capacity readout of GSC samples after knockouts of candidate genes in duplicate (BT954 left, MBT103 right).

Supplementary 2. Antibody Validations.

A) Western blots of all gene knockouts of interest.

Supplementary 3. Gene Correlations.

A) RNAseq correlations of all gene knockouts of interest in TCGA.

Chapter 3 Figure Captions

Figure 1. Identifying GPNMB as a Clinically Relevant Target in Glioblastoma.

A) GSC and NSC cell lines were flow sorted into CD133+ and CD133- populations followed by RNAseq to reveal differentially expressed genes (right).

B) Analysis comparing GPNMB in GBM tissue subtypes compared to normal brain tissues.

C) Western blot validating GPNMB protein is restricted to GBM specimens.

D) Hematoxylin and eosin stain of CD133- GBM xenograft overlays with GPNMB immunohistochemistry.

E) Normal human brain regions lack GPNMB expression.

Figure 2. GPNMB Contributes To Tumor Progression And Upregulates At Recurrence.

A) Western blots validating reduced GPNMB levels in pooled CRISPR knockouts of primary GBMs.

B) Proliferative capacity readout of primary GBM samples after knockouts of GPNMB compared to AAVS1 controls.

C) Orthotopic xenografts display increased survival time in populations with lower GPNMB levels.

D) RNA expression levels of patient GBM samples grown in vitro, in vivo or as intact patient tissue samples.

E) Volcano plots showing differentially expressed whole cell proteomics of a patient

matched primary-recurrent GBM sample grown in vitro.

F) Immunohistochemistry block of PDX block harbouring recurrent GBM (BT972).

G) Comparative whole cell proteomic analysis of 43 intact patient matched primary-recurrent GBM tissues.

H) Representative sample of immunohistochemistry blocks of patient matched primary-recurrent GBM tissues and HALO annotations.

I) HALO quantification of immunohistochemistry blocks of 15 patient matched GBMs.

Figure 3. GPNMB in the Tumor Immune Microenvironment.

A) Single-cell RNA expression levels of GPNMB in bulk GBM tissue.

B) Gene Ontology enrichment analysis of TCGA RNAseq data of GBM revealing biological processes associated with GPNMB.

C) Gene correlations of GPNMB with classic macrophage and inflammatory markers in TCGA GBM samples.

D) Proliferative capacity readout of wild type GL261 compared to GPNMB clonal knockouts.

E) Orthotopic xenografts display increased survival time in populations deficient in GPNMB expression (Clone 3).

F) Schematic of syngeneic mouse single-cell analysis of GPNMB expression.

Figure 4. GPNMB Modulates Hallmark Pathways Of GBM And Well Known Immune Pathways.

A) Readout of upregulated (left) and downregulated (right) pathways in GPNMB-KO mice.

B) Gene set enrichment analysis of pathways modulated in GPNMB knockouts (red) and the top enriched pathways associated with GPNMB in blue.

C) Enriched pathways associated with GPNMB and significant genes differentiall expressed in each pathway, highlighting previously reported biological processes.

D) Co-expression profile of pathways associated with GPNMB expression.

E) Reduced IRF8 transcription factor activity is displayed in GPNMB knockouts, highlighting the most significantly upregulated genes in wild type GL261 cells.

F) GPNMB promoter sequence highlighting transcription factor binding regions of IRF family members.

Figure 5. GPNMB Is Upregulated To Counteract The Proinflammatory Signals of Interferons

A) Inflammation signaling pathways enriched in PDX models treated with SoC

B) Trajectory of GBM evolution in response to SoC, displaying pseudotime progression along with Epithelial–Mesenchymal Transition gene signature and inflammatory genes of interest.

C) Gene correlation of GPNMB and IRF8 in bulk GBM samples in TCGA.

D) Clustered analysis of GPNMB and members of interferon signaling across GBM subtypes.

E) Clustered analysis of GPNMB and members of interferon signaling across cell types in GBM tumors.

Supplementary 1. Examining Enriched Pathways Comparing CD133+/- of GSCs and NSCs.

A) Four Gene Set Enrichment Analyses, comparing and contrasting groups.

B) Analysis comparing GPNMB across GBM subtypes.

C) Pathways enriched in CD133+ populations of both GSCs and NSCs.

D) Pathways enriched in GSC populations compared to NSC populations

E) Pathways specifically enriched in CD133+ or CD133 GSC populations.

Supplementary 2. Preliminary data identifying the distribution of GPNMB through multiomic examination in patient derived GBM samples.

A) Immunohistochemistry optimization of GPNMB in treatment naïve PDX blocks.

B) Patient matched primary-recurrent GBM whole cell proteomics.

C) Transmembrane protein structure of GPNMB with posttranslational modifications.

D) UMAP of single-cell data displaying GPNMB distribution throughout primary and recurrent GBMs.

Supplementary 3. Supporting data of GL261 single-cell data.

A) Western blot validating successful clonal knockouts of GPNMB compared to wild type (WT) lines.

B) UMAP of single-cell data highlighting GL261 wild type and clonal knockout, showing absence of GBM cells in sham control populations.

C) GPNMB distribution comparing wild type and clonal knockout lines, highlighting GBM and immune populations.

D) Enrichment scores of transcription factor activity.

Chapter 4 Figure Captions

Figure 1. Chimeric Antigen Receptor T Cells Are a Viable Immunotherapy Modality.

A) Tissue microarray of 23 normal tissues throughout the human body.

B) Western blot validating clonal knockouts of GPNMB in SK-MEL-2 cell lines and target specificity of GPNMB antibody (R&D Systems AF255).

C) Titration curve of dose response of AF2550 detecting surface expression levels of GPNMB on SK-MEL-2.

D) Flow cytometry analysis of multiple GBM cells lines indicating surface accessability for CAR-Ts.

Figure 2. CAR-T Validations in vitro.

A) Chimeric Antigen Receptor, second-generation schematic of GPNMB and CD19 constructs.

B) Transduction efficiency readout as determined by GFP+ expression indicating successful integration of lentivirus into T cells.

C) Cytotoxicity assays revealing time and dose dependent killings in GBM8 (left) and GBM4 (right) lines.

D) EVOS microscope view of CAR-Ts variably swarming and engaging target cells.

E) CAR-T activation readout at 24 hour timepoint.

F) Proliferation readout of CAR-Ts three days after exposure to target cells.

G) IFN-gamma production levels determined by ELISA of multiple target cells.

H) TNF-alpha production levels determined by ELISA of multiple target cells.

Figure 3. Monotherapy treatments of PDX models with intracranial CAR-Ts.

A) Visual representation of experimental timeline for in vivo CAR-T trials.

B) Weekly bioluminescent measurements using IVIS in PDX models.

C) Tumor volume measurements and survival times in GBM8 bearing mice after single doses of monotherapy treatments.

D) Tumor volume measurements and survival times in GBM4 bearing mice after single doses of monotherapy treatments.

E) Examination of residual tumors using H&E and IHC (GPNMB) for PDX mice treated with CD19 CAR-Ts (left) or GPNMB CAR-Ts (right).

F) Plasma membrane expression levels of antigens of interest in freshly processed brains of PDX mouse brains 10 days after treatment with CAR-T constructs.

Figure 4. Rational combination treatments using CAR-Ts in GBM models. .

A) Flow cytometry showing distribution of GPNMB and CD133 in GBM populations showing distinct populations.

B) Therapy regimens of CAR-Ts injected intracranially.

C) Weekly bioluminescent measurements using IVIS in PDX models.

D) Tumor volume measurements and survival times in GBM8 bearing mice after sequential doses of treatments.

E) Kaplan-Meier survival analysis of tumor bearing mice.

Figure 5. Rational combination treatments using CAR-Ts in GBM models. .

A) Western blot showing relative abundance of GPNMB in myeloid lineage cells types.

B) Surface expression levels of GPNMB in myeloid lineage cells types.

C) Cytotoxicity assays revealing time and dose dependent killing of macrophages in response to CAR-Ts

D) Western blot indicating positive presence of GPNMB in recurrent GBM, BT972 (HEK-negative control).

E) Examination of PDX mouse engrafted with BT972 showing tumor distribution (H&E) and GPNMB distribution specific to tumor regions.

F) Tumor volume measurements and survival times in NOG-EXL humanized mice after sequential doses of treatments with GPNMB CAR-Ts or untransduced T cells.

G) Kaplan-Meier survival analysis of NOG-EXL humanized mice after sequential doses of treatments with GPNMB CAR-Ts or untransduced T cells.

Supplementary 1. Immunohistochemistry optimization of GPNMB antibody.

A) Positive control PDX (GBM8, left) and negative control (BT935, right)

Supplementary 2. Rational combination treatments using CAR-Ts in GBM models.

A) Therapy regimens of CAR-Ts injected intracranially including staggered treatment combinations.

B) Tumor volume measurements and survival times in GBM8 bearing mice after sequential doses of treatments. C) Cytotoxicity assays revealing time and dose dependent killing of macrophages in response to CAR-Ts

C) Weekly bioluminescent measurements using IVIS in PDX models and subsequent survival times including staggered treatment combinations.

D) Tumor volume measurements and survival times in GBM8 bearing mice after sequential doses of CD133 CAR-Ts or staggered with GPNMB CAR-Ts.

E) Kaplan-Meier survival analysis of tumor bearing mice after sequential doses of CD133 CAR-Ts or staggered with GPNMB CAR-Ts.

F) Tumor volume measurements and survival times in GBM8 bearing mice after sequential doses of CD133 CAR-Ts or staggered with GPNMB CAR-Ts.

G) Kaplan-Meier survival analysis of tumor bearing mice after sequential doses of GPNMB CAR-Ts or staggered with CD133 CAR-Ts.

Chapter 2, Figure 1

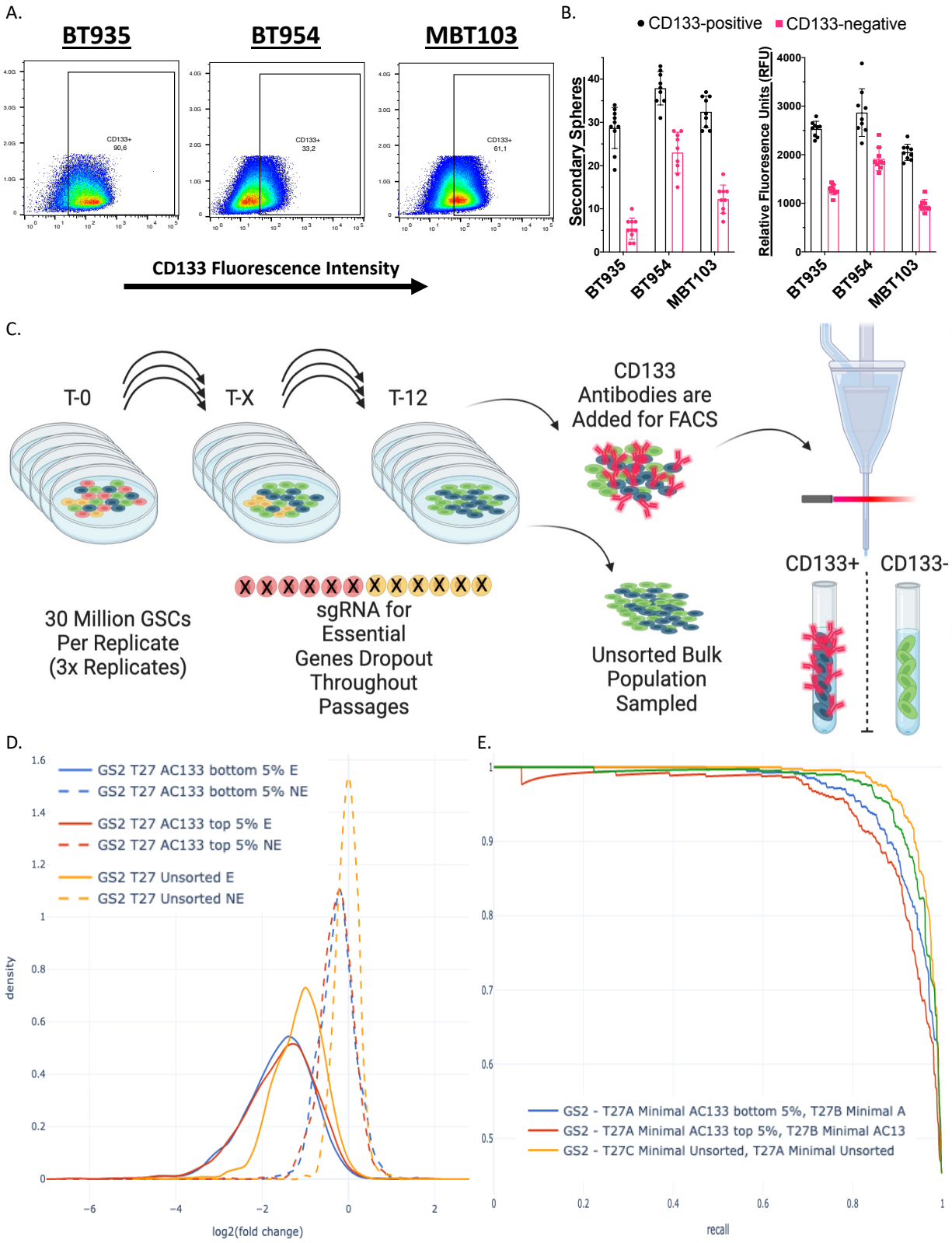

Chapter 2, Figure 2

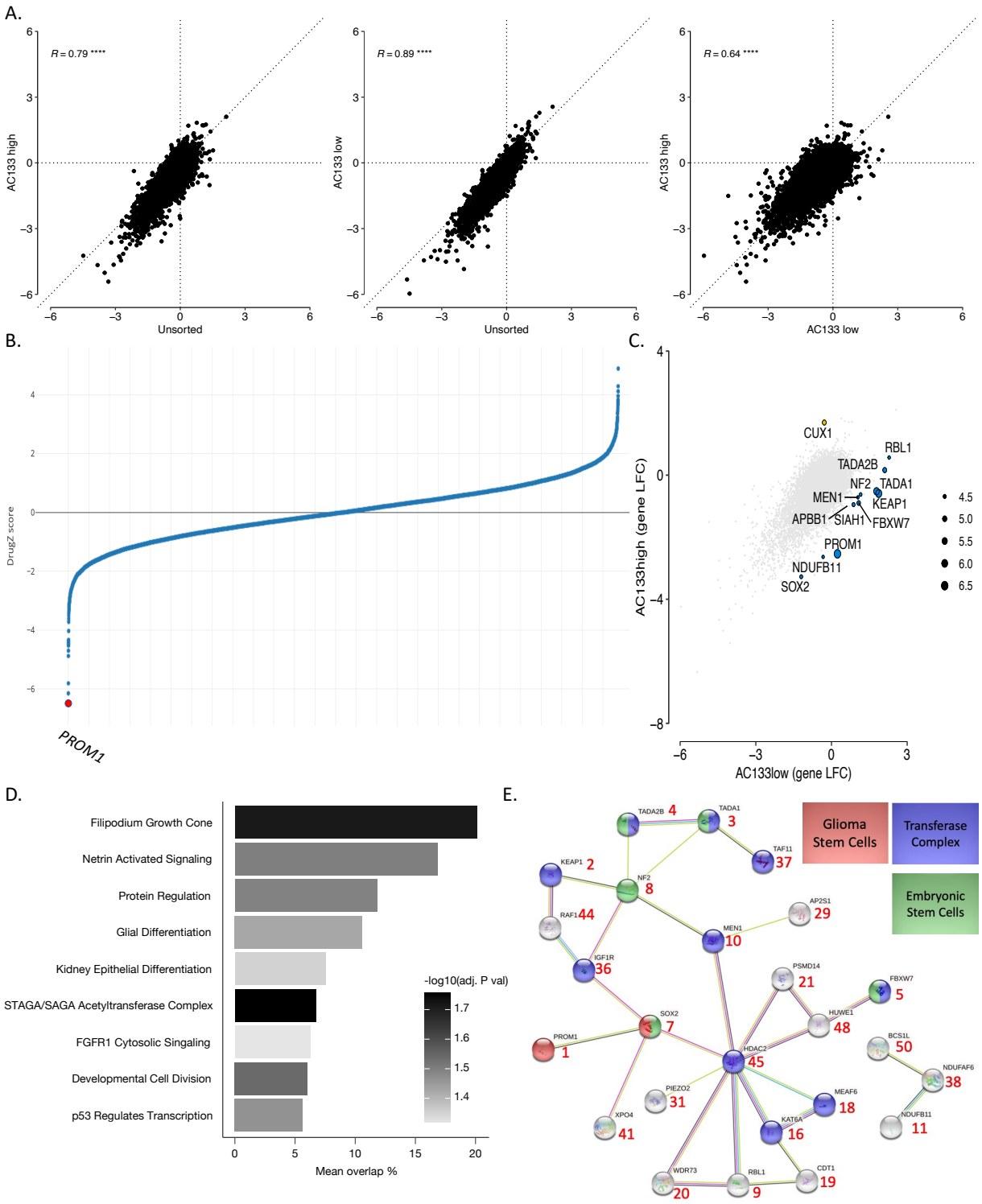

Chapter 2, Figure 3

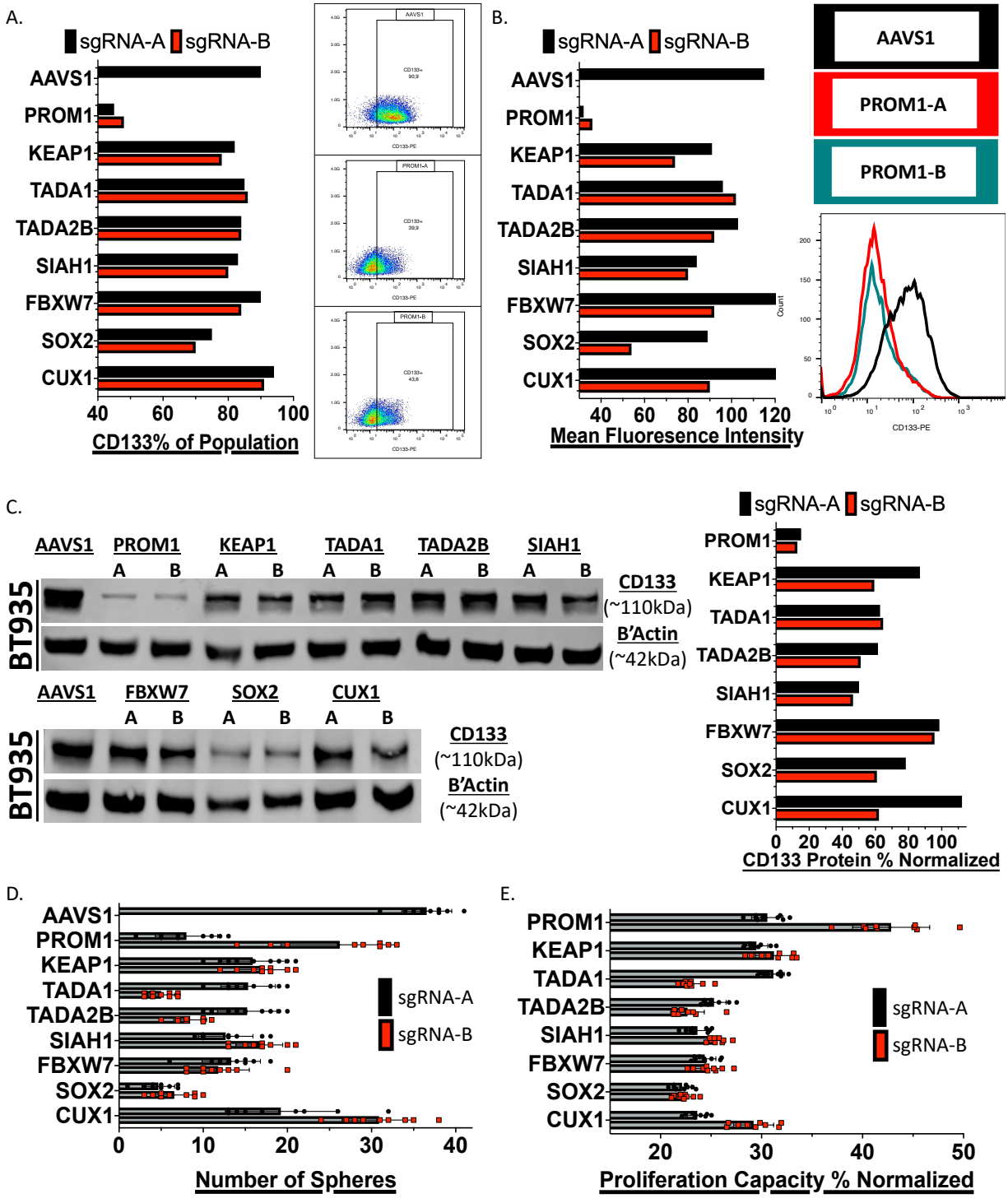

Chapter 2, Figure 4

A.

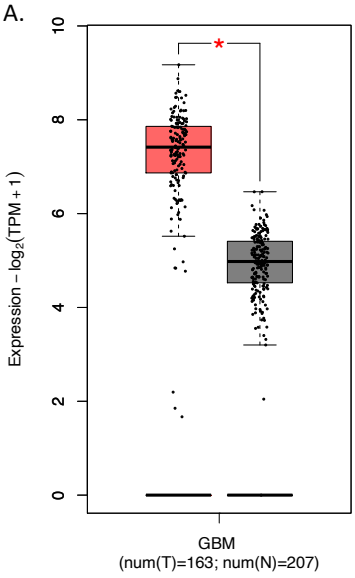

B.

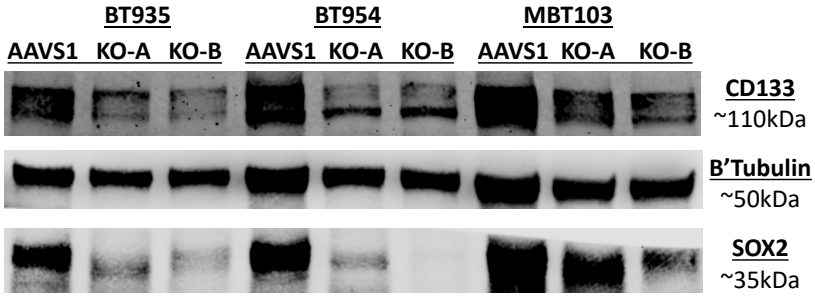

C.

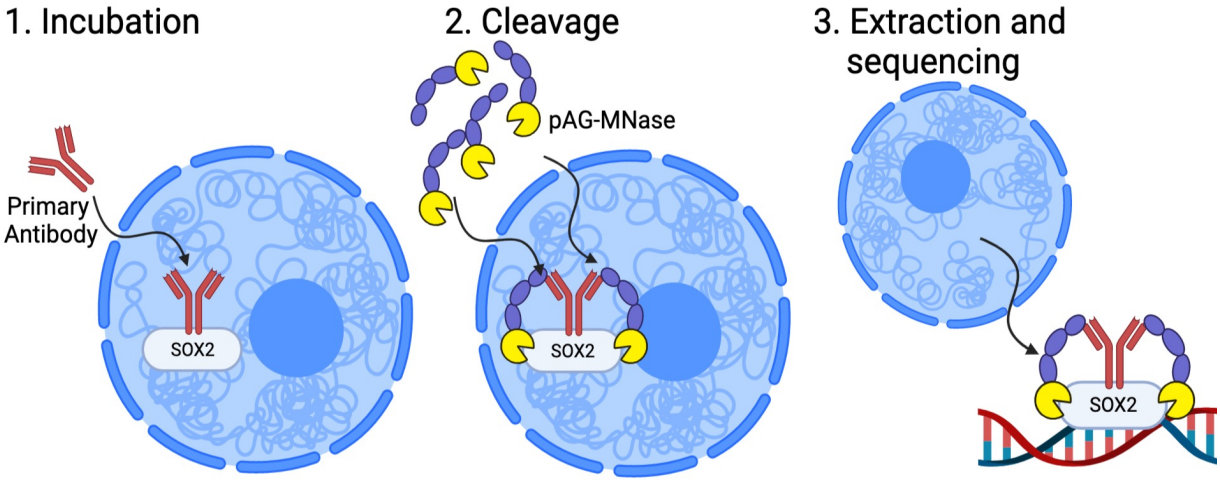

D.

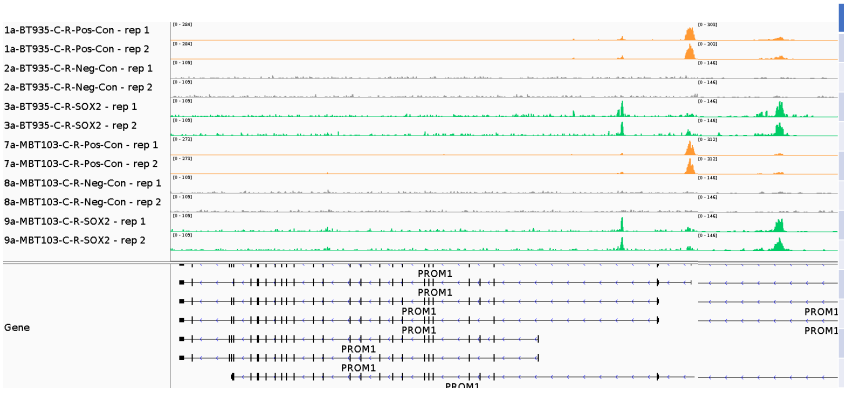

Sample	Number of Peaks
BT935 Pos. Control	20,112
BT935 Pos. Control	20,283
BT935 Neg. Control	16
BT935 Neg. Control	14
BT935 SOX2	9,663
BT935 SOX2	9,903
MBT103 Pos. Control	17,482
MBT103 Pos. Control	17,519
MBT103 Neg. Control	734
MBT103 Neg. Control	728
MBT103 SOX2	16,074
MBT103 SOX2	16,244

Chapter 2, Supplementary 1

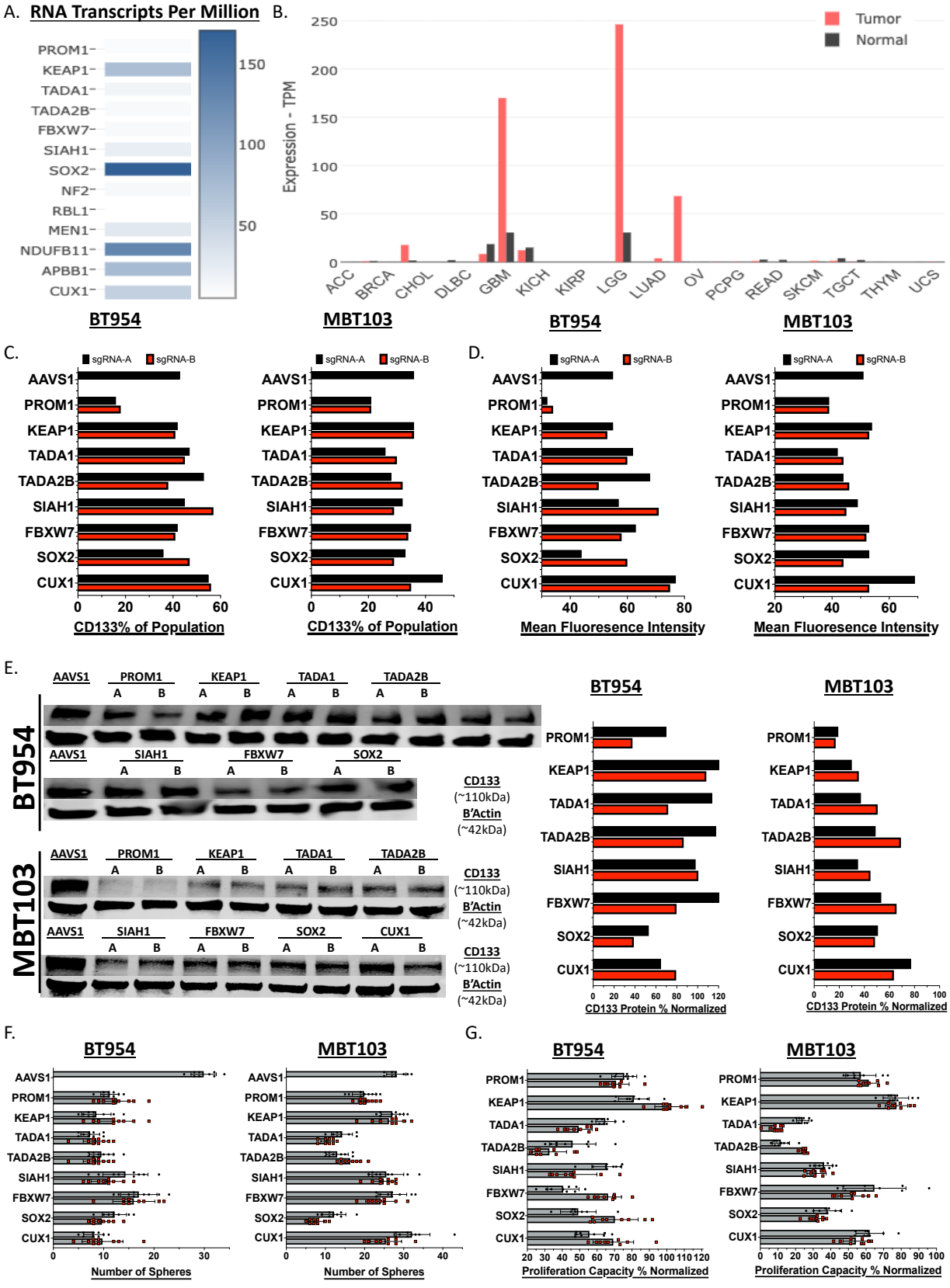

Chapter 2, Supplementary 2

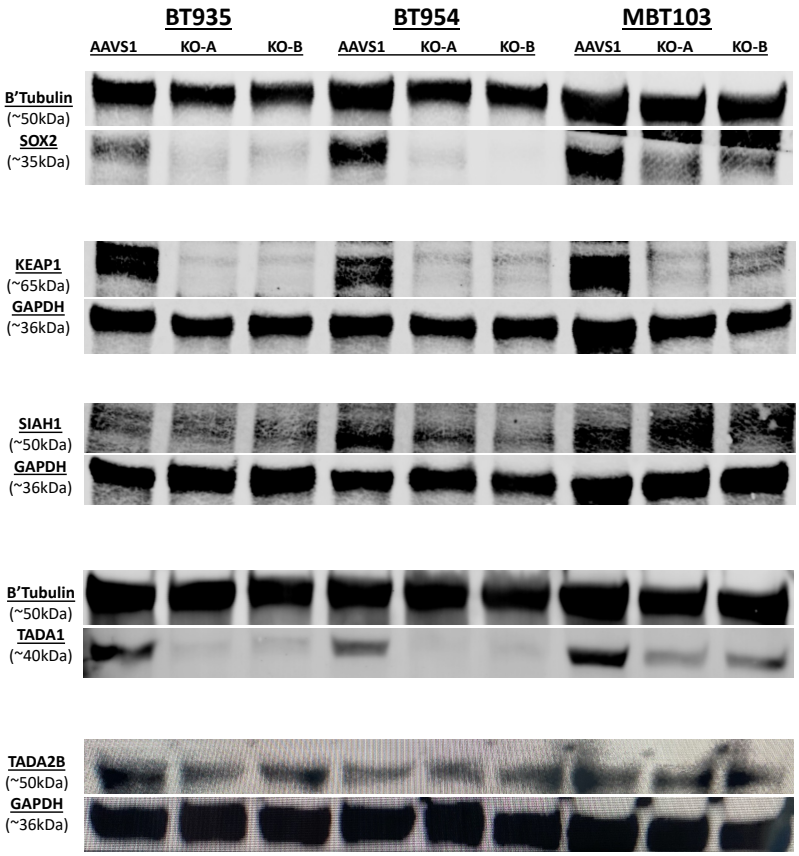

Chapter 2, Supplementary 3

All GBM

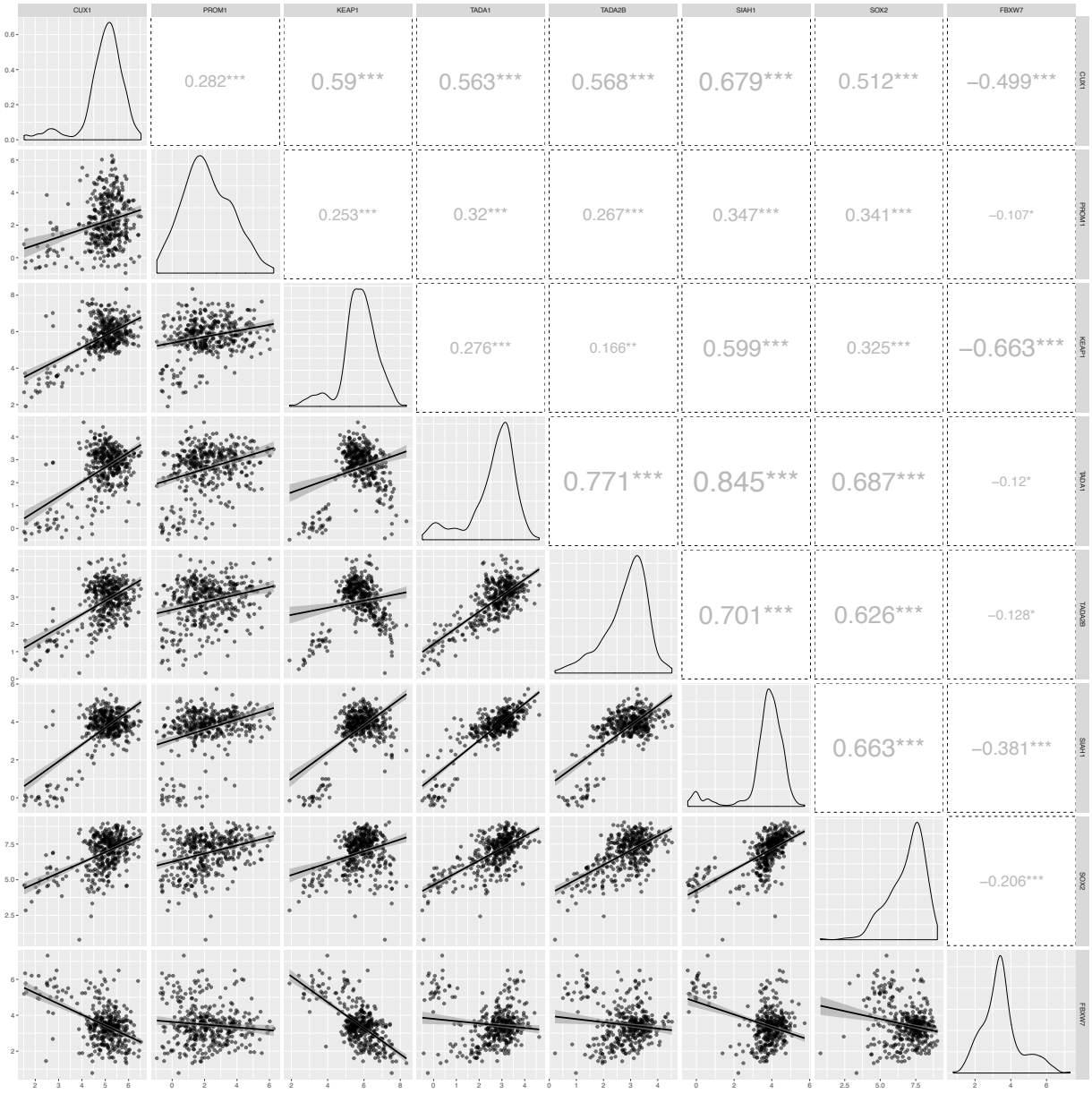

Chapter 3, Figure 1

A.

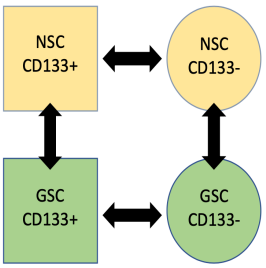

Gene	LogFC	Rank Score	P-Value
GPNMB	-1.63	-1.36	0.04
FAR2	-2.25	-1.33	0.05
MIR4458HG	-4.58	-1.32	0.05
ST8SIA3	-7.21	-1.32	0.05

B.

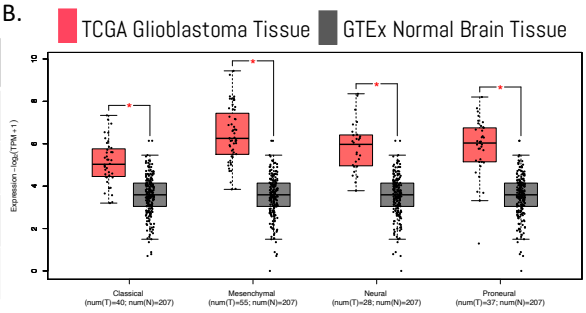

C.

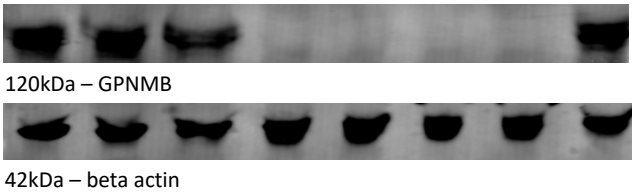

D.

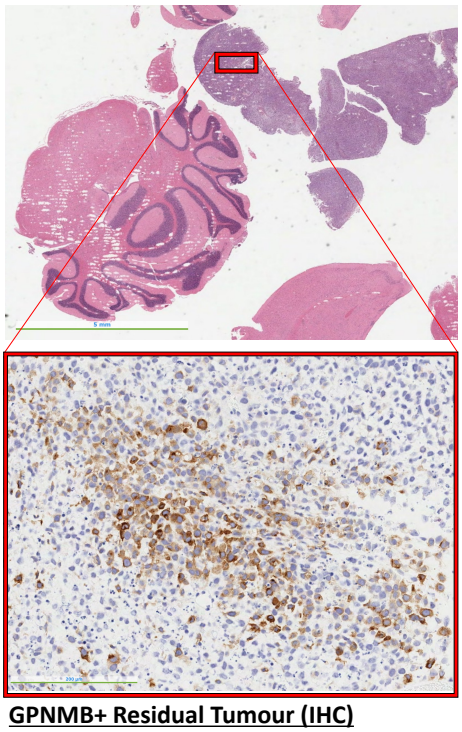

E.

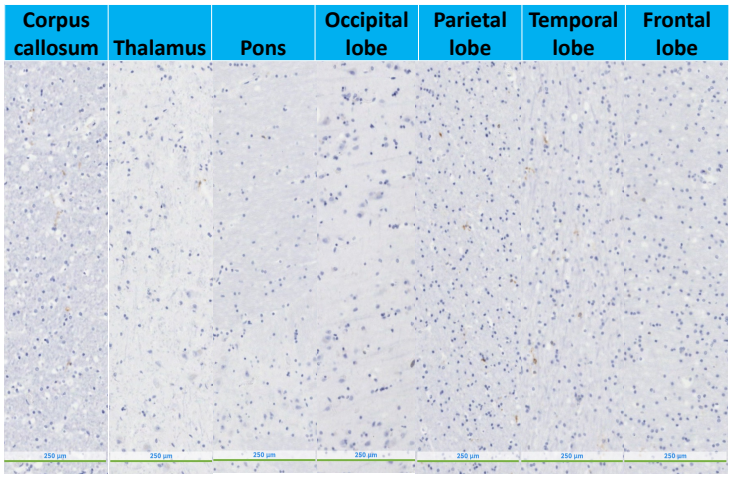

Chapter 3, Figure 2

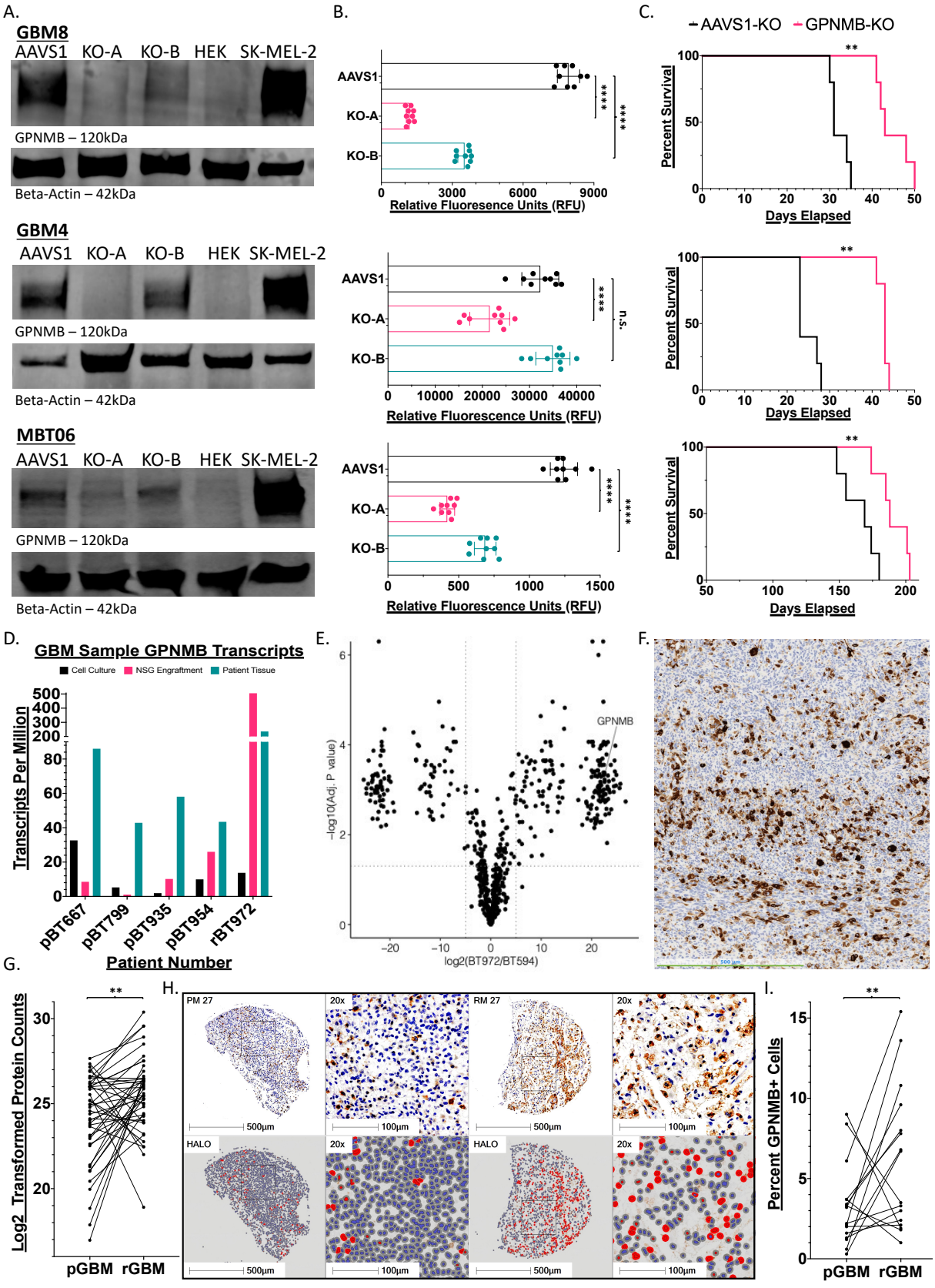

Chapter 3, Figure 3

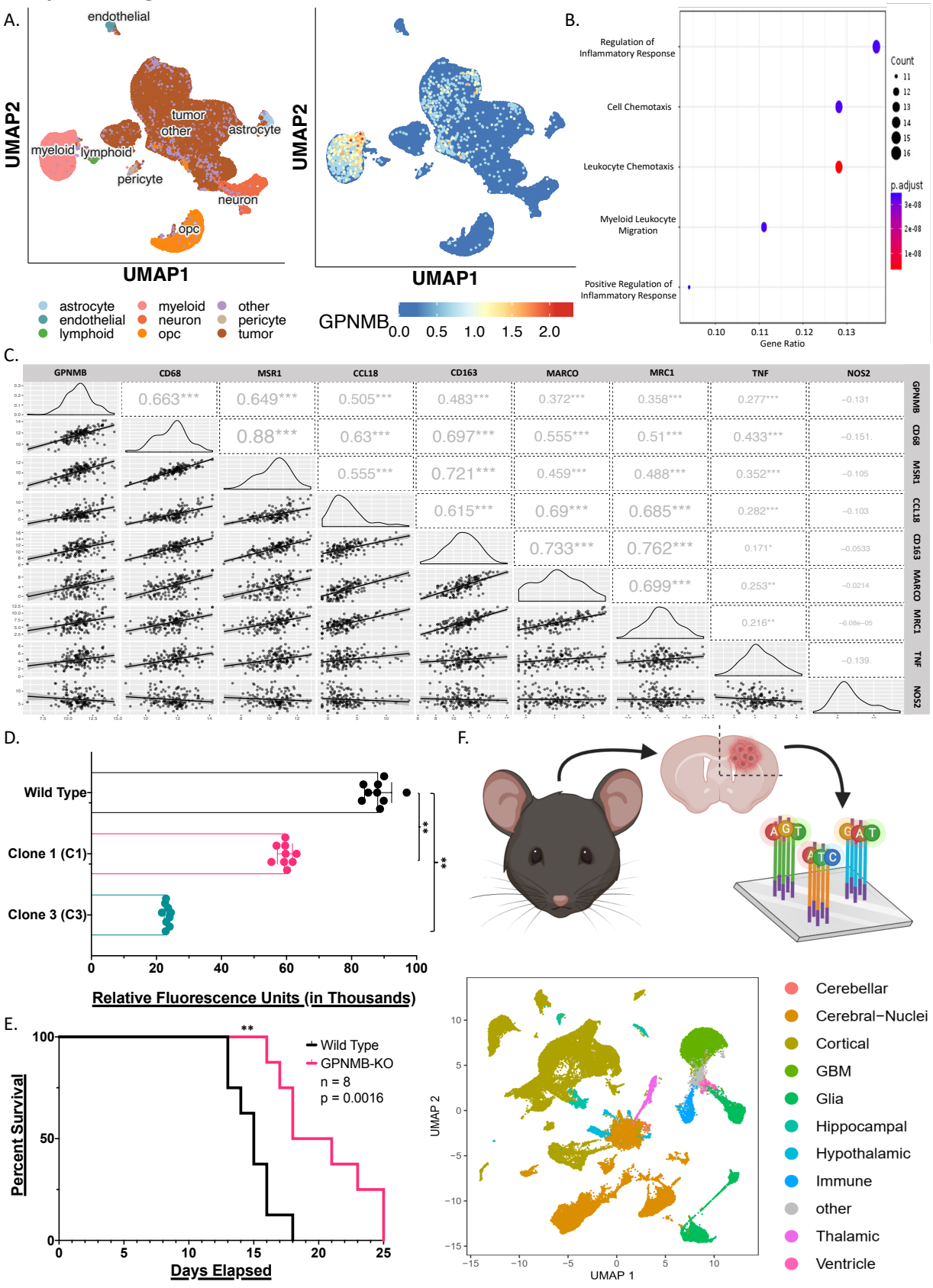

Chapter 3, Figure 4

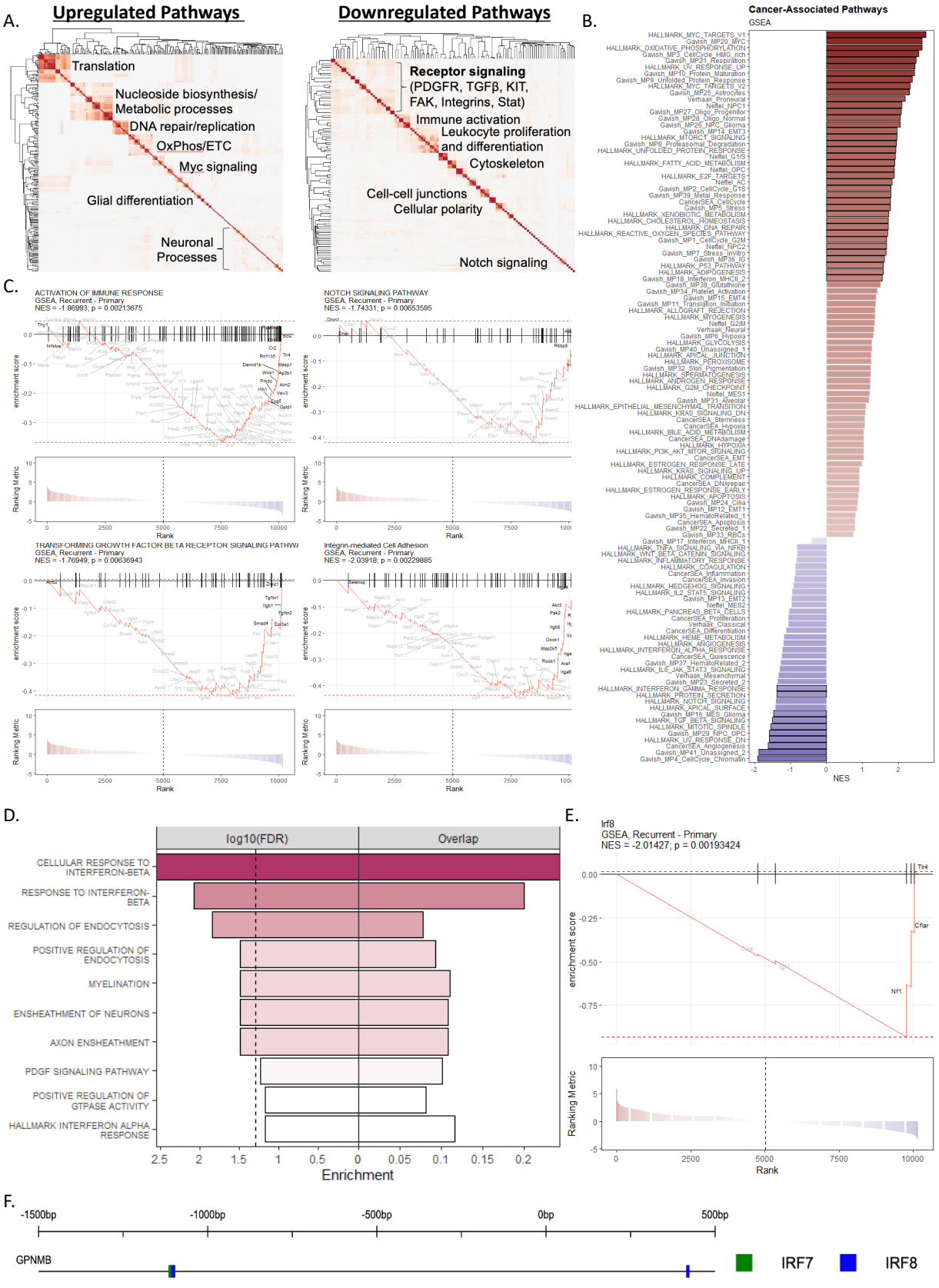

Chapter 3, Figure 5

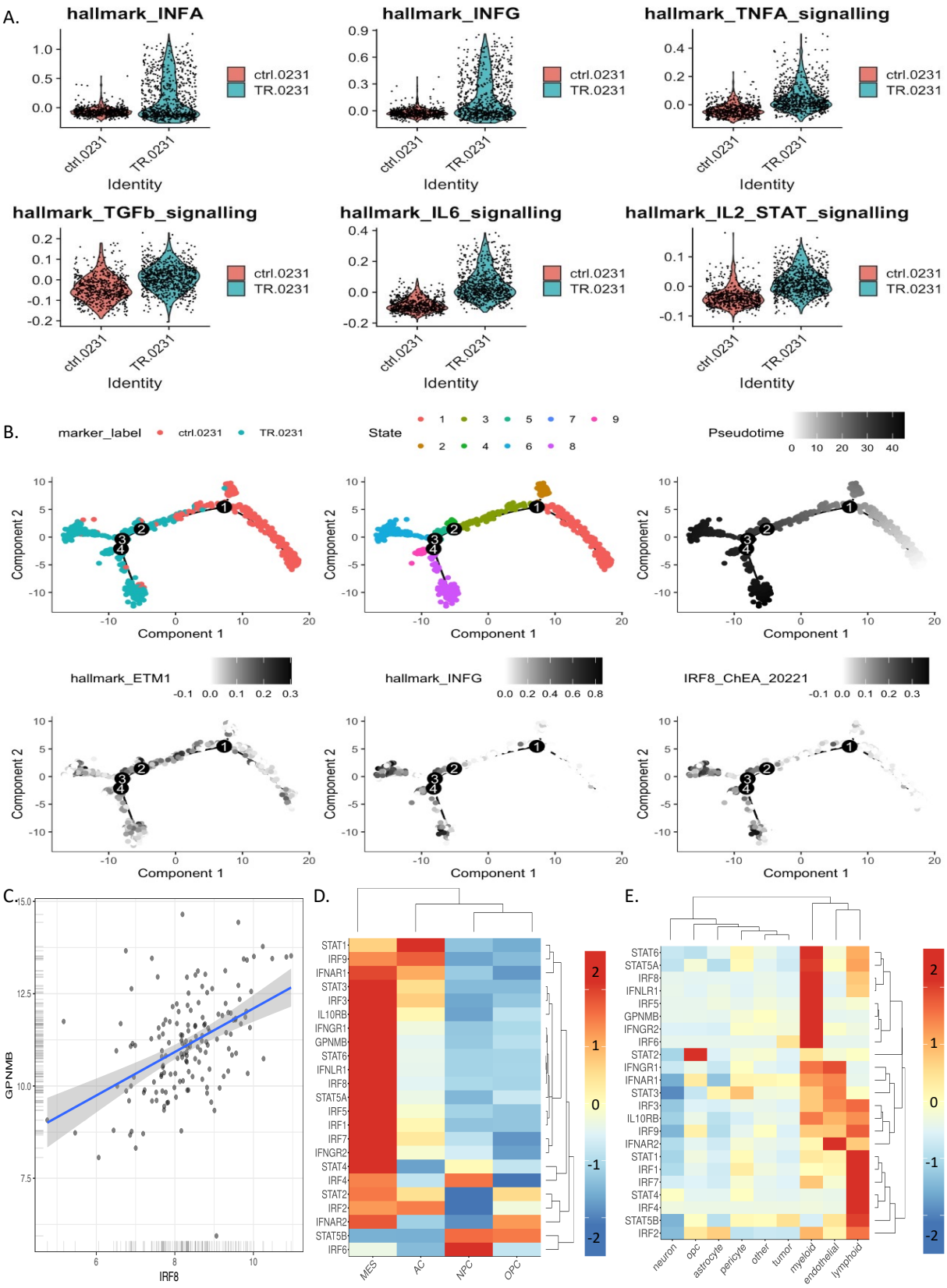

Chapter 3, Supplementary 1

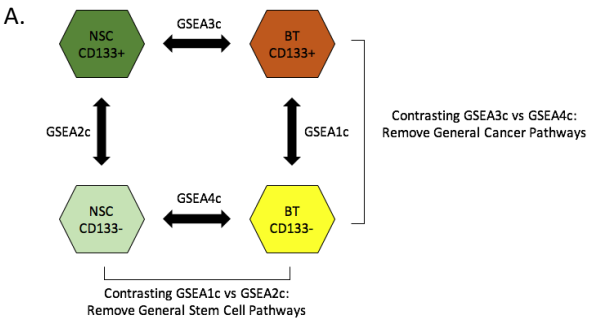

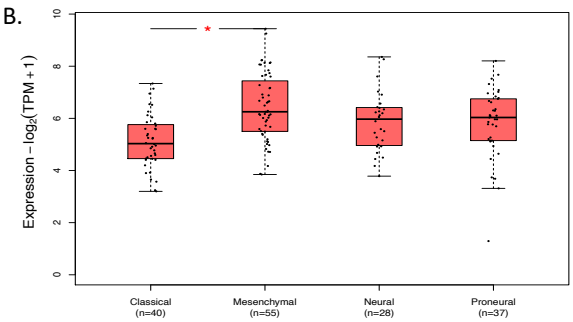

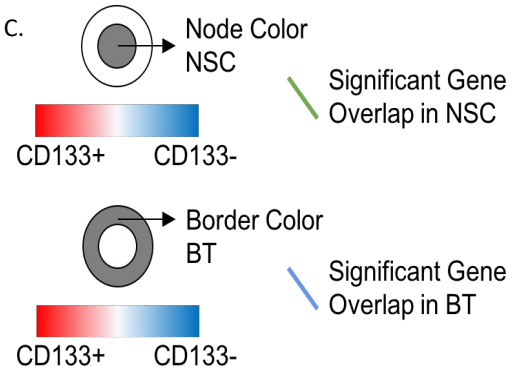

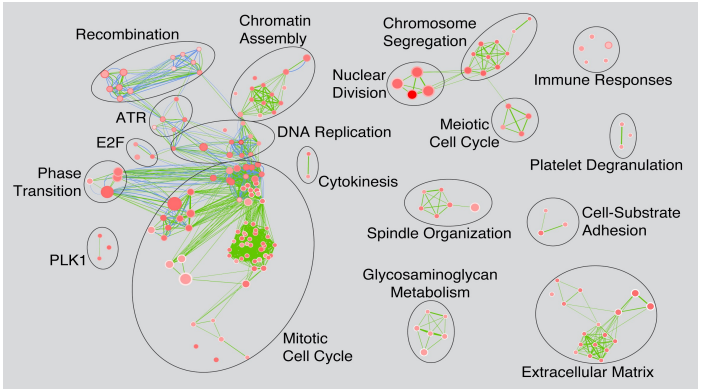

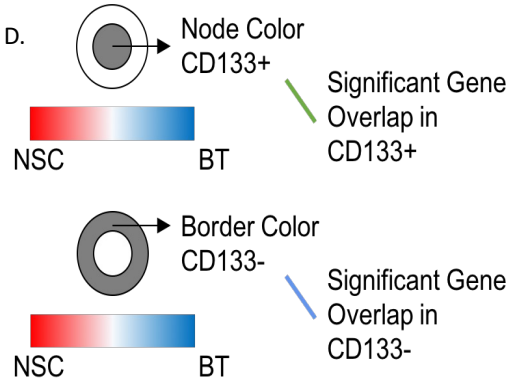

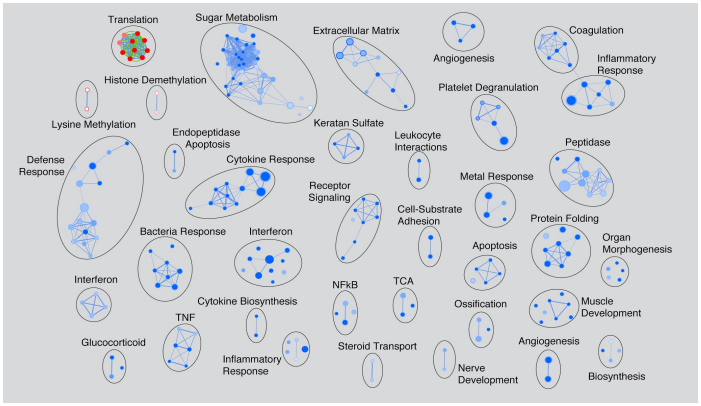

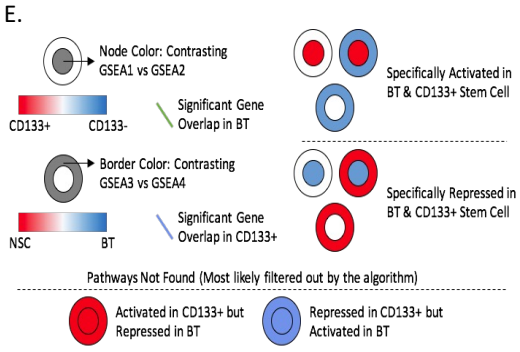

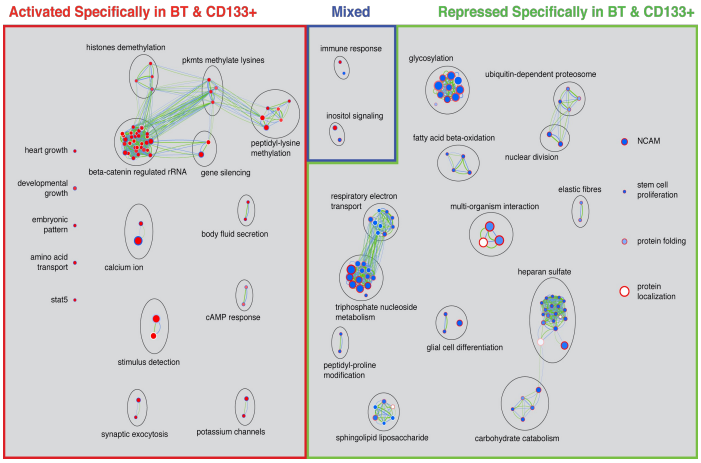

Chapter 3, Supplementary 2

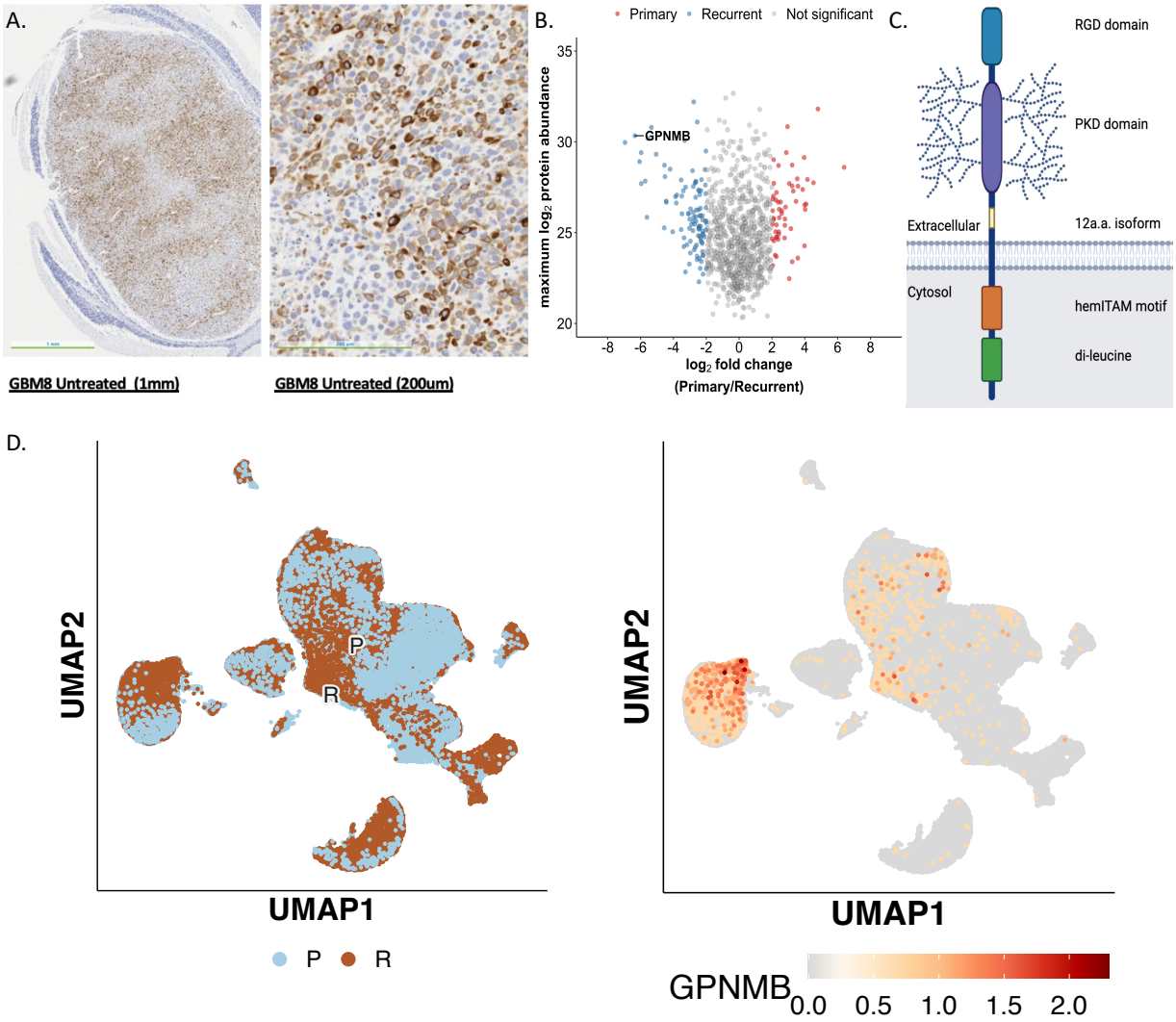

Chapter 3, Supplementary 3

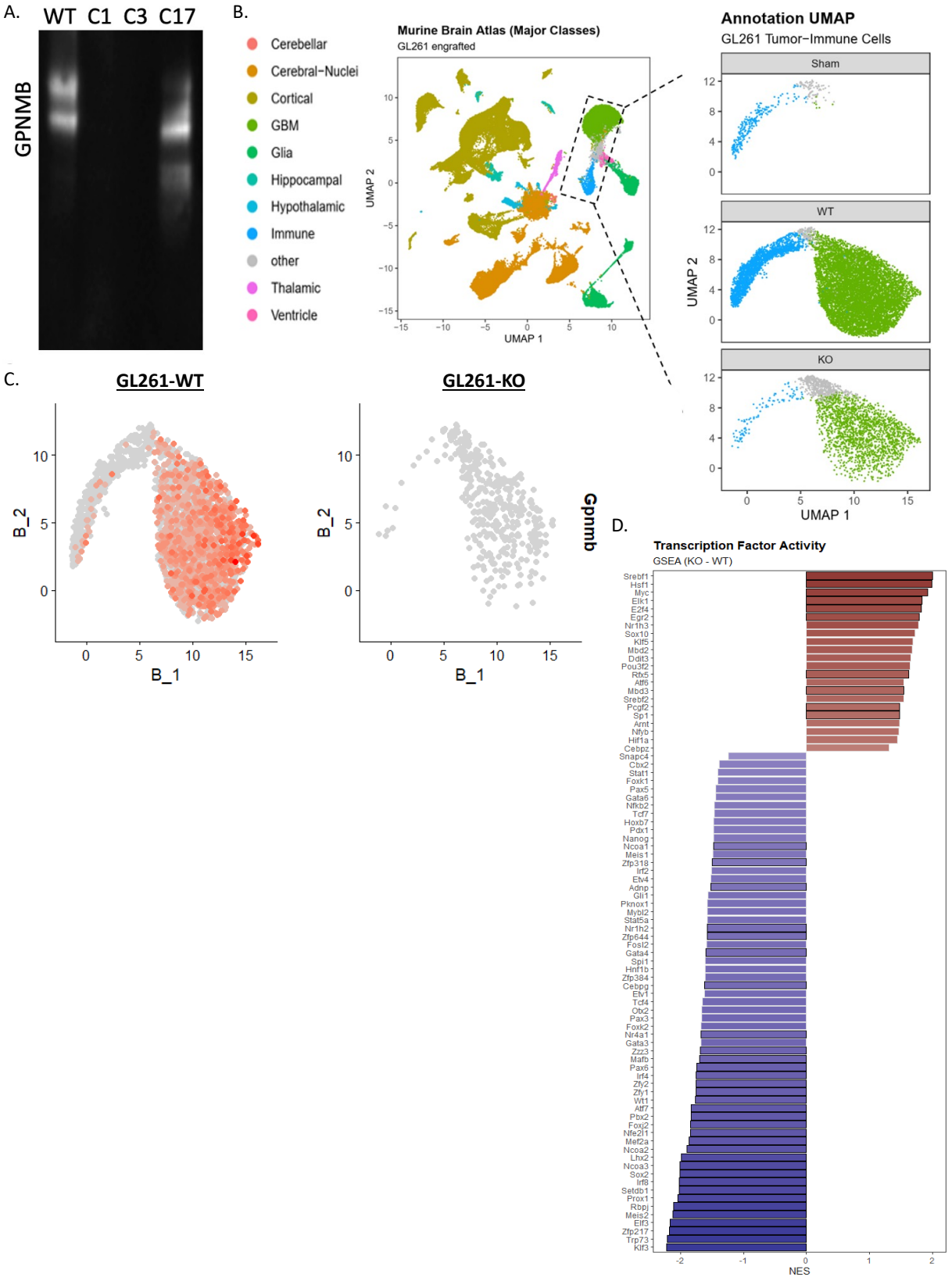

Chapter 4, Figure 1

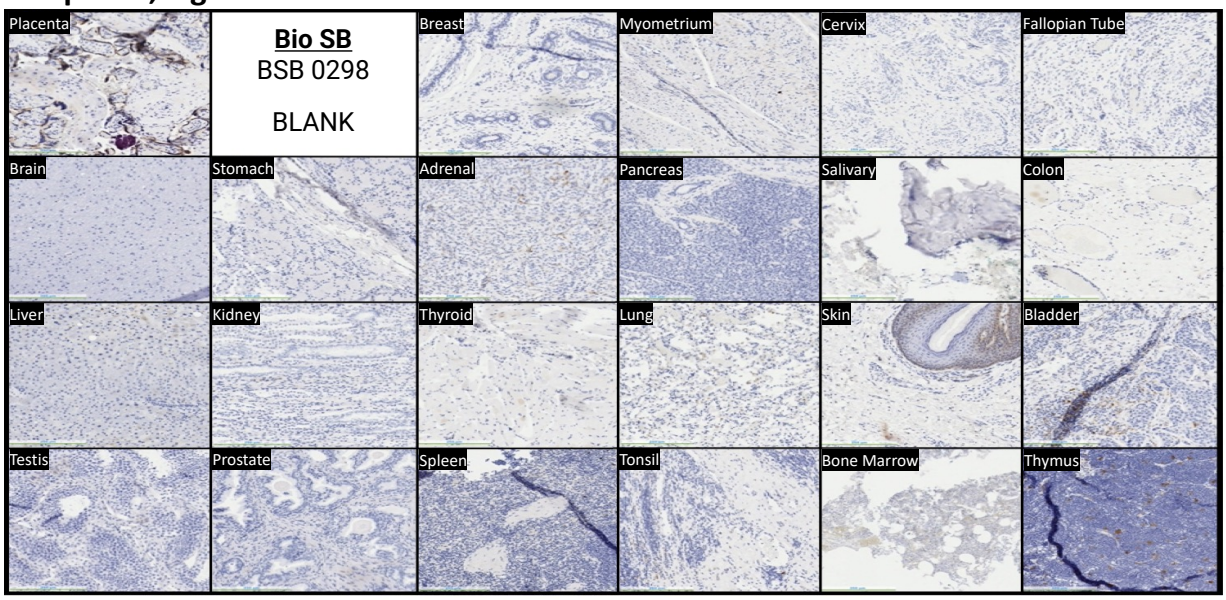

B.

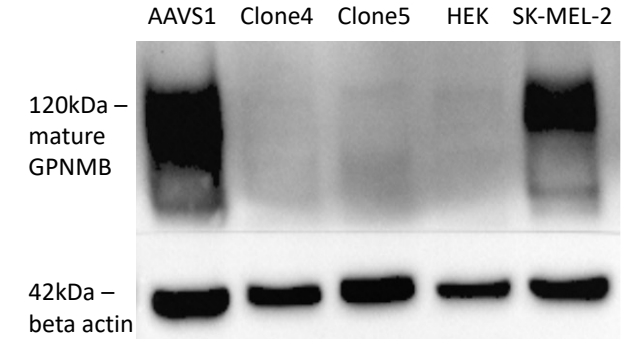

C.

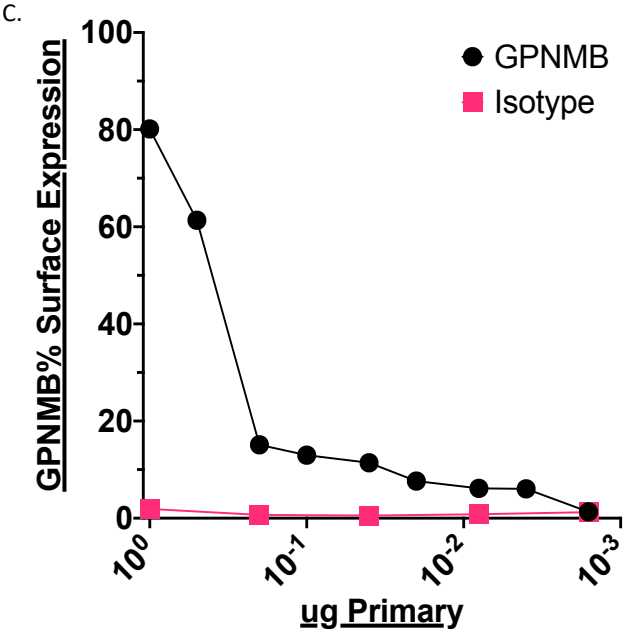

D.

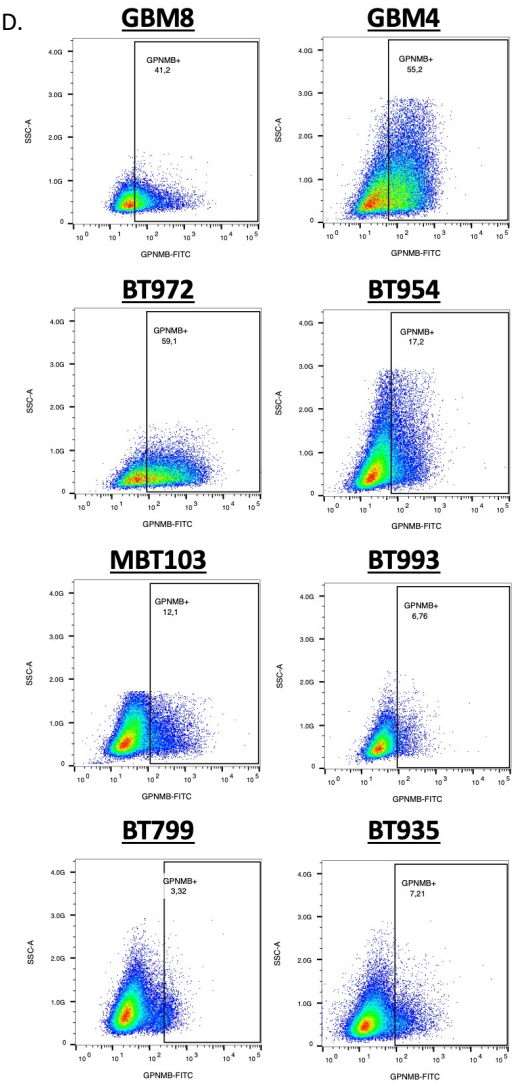

Chapter 4, Figure 2

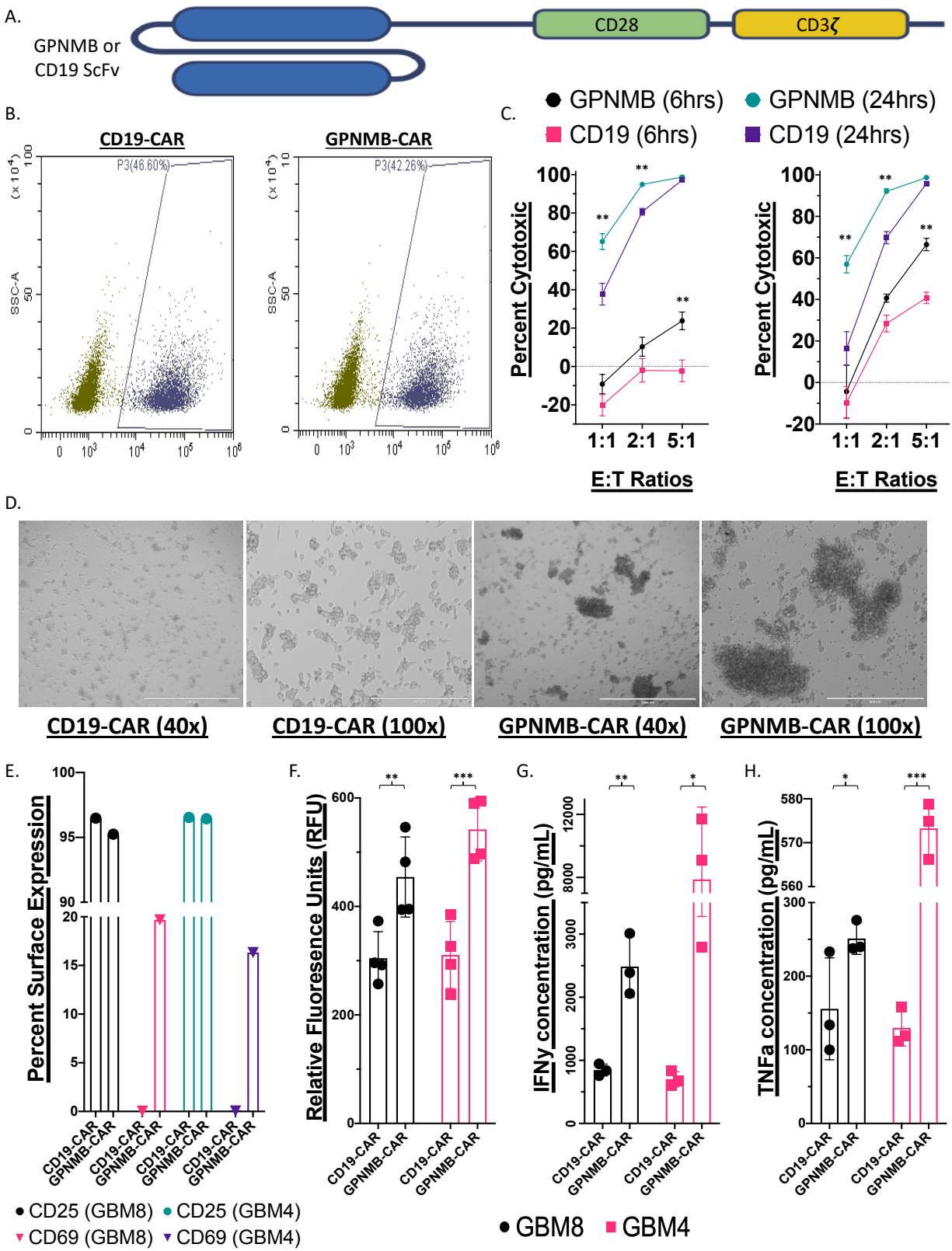

Chapter 4, Figure 3

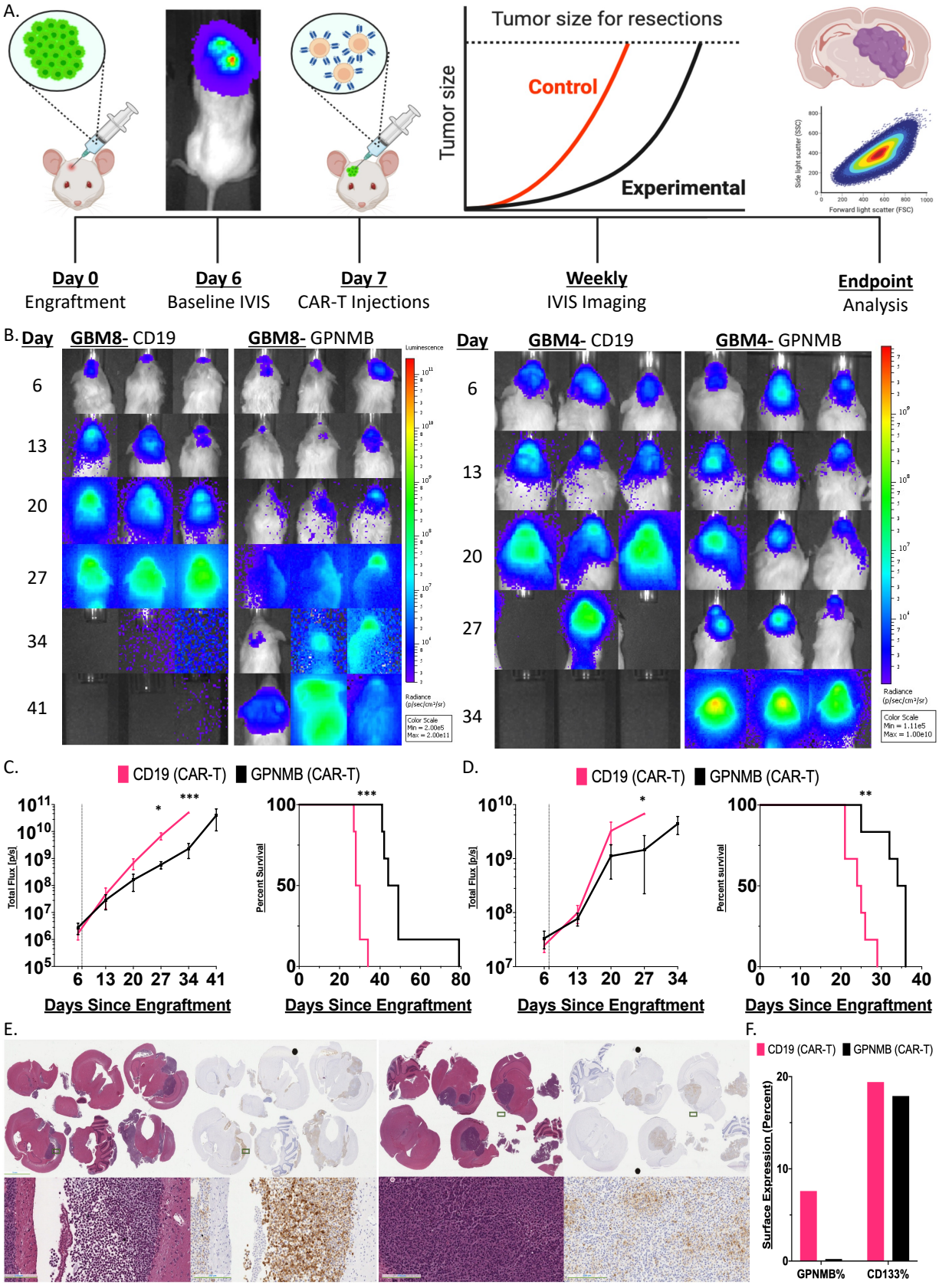

Chapter 4, Figure 4

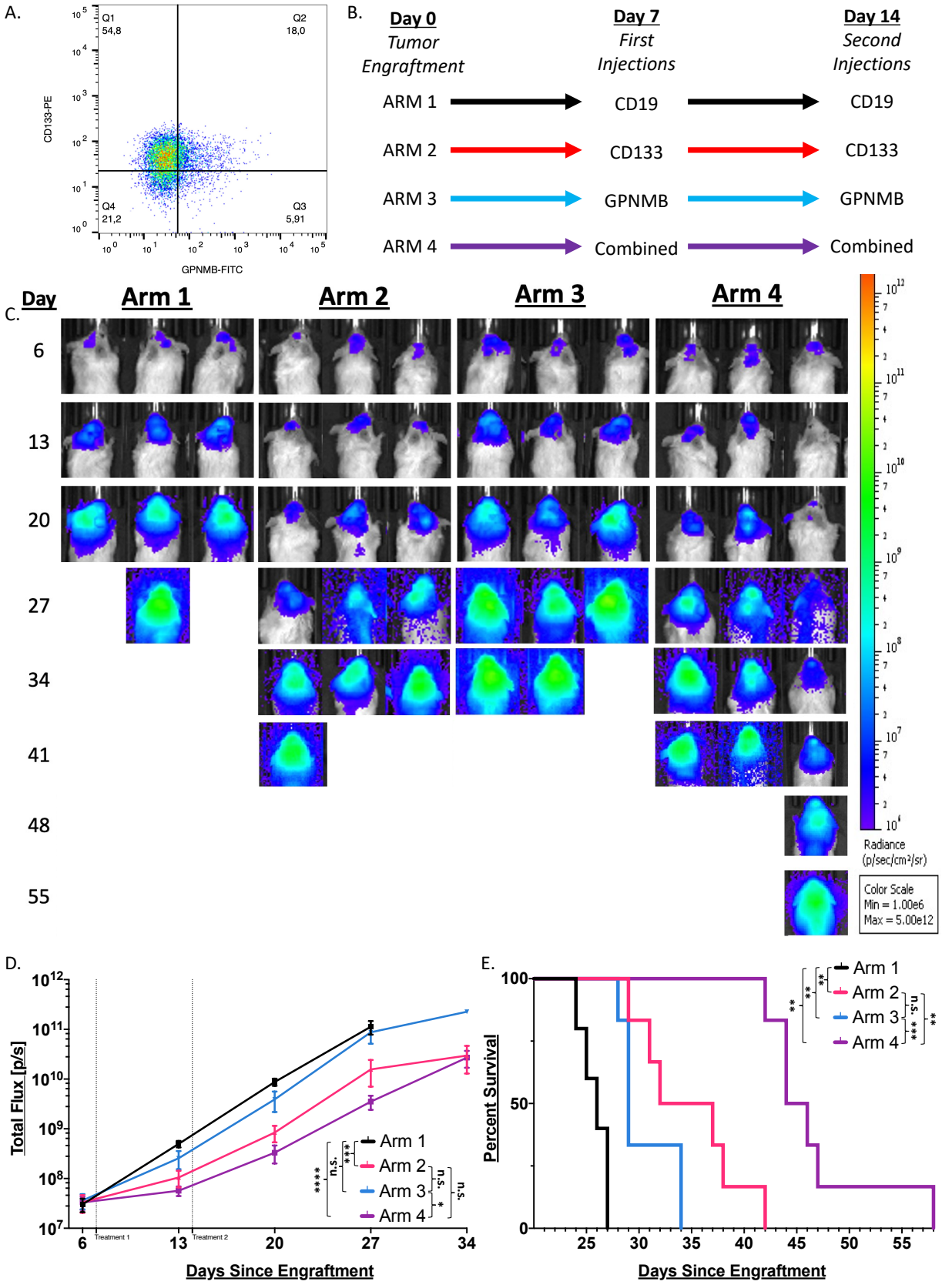

Chapter 4, Figure 5

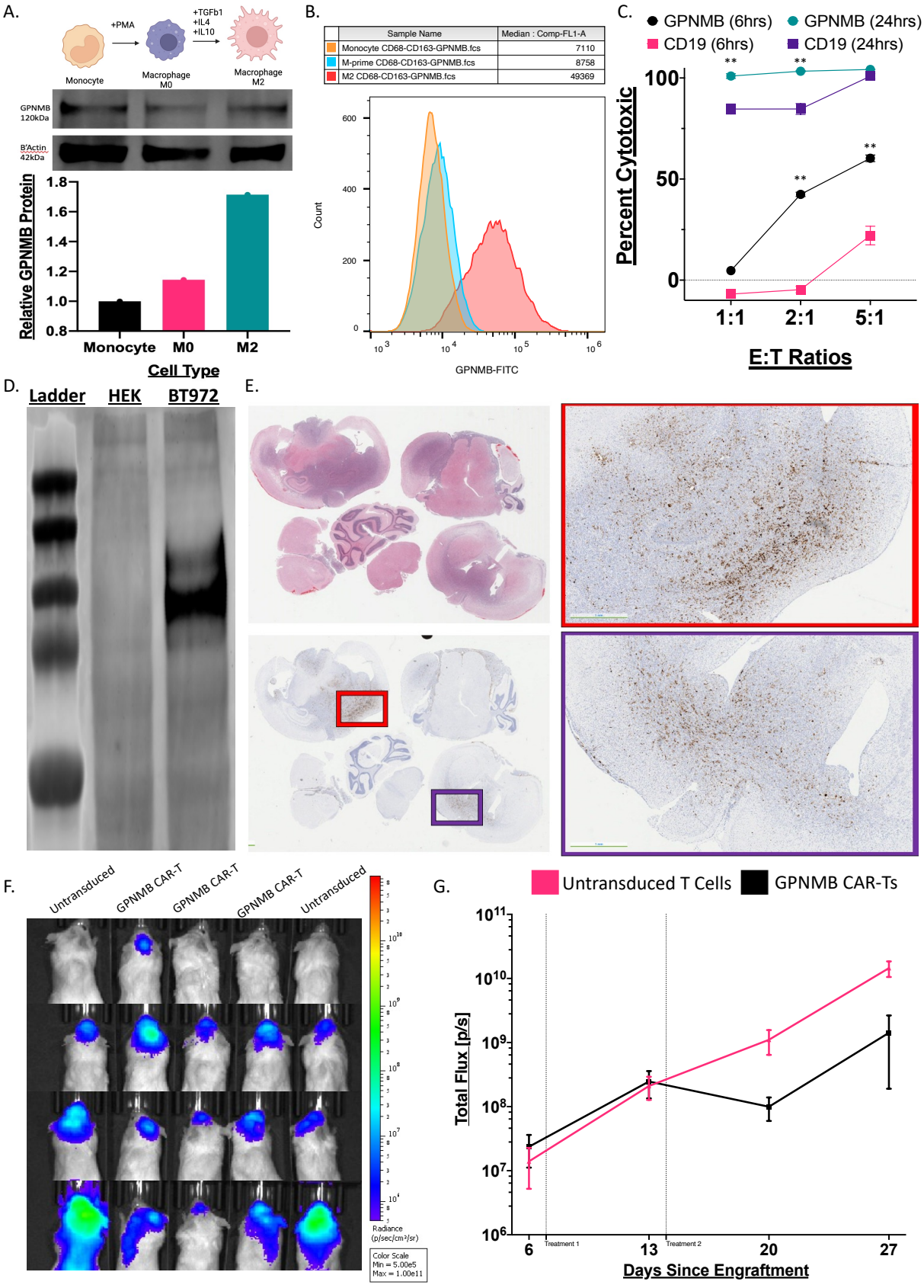

Chapter 4, Supplementary 1

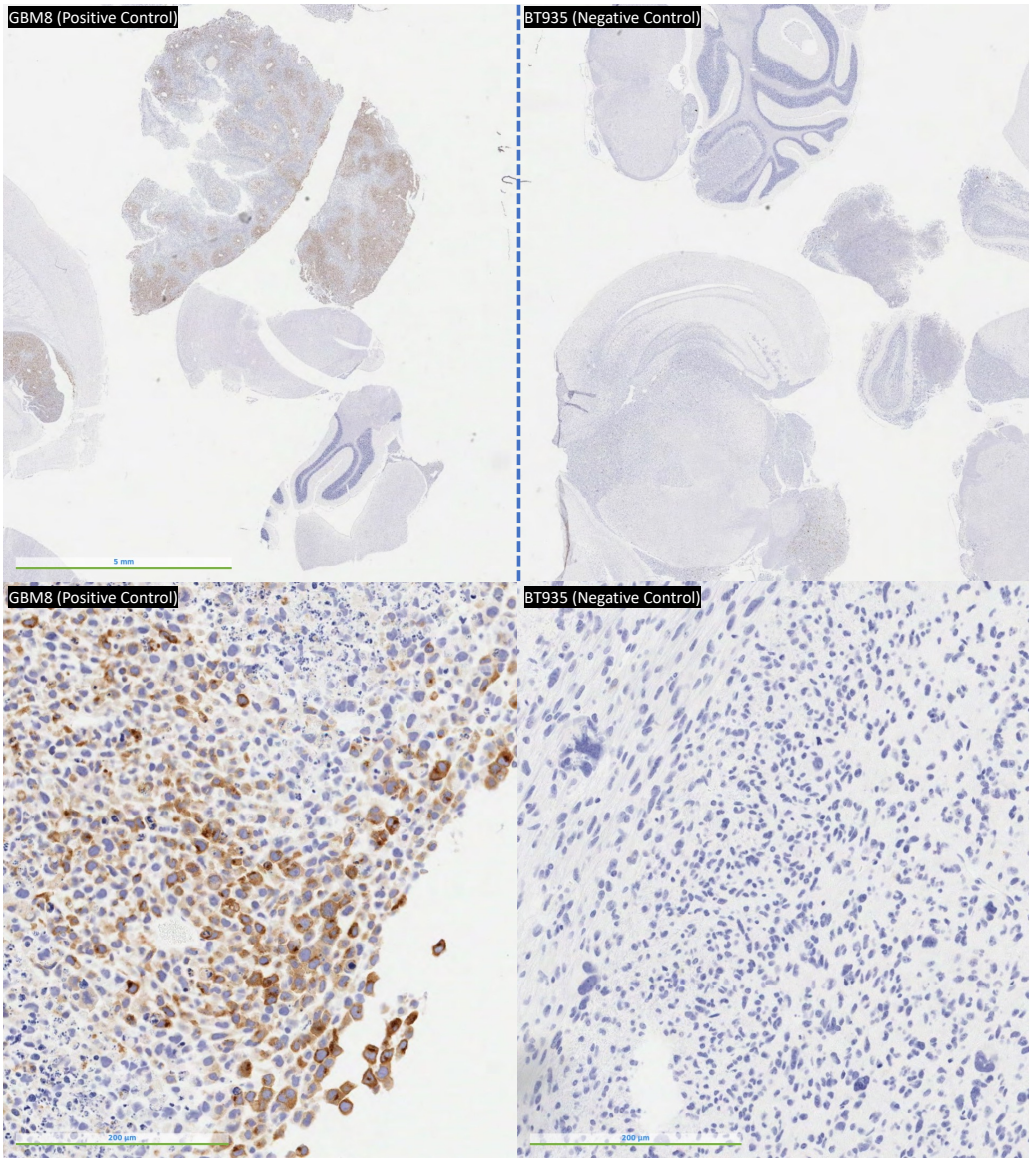

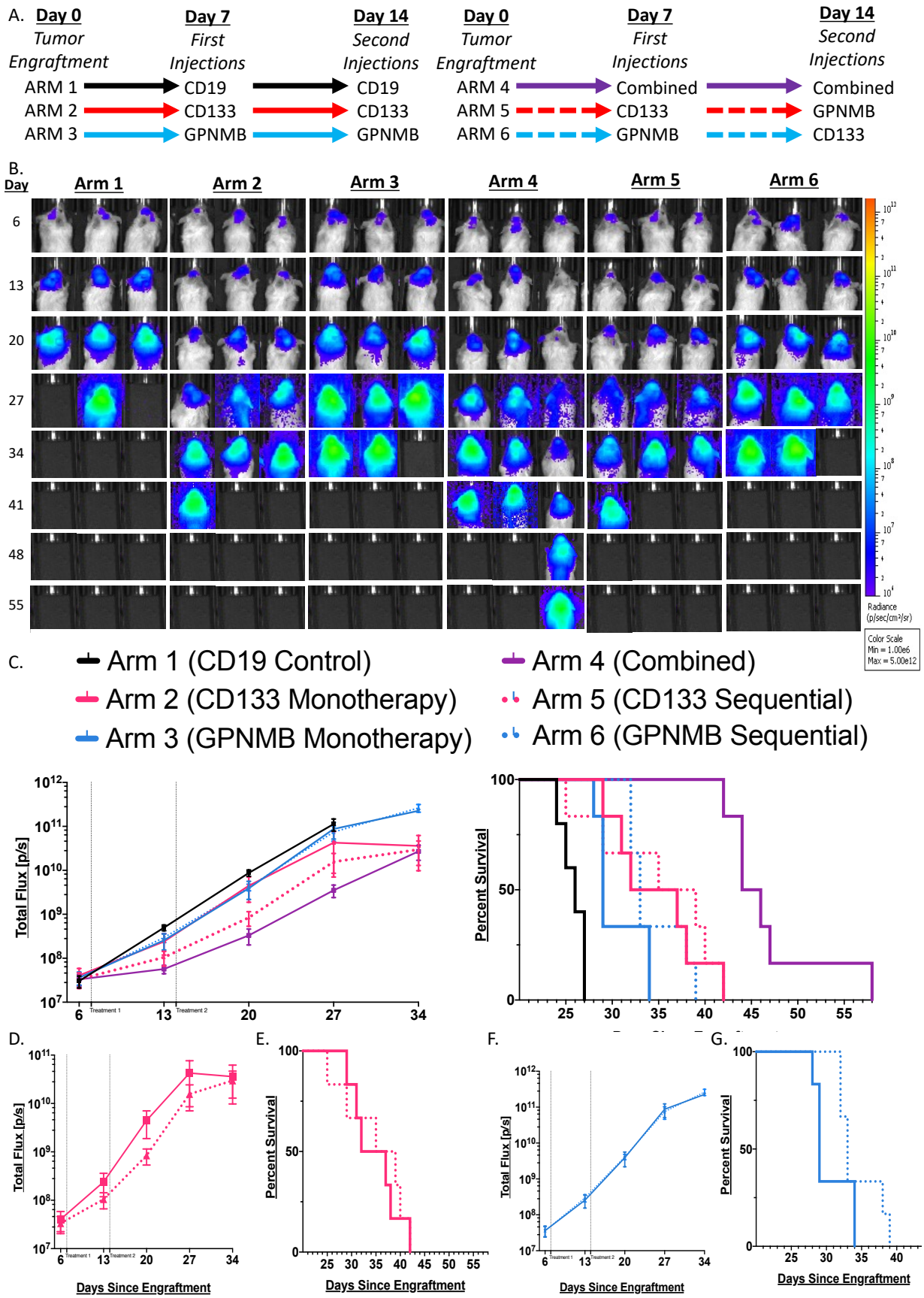
A.
Day 0
Tumor Engraftment
Day 7
First Injections
Day 14
Second Injections
ARM 1
CD19
CD19
ARM 2
CD133
CD133
ARM 3
GPNMB
GPNMB
Day 0
Tumor Engraftment
Day 7
First Injections
Day 14
Second Injections
ARM 4
Combined
Combined
ARM 5
CD133
GPNMB
ARM 6
GPNMB
CD133
B.
Day
Arm 1
Arm 2
Arm 3
Arm 4
Arm 5
Arm 6
6
13
20
27
34
41
48
55
Radiance (p/sec/cm²/sr)
Color Scale
Min = 1.00e6
Max = 5.00e12
C.
Arm 1 (CD19 Control)
Arm 2 (CD133 Monotherapy)
Arm 3 (GPNMB Monotherapy)
Arm 4 (Combined)
Arm 5 (CD133 Sequential)
Arm 6 (GPNMB Sequential)
Total Flux [p/s]
Treatment 1
Treatment 2
Percent Survival
D.
E.
F.
G.
Days Since Engraftment